

19th INTERNATIONAL SHIP AND
OFFSHORE STRUCTURES CONGRESS

7–10 SEPTEMBER 2015
CASCAIS, PORTUGAL



VOLUME 1

COMMITTEE III.2 FATIGUE AND FRACTURE

COMMITTEE MANDATE

Concern for crack initiation and growth under cyclic loading as well as unstable crack propagation and tearing in ship and offshore structures. Due attention shall be paid to practical application and statistical description of fracture control methods in design, fabrication and service. Consideration is to be given to the suitability and uncertainty of physical models.

COMMITTEE MEMBERS

Chairman: F. P. Brennan, *UK*
K. Branner, *Denmark*
J.H. den Besten, *The Netherlands*
A. M. Horn, *Norway*
B. Ki Choi, *Korea*
W. Mao, *Sweden*
T. Nakamura, *Japan*
E. Oterkus, *UK*
I. Paranhos Pasqualino, *Brazil*
G. Parmentier, *France*
C. Rizzo, *Italy*
J. Romanoff, *Finland*
J. Rörup, *Germany*
A. Samanta, *India*
A. Theodoulidis, *Greece*
F. Wang, *China*
G. Wang, *Singapore*

EXTERNAL CONTRIBUTOR

N. Chen, *USA*

KEYWORDS

Fatigue, Fracture Mechanics, Probabilistic Methods, Materials, Steel, High Strength Steel, Stainless Steel, Aluminium, Inspection, Fitness for Service.

CONTENTS

1.	INTRODUCTION	354
2.	FATIGUE LIFE-CYCLE DESIGN PHILOSOPHIES AND METHODOLOGIES	354
2.1	Fatigue and fracture in marine structures	354
2.2	Preliminary Design	354
2.3	Detailed Design.....	354
2.4	Fabrication	355
2.5	In-service Maintenance.....	355
2.5.1	Inspection techniques	355
2.5.2	Inspection planning.....	355
2.6	Fatigue strength.....	355
2.6.1	S-N curves related to expected workmanship	355
2.6.2	Crack propagation parameters.....	355
2.7	Fracture Strength.....	356
2.8	Fatigue Loads	356
2.8.1	Wave loads.....	356
2.8.2	Loading unloading.....	356
2.8.3	Vibrations.....	356
2.9	Environmental effects	356
2.9.1	In air	357
2.9.2	Seawater.....	357
2.9.3	Other aggressive environments	357
2.9.4	Coating and coating life.....	357
2.10	Fatigue, Fracture & Failure Criteria	357
2.10.1	Failure definition	357
2.10.2	Uncertainties	357
2.10.3	Safety Factors	358
3.	FACTORS INFLUENCING FATIGUE/FRACTURE.....	358
3.1	Resistance.....	358
3.1.1	Thickness and size	358
3.1.2	Environment (corrosion)	359
3.1.3	Temperature.....	362
3.1.4	Residual Stress & Constraint, mean stress.....	363
3.2	Materials.....	364
3.2.1	Metallic Alloys	364
3.2.2	Fatigue & fracture improvements through material changes, surface treatment	364
3.3	Loading	365
3.3.1	Stochastic Loading (load interaction effects (sequence)).....	365
3.3.2	Cycle counting – spectral, time-domain, stress ranges, means stress effect....	365
3.3.3	Complex stresses	366
3.3.4	Recent developments in multiaxial fatigue criteria	369
3.4	Structural Integrity/Life cycle management	373
3.4.1	Fabrication and repair.....	373
3.4.2	Inspection & Monitoring of structure and coatings.....	374
3.4.3	Inspection and Maintenance.....	376
3.5	Composites.....	377

4.	FATIGUE ASSESSMENT METHODS	378
4.1	Overview	379
4.2	Fatigue damage models	381
4.2.1	Stress based concepts	381
4.2.2	Strain concepts.....	382
4.2.3	Notch-intensity factor, -integral and -energy density concepts.....	382
4.2.4	Confidence and reliability	383
4.3	Fracture mechanics models	385
4.3.1	Crack growth rate model	389
4.3.2	Crack growth assessment	390
4.3.3	Fracture mechanics based fatigue evaluation of ship structures	391
4.4	Rules, standards & guidance	392
4.4.1	Ship rules	392
4.4.2	Design codes for Offshore Structures	394
4.4.3	IIW recommendation.....	395
4.4.4	ISO Standards	395
4.5	Acceptance criteria	395
4.6	Measurement techniques	396
4.6.1	Crack growth and propagation	396
4.6.2	Fatigue.....	397
4.6.3	Material properties.....	398
4.6.4	Fracture toughness.....	398
5.	BENCHMARKING STUDY	399
5.1	Problem Statement	399
5.2	Analytical Methods.....	400
5.3	Numerical analysis using FEM	402
5.4	Results	403
5.5	Discussion & Benchmarking Study Conclusions	404
6.	SUMMARY & CONCLUSIONS.....	404
	REFERENCES	405

1. INTRODUCTION

This report of the current committee describes the recent activities of the international ship and offshore industry and the researchers that support it, with specific regard to current pertinent issues and trends relating to Fatigue and Fracture. It is important to remember that the subject area is vast and developing rapidly, and that this report should be seen not only in the context of the entire ISSC 2015 Proceedings but also as a continuation of past ISSC reports.

In addition, the committee chose to focus on areas commensurate with the expertise of the committee members to build on the vast knowledge base generated by previous Committee III.2 reports. This report in addition to providing a critique of contemporary research and design methods applicable to fatigue and fracture of ship and offshore structures undertook a detailed Benchmarking Study associated with very thin walled plate structures, a topic gaining prominence as lower weight structures become more commonplace. An important element of ISSC work is to provide an expert opinion on the subject matter reported and readers will find such comments and recommendations interwoven into the report; the most prominent however, are summarised in Section 6.

The report is structured so that Section 2 summarises from a designers perspective *Fatigue Life-Cycle Design Philosophies and Methodologies* aimed to be a gentle introduction to the report and setting the scene for the following two major review sections: *Factors Influencing Fatigue/Fracture* and *Fatigue Assessment Methods*. The former focuses on the generic underpinning scientific literature focusing upon subjects of particular relevance to current and emerging trends in structures operating in the marine environment. The latter section reviews published work associated with assessment methods, both of new design and build, but also for life-extension and reanalysis of fatigue life following unexpected events.

The Benchmarking study illustrates the absolute necessity to perform analyses carefully and for rules, design equations and interpretations to be clear and unambiguous as the fundamental logarithmic relationship between stress and life inherently mean that life predictions are highly sensitive to local stress and the accuracy to which stress is calculated is critical.

2. FATIGUE LIFE-CYCLE DESIGN PHILOSOPHIES AND METHODOLOGIES

Fatigue and fracture phenomena have been known about for a long time, illustrated, for example by the breaks in the liberty ships during World War II.

2.1 *Fatigue and fracture in marine structures*

In current marine structures, fatigue, from local leakage to total structure “brittle fracture” and with the increase of steels’ yielding stress, becomes more and more critical. Even if leakage consequences are generally minor concerning immediate structural strength, pollution resulting from oil loss or other aggressive cargoes may lead to an environmental disaster. Brittle fracture may also lead to a sudden loss of the marine structure.

2.2 *Preliminary Design*

At the preliminary design stage, the objective of the shipyard is to make a quotation. At this stage the issue is not to assess exhaustively the fatigue strength of the structure, as the details have not been designed at this stage, but to assess that the global scantling is sufficient, and that the yard can safely evaluate the structure building cost, before the order and in the next step the planned material. Generally only the global hull girder fatigue strength is assessed at this stage, but the relevant primary structure may also be assessed.

2.3 *Detailed Design*

At the detailed design stage, the structural area with high concentration factors and submitted to significant load ranges is assessed versus fatigue strength. Depending on the case, when local structures do not comply with fatigue strength requirements, the local design is modified. In principle, if the assessment at the preliminary stage has been correctly carried out, target fatigue strength can easily be reached by improving the local design details. Ship and marine structures are very complex and the number of details with significant stress concentration factors is very large and therefore the fatigue assessment of all details is not realistic. Shortlisting the locations where fatigue assessment is to be carried out is one of the most critical tasks in marine structure fatigue assessment.

2.4 Fabrication

Fabrication will never carry out exactly what design has planned. There are misalignments, welding defects, but also sometimes thicker sections used due to supply issues. Tolerance criteria and effects due to workmanship are not always explicitly defined in the rules. In this regard, Jonsson et al. (2013) has analysed the parameters relevant for fatigue among the parameters considered by inspection standards.

2.5 In-service Maintenance

Fatigue damage, on actual marine structures can neither be detected nor measured during initiation, but during crack propagation the size of the flaw should be sufficient to be detected by non-destructive techniques. The efficiency of maintenance depends on inspection efficiency and inspection planning allied to inspection reliability.

2.5.1 Inspection techniques

Due to the complexity of marine structures, exhaustive close inspections are not always possible everywhere.

Inspection techniques are chosen according to the cost, including delivery time constraints, and efficiency/reliability. At the design stage, inspection areas are defined according to the probability of failure and consequences of that failure. Efficiency in terms of ability of crack detection is strongly dependent on the chosen Non Destructive Examination (NDE) approach. Cost of inspection is also to be considered as resources are limited; cost includes not only the cost of the inspection itself, but the time of surveyors, inspection devices and work required to make the structure accessible, e.g. for passenger ships or navy ships, as well as the cost due to the unavailability of the ship or marine structure during the inspection.

2.5.2 Inspection planning

From the above information at the design stage, it is necessary to assess that, according to the planned inspection programme, a possible crack can be discovered and repaired before the occurrence of an unacceptable event. It is, for example the case for LNG carriers with their constant monitoring of potential gas leakage, where the designer has to demonstrate that no tank collapse will occur before a harbour has been reached.

2.6 Fatigue strength

Fatigue strength may be either evaluated in terms of ability to resist damage accumulation or the ability to resist crack propagation up to a maximum allowable crack size. Damage accumulation has no clear physical meaning, but is very easy to apply, while crack propagation corresponds to a physical phenomenon in principle well defined, but difficult to apply except for time history loading. In terms of design, the most suitable model may differ from the physical phenomenon as the easiest model will be used as long as the resulting failure prediction does not differ too much from the test results.

2.6.1 S-N curves related to expected workmanship

The S-N curve models using a Miner damage accumulation approach, corresponds predominantly to an initiation model. This model is easily applied to simple details and reflects the welding quality effects using the most applicable S-N curve for the welding process used, including when relevant, the post welding process. The results are less convincing for complex details and design rules provide correction factors, e.g. they propose a weighted combination of membrane and bending loads to fit test results.

2.6.2 Crack propagation parameters

Crack propagation is, up to now, the only approach that allows estimating the residual life when a crack has been discovered. Unfortunately more often than not, the residual life corresponding to a detectable crack is too low to be economically acceptable as a design life. Alternative approaches have been proposed defining an empirical initial crack size. Most of the life corresponds to propagation in short crack conditions that are very complex to model and current approaches do not take into account this complexity, meaning that this initial crack size determination is questionable as it is generally recalculated retrospectively from S-N data. Final fatigue life estimation can be very sensitive to the accuracy of the initial crack size.

2.7 *Fracture Strength*

Fracture strength is not up until now assessed for marine structures as material specifications are generally supposed to fulfil the assessment of fracture strength. Due to the increase of high tensile steel plate thickness in the largest container ships, fracture strength has become more and more critical. Measures are required to stop any possible sudden crack propagation, either by careful structural arrangement or by checking a material's ability to arrest crack propagation.

2.8 *Fatigue Loads*

Fatigue loads are highly complex and in order to simplify design rules, those that contribute the most are considered neglecting the others. Wave loads are currently considered on all marine structures, whereas other loadings may be considered, e.g. loading/unloading loads may in some cases have a significant contribution.

2.8.1 *Wave loads*

Knowing the future actual route, the corresponding climatology, speed and sea-state distribution, relative heading and encountering frequency can be deduced and then global and local loads applied to the marine structure. At the design stage, generally the ship route is unknown except for specific ships such as fast ferries with a dedicated area and the design climatology is necessarily arbitrary. For offshore structures the site of operation is known and is an essential part of the design.

2.8.1.1 *Definition of a fatigue load Standard*

Taking into account the difficulty in anticipating the actual load applied to a ship's structure, the rules aim to define a standard load condition as a reference for checking fatigue strength.

2.8.1.1.1 *Worst case e.g. North Atlantic*

The first possible approach is to select a conservative navigation area. Generally IACS Recommendation 34 is the base of scantling for yielding ultimate strength and fatigue. The assumption for speed, e.g. 0.66 of maximum speed, remains questionable and should be considered case by case with attention to the type of ship, which includes the propulsive power of the ship, mission profile, actual service at sea, and likelihood of vibration (springing or slamming).

2.8.1.1.2 *Specific worldwide, or local sea-state model*

Loads resulting from the above approach generally provide very conservative results and do not cater for existing ships that have not experienced fatigue issues. An alternative scatter diagram has been proposed with a less severe wave height; the so-called "Worldwide scatter diagram". Ferry ships, particularly fast ferry ships, may be dedicated to a single route or a single route with a limited navigation, conditional on the sea-state. Offshore structures are generally designed for a given site and a specific climatology analysis is carried out.

2.8.1.1.3 *Storms approach*

When crack propagation is used with random loading it results in fatigue life prediction being dependent on the order of cycles. It has been shown that organising the sequence of cycles in terms of storm and not in terms of short-term does not change the mean value of fatigue life but increases significantly the variance of fatigue life and consequently requires a larger safety margin.

2.8.2 *Loading unloading*

For a marine structure operating in a protected area and with frequent loading/unloading (e.g. FSO (floating storage and offloading vessel) or Dredger), fatigue may be slightly influenced by the "static" load variation or this "static" load may be the major source of fatigue.

2.8.3 *Vibrations*

The vibration effect due to slamming or springing is not commonly assessed, but for large ships such as the recent largest container carriers or high speed craft, the vibration effect will have a significant effect mainly due to its interaction with quasi-static loading.

2.9 *Environmental effects*

References or base-line fatigue testing is carried out to establish S-N curves in dry air and in seawater environments.

2.9.1 *In air*

The reference curve has been established in air and in principle, corresponding to a probability of failure less than 2.5%. There is a change of slope conservatively assumed to correspond to 10^7 cycles. The change of slope takes into account both the fatigue limit and the weakening due to damage of higher number of cycles associated with random loading. It is generally assumed that fatigue in air is not significantly influenced by loading frequency for specimens corresponding to typical details, the issue being more in the control of loading.

2.9.2 *Seawater*

The actual phenomenon of fatigue strength weakening due to corrosion is not fully understood. It is not easy to carry out representative testing of fatigue under corrosion as fatigue strength is very dependent on test duration. Design rules have introduced empirical factors to ensure the design is conservative. As an example, the IACS harmonized Common Structural Rules have chosen to modify the slope of the S-N curve, keeping a single slope, disregarding the fatigue limit and dividing the lifetime by two for the higher stress level. For offshore structure the factors are different.

2.9.3 *Other aggressive environments*

Sea water is not the most aggressive environment for metallic structures. Particularly for offshore structures, oil with the hydrogen sulphide effects should also be considered. There is no general corrective factor; it depends either on the corrosive element, the type of detail or material. Tests are to be carried out and results treated with a suitable methodology, with respect e.g. to the test duration versus the structure exposed time etc. It is generally difficult to define the slope of the S-N curve in such an aggressive environment due to the sensitivity of the results to the test duration.

2.9.4 *Coating and coating life*

Coating is a way to protect the structure against corrosion. As long as the coating protection is efficient it can be assumed that the fatigue strength corresponds to the fatigue strength in air; when the coating fails, it is no longer efficient, then the fatigue strength is reduced and close to the fatigue strength in a corrosive environment. Although some requirements are undertaken to improve coating life, the link between coating life and assumptions of coating protection in the structural fatigue strength assessment remains not fully understood. Moreover, attention should be paid to the link between improvement techniques and coating protection as improvements become ineffective when the coating fails. According to the operating conditions, it may be unrealistic to consider that an effective coating protection can be maintained. For example in bulk carrier ship holds, due to the loading/unloading process, it is unrealistic to maintain coating where ore is abrasive or scrapers are used to assist discharge.

2.10 *Fatigue, Fracture & Failure Criteria*

Fatigue is a progressive weakening process and acceptance criteria are neither obvious nor generic.

2.10.1 *Failure definition*

Fatigue criteria depends both on consequences of failure and on the accepted risk of failure. In the offshore industry three different level of failure are defined: N1 where the stress range is measured by a strain gauge decrease of 10% and considered as corresponding roughly to initiation; N2 corresponding to a through thickness crack; and N3 corresponding to the end of the test due to too large displacements. For simple design details there are small differences in life between these fatigue failure definitions, on the other hand for complex details, N1 N2 and N3 may result in very different lives.

2.10.2 *Uncertainties*

For a given detail, i.e. welded or cut detail, for many reasons there is generally a large scatter in the S-N curves. Most of the sources of uncertainty cannot be controlled either during design or the fabrication process. Probability models related to these uncertainties have been widely discussed. From a practical point of view actual fatigue strength under constant amplitude range is considered as a random parameter. A common approach is that the uncertainty of the fatigue life follows a lognormal law but alternative approaches exist, e.g. the Bastenaire approach where the uncertainty depends on the parameter of the S-N curve. In addition to this uncertainty for constant stress range fatigue strength, there is also an uncertainty for variable stress ranges as applied using the damage accumulation law, i.e. Miner law. Crack growth retardation after overload is one of the phenomena contributing to this model uncertainty.

2.10.3 *Safety Factors*

To take into account the uncertainty in the design rules, safety factors are used. Safety factors may be explicit by requiring that the total fatigue damage be less than 0.5 or even 0.1. They can also be implicit defining a navigation condition as the worst possible condition or defining the design S-N curve as an S-N curve with a probability less than that of a given proportion of the specimen of a sample which has a fatigue life lower than the design curve. There needs to be a rational approach to define this safety factor in order to adapt these factors to new materials or new fabrication processes. Probabilistic methods have been developed to optimize this safety factor. For that reason, the consequences of fatigue failure are to be evaluated, and an acceptable probability of failure clarified. Then a set of partial safety factors may be defined to be applied in respect of design equations in order to reach the target safety level and to obtain a failure probability that is as stable as possible versus the different possible designs.

3. FACTORS INFLUENCING FATIGUE/FRACTURE

A large number of factors influence the fatigue life of component or structure as discussed in the previous section. In the following subsections a comprehensive literature review of the main factors are critiqued under the headings:

- “Resistance” which address thickness and size effects, environmental impact, temperature effect and residual end mean stresses;
- “Material” which address fatigue and fracture improvement through microstructure and surface treatments;
- “Loading” which address different types of fatigue loading such as stochastic loading and multiaxial stresses;
- “Structural Integrity” which address fabrication, inspection, repair and different monitoring techniques.

3.1 *Resistance*

3.1.1 *Thickness and size*

Fatigue design methods for very thin deck plates, down to 3mm, have recently received considerable interest due to increasing demands for energy efficiency and requirements for a more efficient use of natural resources. The production of these panels is nowadays possible due to low-heat-input welding techniques such as laser-; laser-hybrid (Fricke et al., 2013b) and friction stir welding (Azevedo et al., 2014). Many classification societies consider the 5mm thickness as a threshold below which special attention should be paid to the manufacturing and welding methods. Especially, the permissible tolerances for axial and angular misalignment should not be exceeded. Recently considerable efforts have been made to investigate the fatigue resistance of thin-welded deck structures based on nominal, structural and notch stress methods; see for example the PhD theses of Molter (2013), Lillemäe (2014) and Köder (2015). Eggert et al. (2012) performed fatigue tests and their analysis on deck panels with thickness of 4mm and concluded that in panels with these thicknesses the photogrammetric technique to obtain the distortion shapes is important when the response is to be analysed, for example with non-linear FE-analyses. Panel tests are quite expensive, especially if the development and optimization of the welding techniques are to be carried out. Therefore, Fricke and Feltz (2013) and (Lillemäe et al., 2012; Lillemäe et al., 2013) have been discussing the simplification of the testing to simple tensile specimens. It is clear that the highly deformed panels are affected by the redistribution of stresses within the panels, as large deflection plate theory would predict. This means that the test results on small-scale specimens e.g. see the excellent review by Fricke et al. (2013a), are not directly transferrable to the design, but this redistribution of stresses needs to be accounted for. (Lillemäe et al., 2014a, b) showed how this redistribution happens from dog-bone specimens to panels and further to passenger ship hull girders. Based on this research it seems that on the large ships where the thin decks are typically located on moderately loaded decks, linear hull-girder analysis with undeformed decks is sufficient. However, as we move towards panel analysis the influence of initial deformations become more important and these should be modelled. Geometrical non-linearity must also be considered as we analyse the small-scale specimens. When this is done, it has been shown by Fricke et al. (2013a) that the nominal and structural stress approaches can be used to predict the fatigue strength of the butt and cruciform joints, even with very low plate thickness. It has been noted that the scatter, especially in the nominal stress approach, is larger than in thicker plates; utilization of the structural stress approach improves the situation. Köder (2015) conducted fatigue tests of 5 mm thickness butt-welded specimens as well as fillet-welded floating frame joints with 3.5mm plate thickness. A laser scanner was used to measure the actual shape of the weld seams. It was found that the fatigue strength of the fillet-welded floating frame joints is mainly influenced by the toe radius, undercut

depth and throat angle. Further research is needed on large-scale structures where the welding process of secondary (web-frames, girders) and even primary structures (bulkheads) induces initial deformations to the panels. In addition, the permitted deformation limits within standards need further investigation.

The thickness effect has been investigated already, decades ago, and is still considered in design standards with the simplified formula $f(t) = (t_{ref}/t)^n$. Where t is the relevant plate thickness, t_{ref} is a reference thickness, usually 22 or 25 mm, and n is an empirical exponent. Different exponents should be considered for different details/cases according to the current recommendations, such as those from the International Institute of Welding, Hobbacher (2009). This factor reduced the used FAT-class for larger thicknesses, e.g. down to 70% for a cruciform joint with 80 mm thickness. However, research demand still exists in respect of the mechanism on the thickness effect and the influence for different structural details.

Doerk et al. (2012) compared fatigue tests for butt weld and longitudinal stiffener specimens with thicknesses from 25 to 75 mm under axial load. For the butt welds a clear thickness influence could be observed. The resulting thickness exponent of $n = 0.21$ complies well with the value given by Hobbacher (2009). For the longitudinal stiffener specimens, where regardless of the main plate thickness a small stiffener with $t = 15$ mm and 200 mm length was always attached, no distinct thickness influence could be detected.

Yamamoto et al. (2012) investigated, using experiments, cruciform joints for various thicknesses from 12 to 80 mm under axial load. As a result, it was found that no thickness effect was observed in the case that the thickness of the attached plate is constant irrespective of the thickness of the main plate. On the other hand, in the case that the thickness of the attached plate increases in proportion to the thickness of the main plate, a thickness effect of the exponent of 0.27 was estimated. Furthermore it was confirmed that the thickness effect on fatigue strength is dominated by the stress concentration and stress gradient at the weld toe which would change according to the form of the joint.

3.1.2 Environment (corrosion)

As recently assessed by Lieser and Xu (2010), the annual worldwide cost of maintenance due to corrosion, repair and replacement is around 3%–4% of GDP of an industrialized country. This fact justifies the continued effort undertaken by the scientific community to understand this damaging phenomenon which, if not detected in time, could lead to a catastrophic failure of a component or structure. Corrosion is well known to reduce the fatigue life of structures. In recent years there has been an increasing interest in using high-resolution microscopic techniques for observing the behaviour of the material during fatigue tests. Li et al. (2012b) used a scanning electron microscope (SEM) to capture the formation of a fatigue crack as a result of the coalescence of individual discontinuities (Figure 1) and the surface exfoliation of a sample affected by pitting corrosion (Figure 2) in Aluminium. They concluded that the corrosion's pit is not only responsible for promoting the nucleation of fatigue cracks, but also for influencing the crack propagation path, together with pre-existing flaws, grain size and pits distribution.



Figure 1. Fatigue crack path resulting from the coalescence of three individual discontinuities: a notch (A), a corrosion pit (B) and a grain boundary (C).

As it is possible to see in Figure 2, the images obtained from SEM allow appreciating the growth in size of the corrosion pits and their coalescence, resulting in the formation of a much larger void. Li et al. (2012b) were also able to derive an empirical formulation for 6151-T6 aluminium alloy, which relates the average pit depth (\bar{D}) with the equivalent corrosion time (T_{eq}):

$$\bar{D} = 0.95 + 15.08 \cdot T_{eq} \quad (1)$$

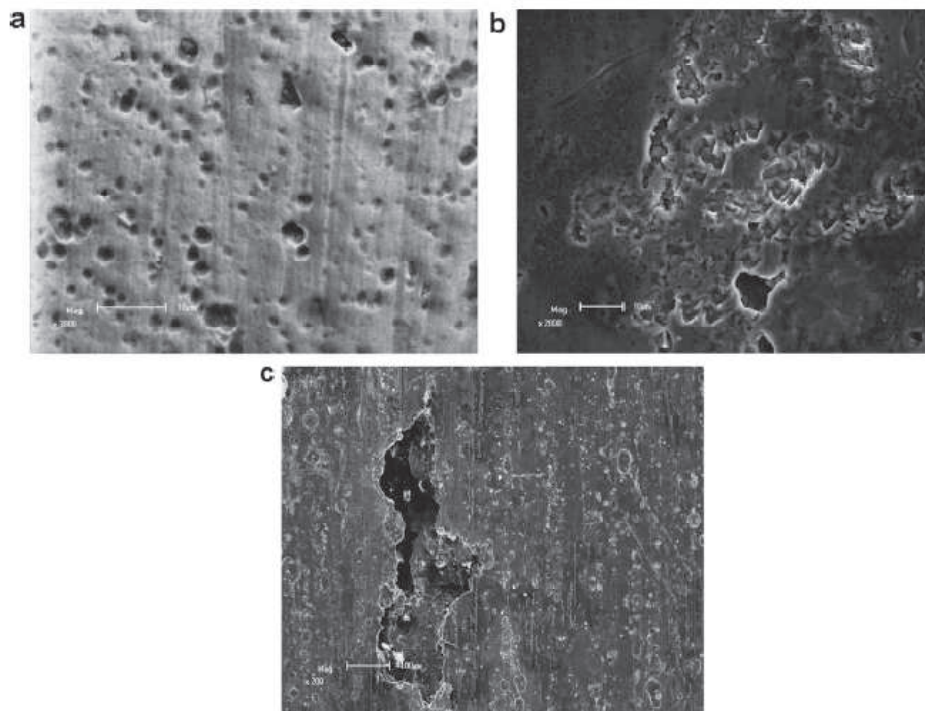


Figure 2. Time evolution of pitting corrosion: (a) 7 equivalent corrosion years, (b) 15 equivalent corrosion years, and (c) 19 equivalent corrosion years.

As shown in the study of Lee et al. (2013), high-resolution digital images of specimens during fatigue tests can be transformed into binary images, using an image segmentation method called “Binarization”. Apart from the advantage of having images of a smaller size, the most important advantage is the possibility of evaluating quite accurately the morphology of the corrosive phenomenon. In addition the authors showed that the data could be used to create a 3D model of the specimen, which was modelled; von Mises stresses were successfully extracted and predicted the onset of the crack observed in the specimen.

Problems become even more complex when considering structures such as oil & gas pipelines. It is known that the corrosion rate of welded joints (WJ) is higher than for the base metal (BM). Moreover, according to Slobodyan et al. (2009), electrochemical differences are expected between the heat-affected zone (HAZ) and BM and lower mechanical properties are expected in the fusion zone (FZ) with respect to the rest of the joint. These non-homogeneities are responsible for different corrosion rates. The current approach to designing these structures is based on laboratory testing, engineering evaluations and safety factors. To further complicate the matter, oil & gas pipelines are exposed to the fluids they transport. According to Andreikiv and Hembara (2013), the hydrogen absorbed by the metal can double the corrosion rate and they proposed a method to quantitatively evaluate the influence of hydrogenation on soil corrosion rates of oil & gas pipelines.

Sahu et al. (2013) studied the effect of type I hot corrosion on the low-cycle fatigue life of a nickel base super-alloy used in marine and offshore gas turbine engines. The phenomenon is caused by the high operating temperatures and the exposure of the material to saline atmosphere, leading to the deposition of a mix of fused salts. They used SEM to show the typical morphology of the phenomenon (Figure 3):

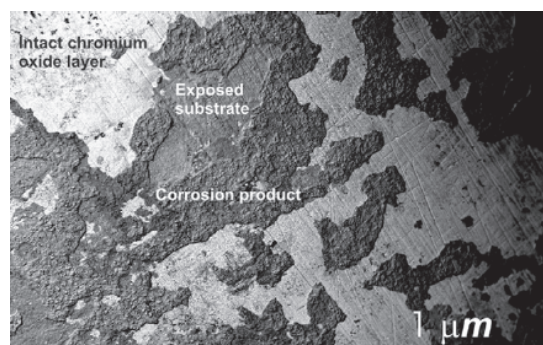


Figure 3. Typical morphology of type I hot corrosion: intact chromium oxide layer, exposed substrate and corrosion product, (Sahu et al., 2013).

They concluded that the reduced low-cycle fatigue life induced by type I hot corrosion is due to the oxidation of grain boundaries (Figure 4):

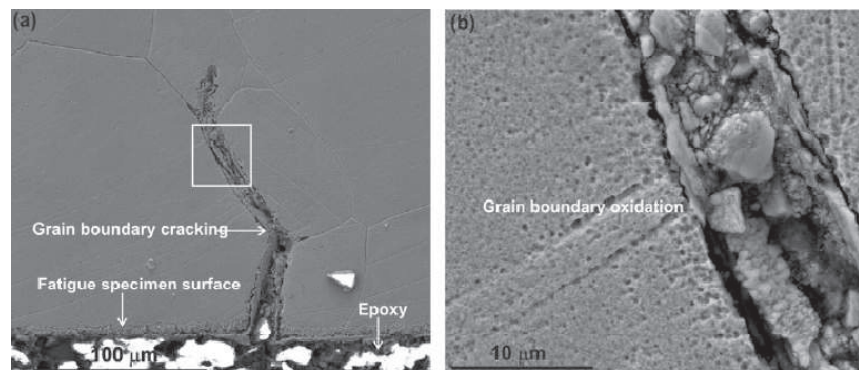


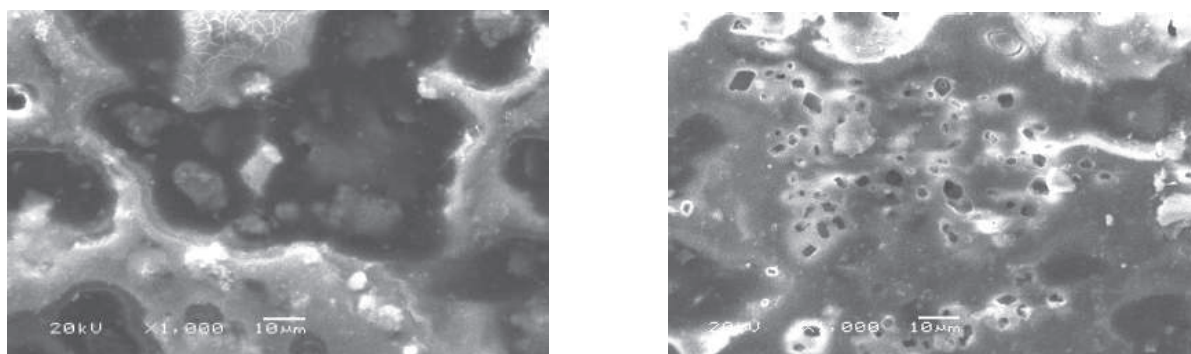
Figure 4. Grain boundaries oxidation due to type I hot corrosion, (Sahu et al., 2013).

According to Magdziarz et al. (2013), type I hot corrosion consists of two stages: (1) incubation period with low corrosion rate and formation of the protective oxide layer and (2) accelerated corrosion attack leading to the rupture of the protective oxide layer, consequent exposure of the substrate and formation of corrosion products (Figure 4).

Corrosion has a critical influence on the ship structure because ballast tanks are fitted along the mid-ship. Once the mid-structure is significantly corroded, it can cause a catastrophic failure as a result of the large bending moment applied by dynamic sea loads. De Baere et al. (2013) indicated that the ship's ballast tanks are usually coated with epoxy and backed up by sacrificial zinc anodes in order to decrease the effect of corrosion; however, this construction method has not been altered for many years. They proposed that durable coating, combined with lifetime lasting aluminium anodes, can improve the ballast tank concept. It was concluded that corrosion resistant steel also becomes attractive when the steel price becomes competitive.

The microbiological corrosion behaviour of ship plate was studied by Li et al. (2012b) who proposed that LaCl_3 -Zn epoxy coating offers better protection, since the resistance of LaCl_3 -Zn coating is much better than Zn-epoxy alone. In this study, the images obtained, by using a scanning electron microscope, from Zn-epoxy and LaCl_3 -Zn-epoxy coated specimens after 30 days' exposure in sulphate-reducing bacteria solution, are shown in Figure 5 (a) and (b) respectively. From Figure 5 (b), it can be seen that the continuity of the organic rosin of LaCl_3 -Zn-epoxy coating is much better than that of the Zn-epoxy coating presented in Figure 5 (a), and hence the structure was more successfully preserved by using the LaCl_3 -Zn-epoxy coating.

There are two main limitations to the empirical analyses presented so far: (1) corrosion tests take a long time to be executed and (2) the results of the analyses can be considered relative only to the particular tested material and conditions. The first limitation is overcome by using accelerated corrosion tests, whilst the second limitation, as well as the first, may be overcome thanks to numerical models able to predict the material's degradation caused by the particular corrosive phenomenon.



(a) Zn-epoxy coating

(b) LaCl_3 -Zn-epoxy coating

Figure 5. SEM of specimen after 30 days' exposure in SRB solution (Li et al., 2012b).

3.1.3 Temperature

It is well known that temperature is one of the most influential environmental parameters that affect the behaviour of materials. Certain damaging phenomena occur or become significant only when the temperature is higher than a certain critical value (e.g. creep) or when the temperature is low enough (e.g. embrittlement of the material).

According to the literature, generally the low-cycle fatigue resistance and even more generally, the mechanical properties of metals, decrease at high temperatures due to phenomena such as creep, thermal fatigue and oxidation. However, this is not always the case: the study conducted by Zhang et al. (2012b) reported a material with higher low-cycle fatigue resistance at high temperatures. Their study was about the assessment of the effect of temperature on the low-cycle fatigue resistance of a particular type of aluminium alloy used for components in internal combustion engines. As shown in Figure 6, the material presents higher low-cycle fatigue resistance at high temperatures for large total strain amplitudes:

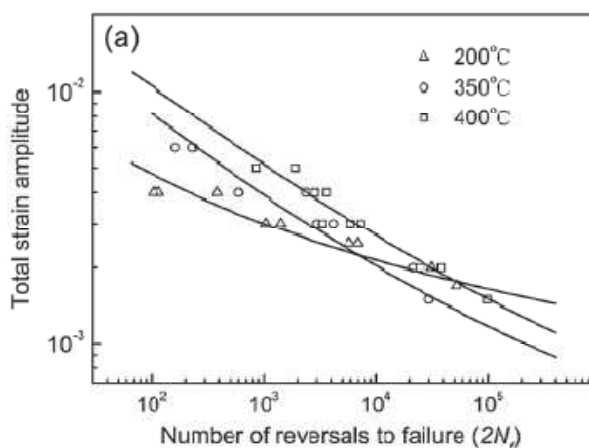


Figure 6. Total strain – fatigue life at 200°C, 350°C and 400°C (Zhang et al., 2012b).

The SEM analysis of the fracture surface of samples tested at high temperature and large strain amplitudes showed the presence of tear ridges, which are considered to impact positively on the low-cycle fatigue resistance of the material by lowering the local stresses and slowing down the crack propagation. Yu et al. (2010) studied the high temperature creep and low-cycle fatigue resistance of a nickel super-alloy and reported a similar behaviour.

Steam generators are another application where the material is required to operate at high temperatures. For this reason, Choudhary et al. (2013) studied the deformation and fracture behaviour of a particular type of ferritic steel used in steam generators under tensile loading. They reported SEM fractographs showing the morphology of the fracture surface at different tested temperatures (Figure 7):

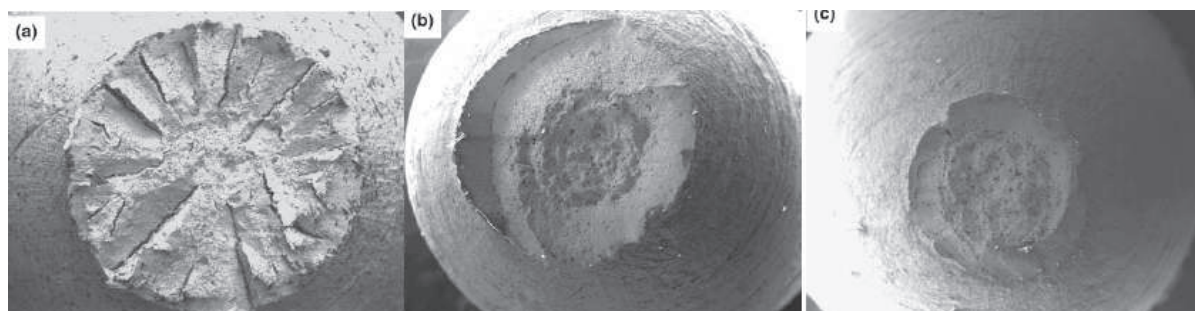


Figure 7. SEM fractographs: (a) 27°C, (b) 300°C and (c) 600°C.

According to Figure 6, the necking of the fracture surface occurs only when the temperature is high enough.

The Arctic presents a challenging environment both to humans and structures operating in the harsh environment. Today's design codes and rules provide limited information and guidance on the quantified requirements for steels and weldments at lower temperatures. NORSOK standards are only applicable down to -14°C and ISO 19906 Arctic Offshore Structure is not very specific when it comes to laying down materials guidelines. The standard only states that material shall have adequate

toughness in order to be ductile at low temperatures, fatigue shall be given particular attention at cold temperatures and in particular the validity of S-N curves with respect to low temperature applications need attention. Hence for lower temperatures, it is up to the designer to show fit for purpose of the selected material and some guidance can be found in (Hauge and Østby, 2013; Horn et al., 2012b; Østby et al., 2013b).

Literature discussion on fatigue testing at low temperature is scarce; especially limited data are reported on the fatigue behaviour of weldments. Low temperatures can have both a positive and negative effect on fatigue resistance, depending on the specific load conditions. Evaluations of fatigue take into account both the toughness and strength of the material. Alvaro et al. (2014) carried out a literature study and recommended that S-N curves and fatigue threshold variation with temperature and weldments should be studied further.

Crack growth testing was performed by Walters (2014) on base material grade S980 and S440 at room temperature and -70°C ; he concluded that fatigue properties decrease with lower temperature until the Fatigue Ductile-Brittle Transition, while below this level the fatigue increases again due to brittle material. A recommended minimum toughness limit was set at T_{27} where a fatigue ductile to brittle transition occurs below this value. The same recommendation is being discussed for being implemented by the new ISO TC67 SC8 Arctic Operations Working Group on Arctic Materials.

The steel industry is currently improving their steel material in order to meet cold climate requirements. Ichimiya et al. (2014) tested offshore grade steel YP420 achieving a CTOD >0.3 at -40°C . Akselsen and Østby (2014) investigated different welding wires for structural steels under arctic conditions and found that toughness tests showed a wide scatter, and coarse grained (CGHAZ) and the intercritically coarse grained HAZ (ICCGHAZ) appeared to have low fracture toughness in the range of CTOD values of 0.05 to 0.15.

Also, the ship industry needs steel grades with low temperature toughness; Nakashima et al. (2014)'s work on YP390MPa steel shows J far above the requirement of 39 J toughness at -40°C for large heat input welding. Choung et al. (2014) investigated crashworthiness of a high strength steel grade FH32 for arctic marine structures against ice impact. From their work consisting of both analytical and material testing, they concluded that since the material strength properties increase (both the yield and tensile strength) at lower temperatures, the effect of lower temperatures was beneficial and the impact provided less deformation compared to a possible impact at room temperature.

For transportation and storage of LNG, such as the cargo tanks of LNG carriers, temperatures as low as -196°C are common and in order to ensure the material is tough, nickel is used; the most common grade is 9% nickel. Kim et al. (2014) investigated the use of 7% nickel TMCP steel and found that the fatigue limits for base metal, butt weld, and fillet weld increase by more than 30%, 33% and 15%, respectively, as temperature decreases from room to cryogenic temperatures (20°C to -163°C). The crack growth results were also compared with 9% nickel material and found to behave similarly.

3.1.4 *Residual Stress & Constraint, mean stress*

Due to high residual tensile stresses, the fatigue strength of WJs is often considered as independent of the mean stress, Hobbacher (2009). On the other hand, theoretical considerations concerning stable crack growth indicate a positive effect of mean compressive stresses on the fatigue life. These positive expectations of the influence of compressive mean stresses are supported by operational experiences with ships, e.g. full container vessels and open multipurpose vessels, exhibiting in still waters a pronounced hogging bending moment. On such so-called "hogging" ships, fatigue cracks were found within the deck area, which is loaded in the still water by tensile stress, but hardly at all in the compressively loaded bottom area. Thus an increased effective material utilization exists and a more economical design for structures which are continuously loaded by compressive mean stresses. The effect of the mean stress on fatigue life can be interpreted for cracks which propagate under axial load (Mode I) as follows: The crack undergoes partial closure during the loading cycle and the stress intensity at the crack tip is reduced due to load carrying via contacting crack surfaces. Thus the effective stress intensity factor is regarded as being proportional to the crack opening part during a load cycle. The effective portion of the stress intensity factor, designated as effectiveness factor U , is often defined only as a function of the stress ratio R . However, it is actually affected by further parameters such as residual stresses, external load, structural configuration and crack geometry. Therefore, a general quantification of the mean stress effect is much more difficult.

Yuen et al. (2013) reported a lack of commonality between different approaches to fatigue analysis and design codes and standards when dealing with mean stress. Therefore, the objectives of their work were to validate the models adopted in the various approaches, to seek to harmonize these approaches across the

codes and to develop an appropriate methodology for assessing the effects of mean stress. These objectives were accomplished through a review of the available data on the effects of mean stress on fatigue strength and they analysed the available fatigue data in order to develop an appropriate methodology for the assessment of the mean stress effects in fatigue analysis for marine applications. Together with Polezhayeva et al. (2013), they recommended using improvement factors on a fatigue strength of 1.2 for steel if the applied stress is fully compressive and linear interpolation between 1 and 1.2 if the applied stress range is between alternating or fully compressive. This applies to the loading patterns where the mean stress level is not changing. Furthermore, Polezhayeva reported that residual stress relaxation due to the applied tensile fatigue or static loading is beneficial if the subsequent fatigue loading produces stress ranges that are partly or fully compressive.

3.2 *Materials*

3.2.1 *Metallic Alloys*

Although propeller design is mainly based on assumed quasi-static hydrodynamic loads (thrust, torque and centrifugal load), propellers are subjected instead to cyclical stresses because of the non-uniform flow behind the ships' hull and because of the inclined flow due to shaft axis inclination. Indeed, fatigue failure becomes a concern for high performance propellers, as propeller blades for common merchant ships are relatively thick.

In fact, acting stresses are generally below the fatigue limit of the material. However, in the case of fast ships and/or specific performance requirements (e.g. low radiated pressure and noise), blades become rather thin and show high values of skew and rake. Moreover, detailed fatigue strength assessment procedures would be beneficial to reduce the relatively high safety coefficients currently considered in rules and guidelines, overcoming rather "old-fashioned" approaches.

Bertoglio et al., (2014); Bertoglio et al., (2015) analysed a high performance propeller blade and proposed a procedure for the evaluation in time of the stress field acting on a blade during one revolution, which is then considered for fatigue assessment. Comparing different computation approaches, assumption and approximations were highlighted both as far as the loading conditions and the fatigue strength is concerned.

3.2.2 *Fatigue & fracture improvements through material changes, surface treatment*

As discussed under section 3.1.3, low temperature affects the material properties and research is being carried out in order to build more robust materials to prevent brittle fracture. One challenging issue for the pipeline industry is the possibility of local brittle zones in longitudinal and girth welds, especially for low temperature pipelines or pipelines subjected to high strain from reeling or environmental loading; these local brittle areas are of particular concern. Moore and Nicholas (2013) investigated this effect on X70 grade pipe with a service temperature of -40°C . HAZ toughness properties were measured and they recommended that modifications were made to the steel making process to reduce the number of large and elongated inclusions in the steel, and to ensure they were well distributed throughout the steel in order to obtain adequate toughness in the HAZ. Tronskar and Andresen (2013) investigated the effect of reeling and the study recommended that welding procedure qualification should involve CTOD in order to demonstrate adequate toughness in the weld zone. They also found that it was beneficial to have steel with a relatively low silicon content ($< 0.2\% \text{wt}$) and vanadium as the main micro-alloying element ($V \leq 0.06\% \text{wt}$), with high Si ($> 0.29\% \text{wt}$) and niobium content at $0.029\% \text{wt}$ or greater, in order for the material to be susceptible to formation of LBZs. To prevent/limit the possibility of a brittle crack to initiate, or to prevent crack propagation in large container ships, Murakami et al. (2013) developed YP460 Class steel plate (EH47 grade) with excellent brittle crack arrestability.

In order to investigate microscopic fractures in 420 MPa steel, acoustic emission (AE) was performed by Østby et al. (2013a). Based on this testing technique they could document the local arrest of propagating microcracks in the HAZ, microcrack nucleation rate and the cumulative distribution of arrested microcrack sizes, which are data of interest, in order to gain an understanding of micromechanical brittle fracture models. A numerical model for dynamic crack propagation and arrest in steel plates based on the local fracture stress criterion was developed by Aihara et al. (2014). Their model was compared with test data and showed good alignment with the physical tests.

The makers of steel and weld consumables are developing steels and weld metal in order to meet the demands for pipelines operating in more challenging environments such as e.g. ultra deep water, sour service, low temperature or high strains from e.g. reeling, earthquakes, soil movements etc.

Harksen et al. (2013) investigated X-65 line pipe steel in the as-rolled condition (AR), quenched condition (Q), and quenched & tempered condition (QT), in order to gain an understanding of the mechanical material characteristics during the different processes. Nash (2013) presented the qualifications of Line-Pipe for the Middle East to India Deepwater Pipeline project, with a water depth of 3500 m. The effect of heat treatment on the hydrogen diffusion of process pipe steel was investigated by Han et al. (2013) who found that post weld heat treatment degraded the pipe steel ability to resist hydrogen diffusion when the micro structure had acicular ferrite compared to non-heat treated steel, this finding is opposite to other microstructures such as ferrite/pearlite or bainite structures.

3.3 Loading

3.3.1 Stochastic Loading (load interaction effects (sequence))

The traditional approach to fatigue damage under varying loading is still widely used, based on the S-N curve and the assumption of linear cumulative damage (Palmgren-Miner's rule). Accordingly, the total damage is expressed as the accumulated damage from each load cycle at different stress levels, independent of the sequence.

Renaud et al. (2013) shows that the inclusion of flexible modes in the calculation of fatigue damage accounts for a large share of the total fatigue damage by analysing measurements recorded onboard a 9,400 TEU class container vessel. Schaumann et al. (2012) investigated the effect of load sequence on the fatigue performance of welded spatial tubular joints based on uniform material law and concluded it is important to describe the load chronology and the maximum peaks precisely in order to take into account load sequence effect in a practical way. Concerning the complex and randomness of fatigue loads acting on ship side-shell structures, Li et al. (2013b) proposed a direct calculation procedure to compute the local stress of such details using a so-called local stress factor instead of the conventional stress concentration factor. The method was compared with full-scale measurements of a 4400TEU containership for the fatigue assessment of ship side-shell structures with good agreement. Mao et al. (2015) proposed a modified beam theory using coefficients regressed using bending moments computed by a 3D-panel hydrodynamic analysis and nominal stress calculated by the global FEM analysis. It is able to take into account fatigue damage of containerships caused by horizontal bending and warping in a reliable and fast way with similar accuracy as the direct FE analysis.

Fatigue crack propagation behaviour under the superimposed loading history containing whipping response was studied by Matsuda and Gotoh (2013). Consideration of the high frequency component of the loading history leads to overestimating the fatigue damage factor and shows that the traditional fatigue life calculation method based on the S-N curve approach with the rainflow counting is inappropriate under superimposed loading conditions.

Fricke and Paetzold (2012) carried out fatigue tests using simplified stress histories with superimposed stress cycles of different frequencies and showed that most of the fatigue damage is caused by the wave-induced stress cycles enlarged by whipping stresses. They also proposed the simplified fatigue damage assessment of wave induced stress cycles including whipping effects and this method has been adopted by Germanischer Lloyd.

Gotoh et al. (2012) also performed fatigue tests with stress histories containing superimposed stresses and proposed a procedure for extracting an effective loading sequence from random loading. They compared the traditional S-N approach with RPG (re-tensile plastic zone generating) load criteria which provided better results when considering the load sequence effects on fatigue life. Osawa et al. (2013) proposed carrying out the fatigue tests of superimposed stress signals with a new testing machine powered by two exciting motors and showed that a simplified counting based on the enlarged low frequency cycles yielded a good prediction of the fatigue life.

3.3.2 Cycle counting—spectral, time-domain, stress ranges, means stress effect

In order to apply Miner's rule in the assessment of fatigue life, the complex stress time history is divided into blocks of constant stress amplitude (or range). The rainflow counting method is still the most popular technique in the analysis of fatigue data.

Several different assessment methods were assessed by Nielsen et al. (2011) and a comparison made of the measured strains and results from the frequency domain fatigue analysis with those from a time domain analysis based on the rainflow counting method using the Palmgren-Miner rule.

Fukasawa and Mukai (2014) investigated the effects of the hull-girder vibration on the fatigue strength of a Post-Panamax container ship for short-term sea state. They showed that the fatigue damage factor was reasonably evaluated by the rainflow counting method, even in the case where the smaller amplitude

component of the higher frequency vibration (flexible response) superimposed on the larger amplitude component of the low frequency vibration.

Andersen and Jensen (2013) investigated four spectral methods in order to assess whether spectral methods for fatigue damage estimation are applicable in onboard systems for monitoring the fatigue damage of a 9,400 TEU container ship and compared them with the result of rainflow counting. They showed that the agreement between the spectral method and rainflow counting is generally good and the narrow-band approximation seems to yield a fast and fair estimation of the fatigue damage.

Huang (2013) proposed a new method, which is equivalent to Low's method to estimate the fatigue damage of combined high and low frequency load effects and this method also identified the reduced effects of the rainflow counting.

3.3.3 Complex stresses

Ship and offshore structures are often subjected to complex stress fields due to their unique structural configuration and also due to various wave encounters from the sea. However, the fatigue tests conducted in the laboratory have a simple uniaxial stress field. Conversion of the complex stress field into an equivalent uniaxial state is still a challenging task for the researchers working in the area of fatigue. The following literature highlights the complex stress field as an important factor governing the fatigue life.

Yu et al. (2011) carried out strain controlled multiaxial fatigue experiments on extruded magnesium alloy cylindrical specimens. The experiments included fully reversed tension-compression (path a), cyclic torsion (path b), proportional axial torsion (path c), and 90° out-of-phase axial-torsion (path d), as shown in Figure 8.

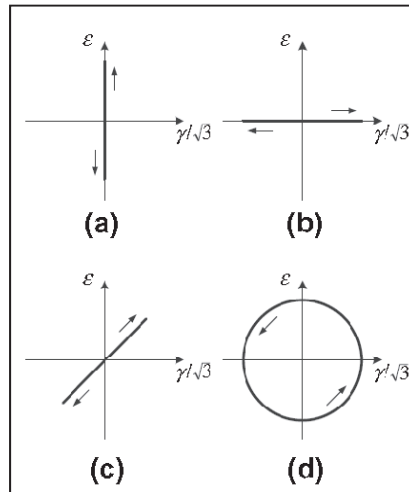


Figure 8. Load paths used in the experiment.

For the same equivalent strain amplitude, fatigue life under proportional loading was higher than in the case of non-proportional loading (Figure 9).

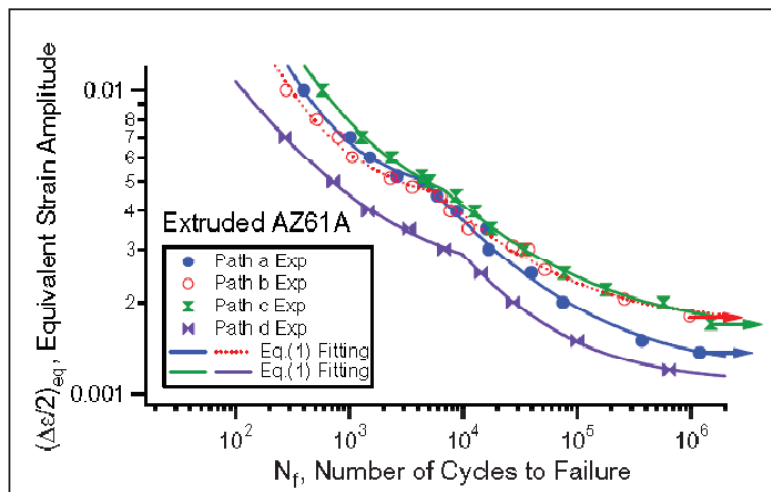


Figure 9. Fatigue lives obtained for various load paths.

It is observed that the Fatemi–Socie criterion predicts the fatigue life well in the low cyclic fatigue regime for all the loading paths investigated, but does not do so for the high cycle fatigue regime. The modified Smith Watson and Topper (SWT) criterion combining the normal and shear components of the stresses and strains on material planes can predict the fatigue lives of the material satisfactorily. Both models (Fatemi–Socie and SWT) fail to predict fatigue life and early cracking behaviour for the loading conditions under cyclic torsion with a high compressive axial stress.

Rozumek and Marciniak (2012) investigated, by the use of experiments, the crack growth in rectangular cross sections subjected to out-of-phase bending and torsion loadings. The tests were conducted in a high cycle fatigue regime for in phase and 90° out-of-phase conditions and it was observed that the fatigue life of the specimen is less when the loadings are applied out-of-phase.

Wu et al. (2012) conducted strain controlled multiaxial low-cycle fatigue experiments on tubular specimens made up of Ti-6Al-4V for both proportional and non-proportional load cases. The strain paths used were push pull (PP), reversed torsion (TP), 90° out-of-phase circular strain path (CP) and 90° out-of-phase elliptical strain path (EP). The number of cycles to failure obtained from the experiments are correlated with the von Mises equivalent strain range and principal strain range (Figure 10). Use of both of these classical methods resulted in scatter of fatigue data which indicates the inaccuracy of the classical methods for predicting fatigue life in non-proportional load cases.

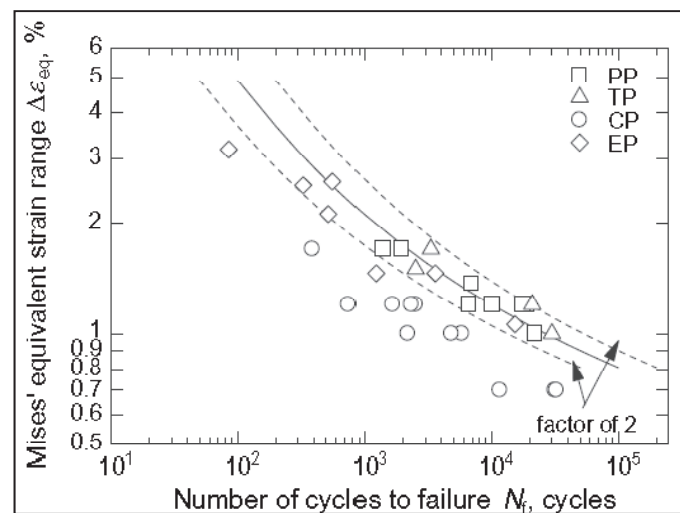


Figure 10. Correlation of number of cycles to failure with the von Mises equivalent strain.

Shamsaei et al. (2010b) investigated the fatigue behaviour of pure titanium and titanium alloy cylindrical specimens under proportional and non-proportional loading conditions. It has been observed that cyclic stress strain data were correlated by von Mises equivalent criterion. This indicates that there is no additional hardening effect observed for this material under non-proportional cyclic loading. However, non-proportional loading resulted in significantly shorter lives and fatigue data could not be correlated by the von Mises criterion which indicates that the non-proportional loading shortens the fatigue life though the non-proportional hardening is not observed. The authors explained that the non-proportional additional hardening is not the only parameter which provides differences in fatigue life in non-proportional cases.

Zhang et al. (2012b) carried out experiments on solid cylindrical aluminium alloy bar specimens to investigate the effect of the stress amplitude ratio (ratio of amplitude of shear stress and normal stress), mean shear stress and phase angle on axial-torsion high cycle fatigue failure of an aluminium alloy under a certain equivalent stress. Macro- and micro-analysis of the specimen fracture appearance were conducted to obtain the fracture characteristics. It was concluded that with increasing stress amplitude ratio, fatigue life reduced gradually under proportional loading and the reduction is more significant under non-proportional loading. This indicated that in tension-torsion fatigue, the effect of the stress amplitude ratio is more severe than for uniaxial fatigue.

Zerres and Vormwald (2013) conducted experiments on thin-walled tubes made of fine grained steel S460N and aluminium alloy AlMg4.5Mn under proportional and non-proportional tension and torsion loading under stress controlled conditions. For both cases, compared to proportional loading conditions the

non-proportional load case provided longer crack growth life compared to the proportional load case (Figure 11).

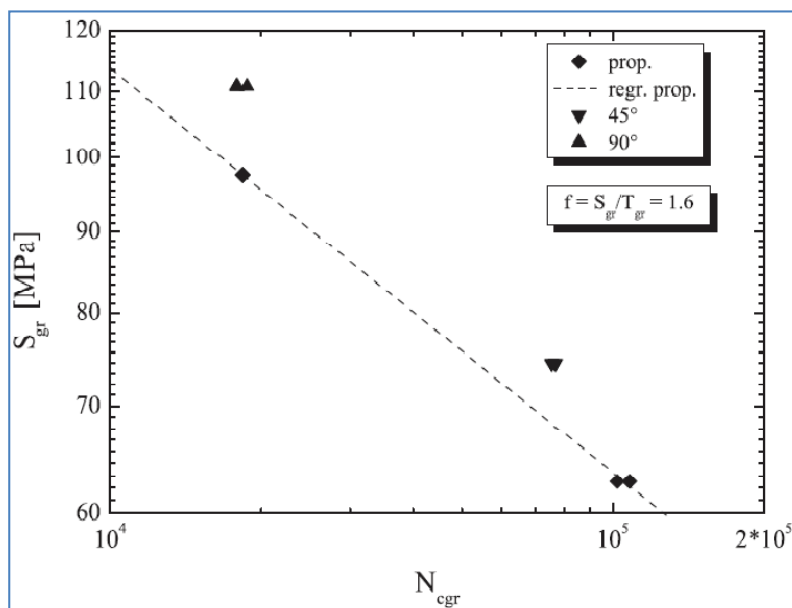


Figure 11. Crack growth lives of steel specimens.

Thévenet et al. (2013) conducted experiments (deformation controlled) on tubular Welded Joints subjected to multiaxial fatigue stresses. The fatigue assessment approaches according to the International Institute of Welding (IIW), Det Norske Veritas (DNV) and American Bureau of Shipping (ABS) were applied for this particular case of tubular joint subjected to multiaxial fluctuating stress. It was observed by the authors that under the loading, the application of these kinds of recommendation does not lead systematically to conservative predictions (Figure 12). Dang van's multiaxial fatigue criterion has been recommended by the authors as a suitable alternative. The authors also highlighted that the approaches mentioned above do not mention the critical point to be assessed when a combination of different load components occurs.

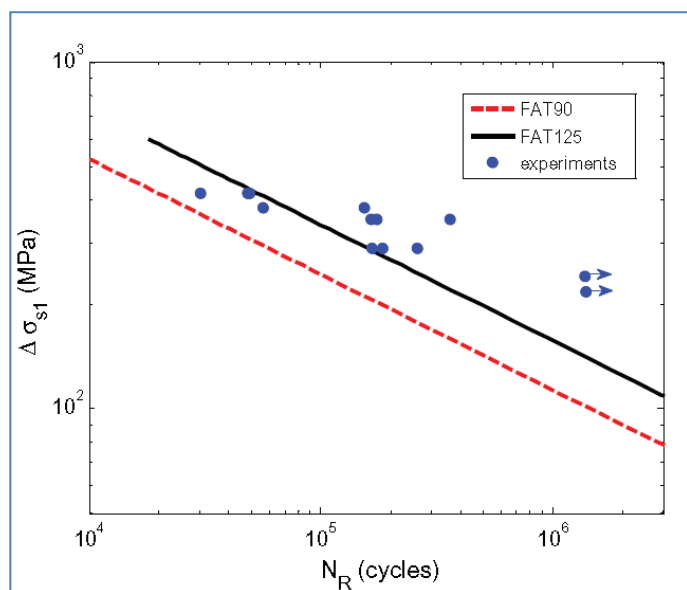


Figure 12. Numerical and Experimental Fatigue Lives.

Shamsaei and Fatemi (2014) investigated small crack growth behaviour of 1045 and 1050 medium carbon steels, 304L stainless steel, and Inconel 718 under multiaxial states of stress. Experimental observations from solid and thin-walled tubular round specimens under various combined stresses including in-phase (IP) and out-of-phase (OP), tension-torsion and tension-tension, with or without mean stresses, were used

to characterise small crack growth behaviour. The effects of friction induced closure, material ductility, stress gradient, strain amplitude, non-proportionality of loading, and mean stress on small fatigue crack growth behaviour were also discussed. The Reddy–Fatemi (RF) effective strain-based intensity factor was used to correlate crack growth rate data for various materials and loading conditions presented. The difference in fatigue crack growth behaviour in proportional and non-proportional loading for 1050 N steel is shown in Figure 13.

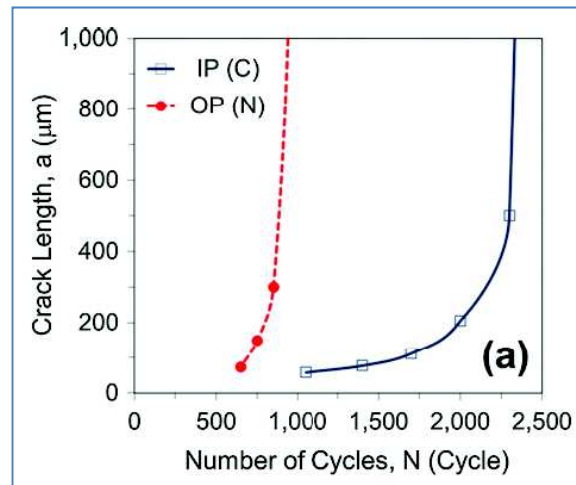


Figure 13. Effect of non-proportionality in crack growth behavior (1050 N Steel).

3.3.4 Recent developments in multiaxial fatigue criteria

In the ISSC 2012 report, multiaxial fatigue was discussed and also included a comprehensive bench mark study of a bulkhead, where the weld seam was subjected to parallel, normal and shear stresses. Different codes were assessed and the results showed a great divergence between the results, which gives clear evidence of the fact that fatigue problems in the case of multiaxial stresses need further research supported by experimental work, which was also pointed out by the official discussor of the report.

Araújo et al. (2011) proposed a new method of finding the shear stress amplitude on the critical plane for both synchronous and asynchronous loadings. The authors used the Maximum Rectangular Hull (MRH) method for finding the shear stress amplitude in the critical plane. It has been observed that the use of this MRH method instead of Minimum Circumscribed Circle (MCC) method improves the fatigue life prediction for the data evaluated.

Fatemi and Shamsaei (2011) presented an overview of some important issues in multiaxial fatigue and life estimation. The authors focused on damage mechanisms and damage quantification parameters, material constitutive response and non-proportional hardening, cycle counting and damage accumulation in variable amplitude loading, and mixed-mode crack growth. It is highlighted that capturing the correct damage mechanism is essential to develop a proper damage quantification parameter. Also the authors emphasized that critical plane damage models with both stress and strain terms are more appropriate since they can reflect the material's constitutive response under non-proportional loading.

It has been emphasized that classical yield criteria, such as the von Mises distortion energy criterion, are commonly extended to multiaxial fatigue life estimations, although these criteria may work for in-phase or proportional loading, they often under-estimate the typically observed shorter lives for out-of-phase or non-proportional loading. The shorter life under non-proportional loading is often attributed to non-proportional hardening. However, materials without this hardening also typically exhibit shorter life under such a loading. Classical criteria, such as von Mises equivalent strain, cannot represent this behaviour and should not be used for non-proportional loading.

Overall, it is concluded by the authors that due to the challenging nature of the multiaxial fatigue problems, much additional research and development work is still needed for accurate and reliable multiaxial fatigue life estimation.

Li et al. (2011) proposed a new multiaxial fatigue criteria based on the critical plane concept. The non-proportional factor proposed by Chen et al. (1996) has been used in this method to evaluate and account for the degree of multiaxiality. It was observed that the fatigue life was reduced when the additional non-proportional cyclic hardening increased.

Matsubara and Nishio (2013) proposed a new criterion to estimate fatigue limit under multiaxial high cycle loading. The proposed criterion consists of two parameters, one for crack initiation and the other for initial crack growth. When compared with the available experimental results, the results are within 10% of error, which is better than other criteria used for comparison.

Marciniak et al. (2013) compared the fracture plane position gained from experimental tests of specimens under multiaxial loading and theoretical ones from calculations according to variance and damage accumulation methods. The authors concluded that the damage accumulation method predicts the fatigue life better than the variance method. However, for the pseudo-random loading, the variance method is better than the damage accumulation method.

Ince and Glinka (2014) proposed two different forms of an original multiaxial fatigue damage parameter related to the maximum fatigue damage plane for performing fatigue life prediction under various loading conditions loadings. Both the damage parameters are correlated to sets of experimental data published in the literature to verify the prediction accuracy of the damage parameters. The damage parameter in the form of the GSA, when applied to the uniaxial loading, provides very good correlations with four sets of experimental mean stress fatigue data for Incoloy 901 super alloy, ASTM A723 steel, 7075-T561 aluminium alloy and 1045 HRC 55 steel. In the case of multiaxial loadings, both the GSE and GSA parameters are found to correlate well with fatigue data of 1045 steel and Inconel 718 tubular specimens under proportional and non-proportional loadings. In addition, the damage parameters show reasonably acceptable correlations with experimental fatigue data of SAE 1045 steel notched shafts subjected to proportional and non-proportional loadings.

Factors affecting multiaxial fatigue performance–Material and Additional hardening due to non-proportional load path

The difference in fatigue life is attributed to the type of material subjected to cyclic loading. This can be explained from a metallurgical point of view. In materials having low stacking fault energy, only planar slip systems evolve under a proportional load. However, during a non-proportional load the principal stress plane rotates and causes plastic strain at different slip mechanisms. This cross slip activation due to plastic strain can result in a significant increase of hardening of the material when compared to a proportional load cycle.

However, for materials with high stacking fault energy, slip is easier and material slip occurs both under proportional and non-proportional load cases. In these materials the additional hardening in a non-proportional load cycle is rarely observed. To illustrate this, aluminium material has a higher stacking fault energy hence, this material shows virtually the same stress strain curve independent of the proportionality of the loading path and no significant additional hardening is observed in this material.

Literature that relates the material as a parameter affecting the fatigue life in non-proportional load case has been reported by several researchers. Shamsaei and Fatemi (2009) who studied the effect of material hardness on multiaxial fatigue behaviour based on experiments conducted on tubular specimens made from a medium-carbon steel with three hardness levels obtained from normalizing (low hardness), quenching and tempering (medium hardness) and induction (high hardness). The authors concluded from the experiments they conducted that the induction hardened tubular specimen lives were 8 and 25 times longer than the normalized tubular specimen in the high cycle fatigue regime, whereas, in the low-cycle fatigue regime, the induction hardened tubular specimen fatigue lives are approximately three times lower than the normalized tubular specimen. Based on these results the authors concluded that the ductile material sustains more in the low-cycle fatigue regime, whereas, in the high cycle fatigue regime, the higher hardness improves the fatigue life. Based on these experiments, it is understood that the fatigue life of the material in the multiaxial stress state depends on the hardness of the material as well as the type of loading (proportional or non-proportional).

Itoh and Yang (2011) studied the material dependence of multiaxial low-cycle fatigue to develop a suitable strain parameter for life estimation under non-proportional loading. Strain controlled multiaxial low-cycle fatigue tests under proportional and non-proportional strain paths were carried out using hollow cylindrical specimens of several materials. Test materials employed were 12 metallic materials of which crystal structures (CS) are of a face-centred cubic (FCC) structure and body-centred cubic (BCC) structure. It is concluded that reduction in fatigue life has a close relationship with additional hardening under non-proportional loading, and depends on the crystalline structure of the tested materials. The authors proposed a material dependent equation to calculate the equivalent strain range which takes into account the additional hardening effect. It has been observed that by using this equivalent strain range parameter proposed by the authors, predicted and experimental fatigue lives were in good agreement (Figure 14).

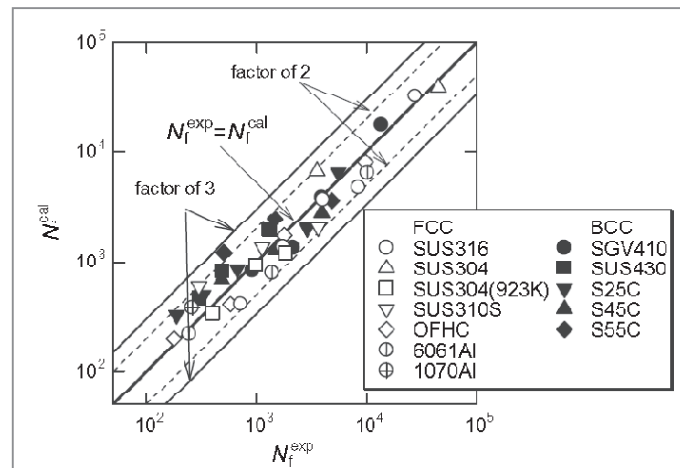


Figure 14. Predicted and experimental fatigue lives of various materials of BCC and FCC category using proposed equivalent strain parameter.

Shamsaei and Fatemi (2010) investigated the effect of micro structure and hardness on non-proportional cyclic hardening of metallic materials. Tubular specimens made from 1050 steel in normalized, quenched and tempered, and induction hardened conditions, as well as 304L stainless steel were used to study the effect of microstructure on multiaxial cyclic deformation. Multiaxial data generated in this study as well as multiaxial deformation data of several materials from literature suggest non-proportional cyclic hardening can be related to uniaxial cyclic hardening. Non-proportional hardening coefficients predicted from a proposed equation based on this observation were found to be in good agreement with the experimental values in this study and from the literature. It was concluded by the authors that a non-proportional hardening coefficient cannot be predicted if only based on monotonic properties, as non-proportional cyclic hardening also depends on the material slip system induced under cyclic loading. The non-proportional cyclic hardening coefficient was found to strongly correlate with the uniaxial cyclic hardening coefficient. Similar trends were observed for both coefficients with a change in total plastic strain. With the proposed non-proportional hardening coefficients, the authors have shown that the predicted and experimental equivalent stress values are in good agreement (Figure 15).

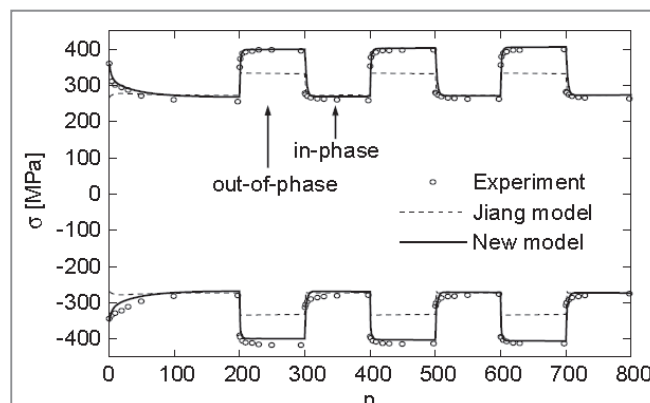


Figure 15. Predicted and experimental equivalent stress values for various materials.

Additional hardening due to non-proportional load path

In general, additional hardening is observed in the low-cycle fatigue behaviour where the stress exceeds the yield stress of the material. When the stress exceeds the yield stress in case of monotonic loading there is strain hardening due to locking of the grain after the initial plastic flow. In the case of the non-proportional cyclic loading it is observed that the hardening is either more or less than the case of proportional cyclic load case/ monotonic load case. Several slip systems are activated in non-proportional loading and block each other, which finally results in additional hardening. This additional hardening is generally noted in the literature as additional hardening due to non-proportional load case.

Literature that relates the additional hardening as a parameter controlling the fatigue life in multiaxial fatigue has been reported by several researchers.

Doring et al. (2006) carried out experiments and numerical simulations using a new plasticity model to compute the additional hardening in the non-proportional load case. The experiments were conducted by altering 100 proportional load cycles and 100 non-proportional load cycles with 90° out-of-phase in the

non-proportional case. It is observed that during the non-proportional loading the stress value rose significantly, which is known as the additional hardening due to non-proportional load cycle (Figure 16).

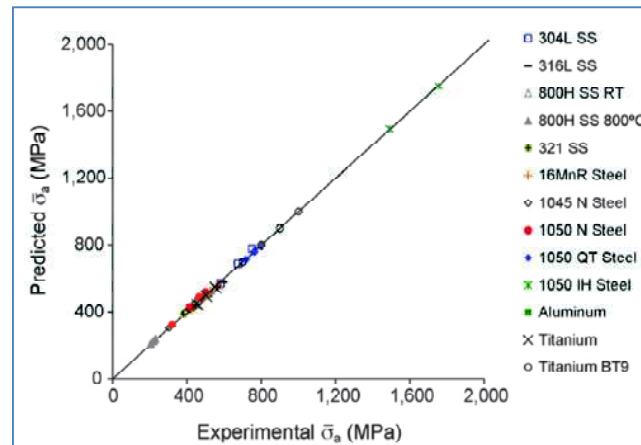


Figure 16. Alternating cycles from proportional and non-proportional loading to observe additional hardening behaviour in non-proportional load case.

Shamsaei et al. (2010a) observed from experiments that the fatigue life of 1050 steel with no non-proportional cyclic hardening was found to be more sensitive to non-proportional loading than for 304L stainless steel with significant non-proportional cyclic hardening. Therefore, additional cyclic hardening due to the non-proportionality of loading is not the only factor causing shorter fatigue lives under non-proportional loading.

Noban et al. (2012) studied the load path sensitivity in the fatigue life estimation of a material (30CrNiMo8HH). Three proportional and seven non-proportional load paths were studied by the authors using strain controlled experiments. In addition, the authors used two different cyclic plasticity models (Mroz and Chaboche) for predicting the cyclic stress strain behaviour. The authors concluded that for multiaxial load paths the Chaboche model produces results in good agreement with the experiment, whereas for uniaxial load paths the Mroz model has been observed to be closer to the experiment.

It is observed that the examined material did not show any significant additional hardening due to non-proportional loading. However, the material showed significant reduction in fatigue life compared to the proportional loading case. The cause of lower lives in non-proportional loading is not necessarily the additional hardening, rather it depends on the sensitivity of material to out-of-phase loading of which additional hardening may be one part.

Based on the cyclic stress strain behaviour of the material for various loading paths, a material dependent non-proportionality modification factor has been proposed to account for the severe path dependency of the material. The fatigue life assessment with this modification factor is observed to be more accurate with the non-proportionality factor for this material (Figure 17).

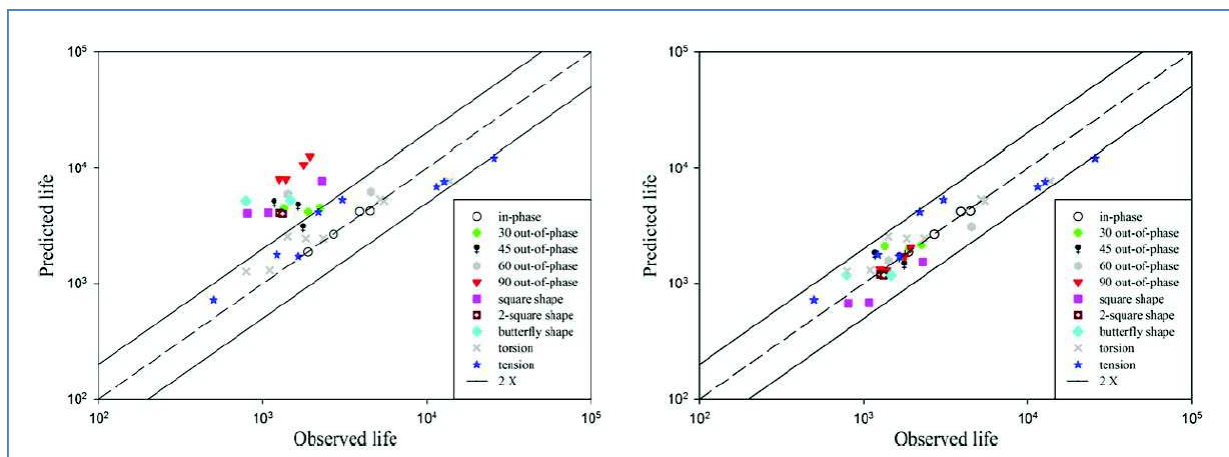


Figure 17. Predicted fatigue life vs. experiments, before (a) and after (b) applying the loading path effect on maximum equivalent strain.

Anes et al. (2013) explained that in shear stress space, the use of a constant factor to convert the axial stress is not appropriate. The authors further explained that the stress scale factor (ssf) on axial stress is dependent on the stress amplitude level and also based on the shape of the loading path. The authors have conducted a series of multiaxial fatigue tests on a high strength steel to determine the multiaxial fatigue strength under proportional and non-proportional loading conditions. An ssf function was mapped based on the experimental results using as arguments, the axial stress amplitude and the stress amplitude ratio, which have proved to be sensitive to the loading path nature. Using the ssf surface, an equivalent shear stress was defined which was used for the fatigue life calculation. Results indicate that the ssf is not a constant value and it is strongly dependent on stress amplitude level and loading path shape. The authors concluded that the equivalent stress was successfully applied to proportional and non-proportional loading paths with satisfactory results.

Fremy et al. (2013) studied the load path effect on mixed mode conditions experimentally on stainless steel. The authors observed that the load path has a significant effect on the rate of crack growth (Figure 18), though the crack path is not significantly different. It is observed from scanning the electron microscope in a non-proportional mixed mode condition that a complex system of slip bands is formed at the crack tip and is used to promote the crack growth. It is concluded that, in non-proportional mixed mode loading conditions, criteria based solely on the maximum, minimum and mean values of the stress intensity factors, cannot provide accurate predictions of the crack growth rate or of the crack path. The entire load path should be considered so as to predict accurately fatigue crack growth in non-proportional mixed mode conditions.

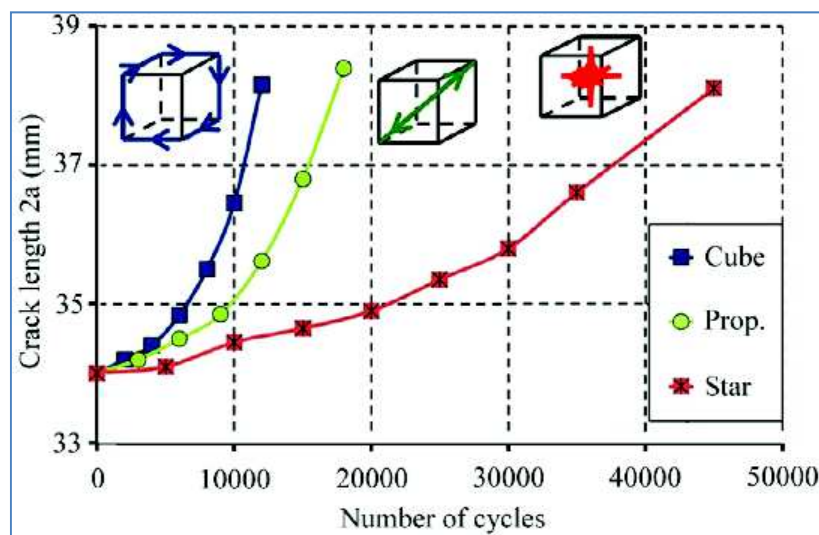


Figure 18. Crack lengths vs. Number of cycles for various cases.

Itoh et al. (2013) proposed a method of evaluating the principal stress and strain ranges and the mean stress and strain, and also proposed a method of calculating the non-proportional factor which expresses the severity of non-proportional loading in 3-dimensional stress and strain space. This study also examines the material constant used in the strain parameter proposed by the authors for life estimation under non-proportional multiaxial LCF and presents a simple method to re-evaluate material constants in relation to the material constants obtained in a static tensile test. For various materials with different non-proportional loading, the authors have shown that the predicted and measured fatigue lives are in good agreement.

3.4 Structural Integrity/Life cycle management

3.4.1 Fabrication and repair

Fatigue improvement methods were discussed in the ISSC 2012 Fatigue and Fracture report and more details regarding the different methods can be found in the ISSC 2015 V.3 report. Hence, only the most applicable research within this topic is listed below.

High frequency mechanical impact (HFMI) technology has undergone a significant amount of research with the aim of improving the fatigue classes of Welded Joints in high strength steels (HSSs) with yield strength up to 950MPa (Yildirim, 2013; Marquis and Barsoum, 2013; Yildirim and Marquis, 2014). The benefits of the technique are small tools, low induced noise levels and compressive residual stresses

produced at the weld. Recommended design curves are proposed for nominal, structural and notch stress approaches when the load ratio is $R=0.1$; see Figure 19. These are collected and presented in Marquis et al. (2013) and Haagensen and Maddox (2013). (Kirkhope et al., 1999a, b) and Yildirim and Marquis (2014) state that future research should be directed towards large-scale structures, variable amplitude loading and other load ratios. The quality control issues have been investigated by Yekta et al. (2013); the varying load ratio by Mikkola et al. (2013) and the residual stress states by Suominen et al. (2013). The IIW Commission XIII design proposal includes proposals for the material strength, high load ratio and variable amplitude loading. The presented investigations show the potential of this method to improve the fatigue strength, which would enable weight reduction or longer design lives for marine structures when high strength steels are considered.

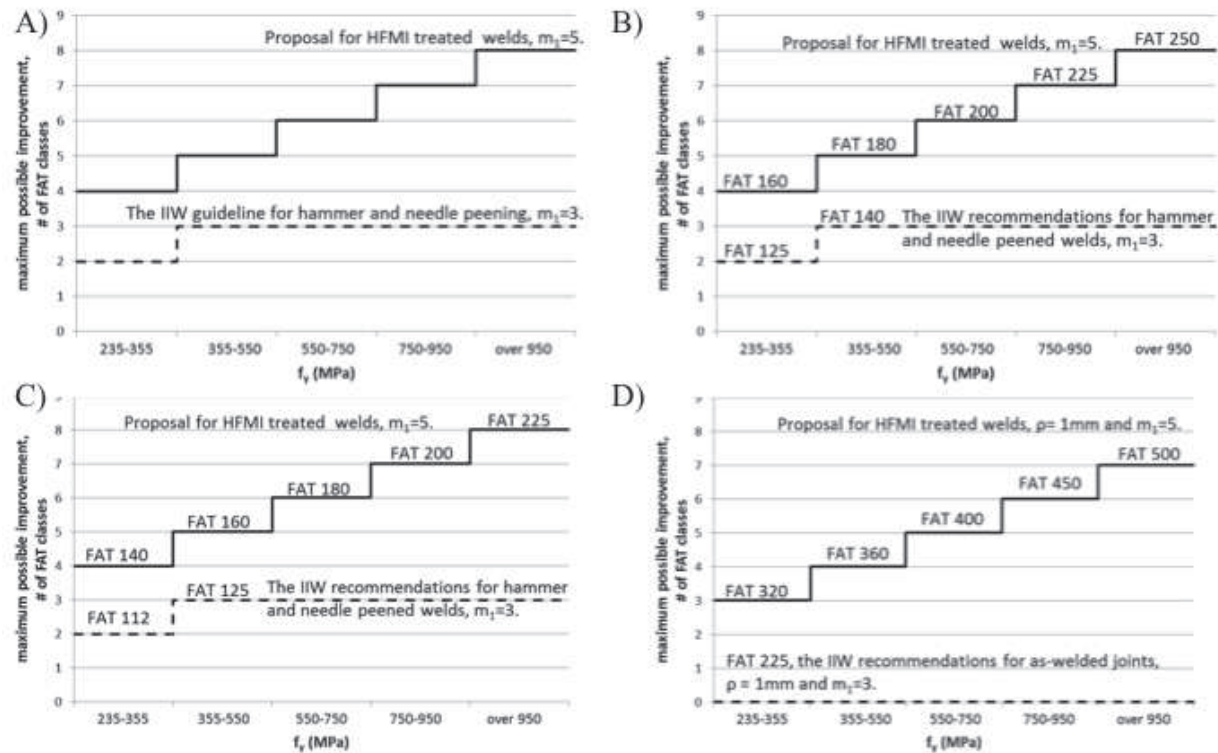


Figure 19. Proposed maximum possible fatigue class improvement in % for A) nominal stress method, B) structural stress method (non-load-carrying), C) structural stress method (load-carrying) and D) all joints using the notch stress method (Yildirim, 2013).

The long term effects of the different improvement methods are not well documented. Haagensen et al. (2014) studied the long term effect of different extension methods applied to the floater Vestlefrik B in the North Sea during 1999-2000. From their study they concluded that toe burr grinding and hammer peening showed an improvement of 4 to 6 in fatigue improvement and only one crack was observed in the treated area during inspection 10 years later, however this crack was due to a lack of penetration not discovered during the first inspection.

3.4.2 Inspection & Monitoring of structure and coatings

Marine structures are exposed to dynamic, continuous loadings coming from the harsh marine environment. This environment can not only cause damage to the structure due to extreme loadings in the short term or cyclic loadings in the long term, but also engenders corrosion. In order to guarantee reliability and integrity of marine structures, an application of structural health monitoring (SHM) is required. The utilization of SHM in the marine industry allows increasing both human and environmental safety in conjunction with reduction in maintenance costs. Sielski (2012) indicated that SHM should have the following main components: (1) accurate information about a structure's failure modes, fatigue characteristics and material corrosion characteristics, (2) damage detection capability in real-time and (3) prediction capability of the forthcoming condition of structural members. In this study it was proposed that SHM can be improved, if the following characteristics are achieved: (1) develop more accurate fatigue and fracture models, (2) improve the model in terms of corrosion detection and (3) install sensors for detecting damage continuously.

One of the most common failure modes of ship structures occurs from fatigue crack initiation and propagation. In the case of a ship being under dynamic sea loading, fatigue cracks are easily initiated since the structural components are assembled by using a welding process. According to stiffened plate fatigue experiments, the combination of lamb wave propagation and power spectral density methods is effective enough to detect fatigue crack initiation and monitor crack propagation. In addition to the development of a fatigue crack model, the selection of an appropriate sensor is crucial to collect strain data accurately. Murawski et al. (2012) suggested that Fibre Bragg Grating (FBG) sensors should be used in marine structures to increase the precision of obtained strain data during the SHM process. In this study, a damage detection experiment was conducted on an offshore platform leg model by using FBG sensors. The location of the FBG sensors on the offshore platform leg model can be seen in Figure 20. The mechanical strain changes due to the dynamic loading are illustrated in Figure 21. The scheme of the SHM system for real marine structures is also discussed in order to calculate strain-stress absolute values with main axis directions by arranging three FBG sensors as a strain rosette.

The conventional non-destructive methods for crack detection consist of strain monitoring, ultrasonic testing, radiographic testing and magnetic testing. The strain monitoring process can be applied to marine structures by allocating strain-gauges on various locations of the structure. However, this process can require a large number of strain-gauges depending on the complexity of the structure. Ultrasonic sound waves can be applied to the structure in order to carry out the ultrasonic monitoring. These waves can become discontinuous when they reach a crack in the structure, and hence the crack inspection can be done by using this process. In contrast, this test system is not adequate for the in-service screening of fatigue cracks. The radiographic testing system generally relies on X-rays and Gamma-rays which can penetrate the structure and allow identification of the crack. Nevertheless, it is impractical for them to be actually applied to marine structures, such as offshore platforms, due to the size of the structure. Although the magnetic testing method is very simple to use, it requires human interpretation to notice the crack on the structure surface. Hence, it is not beneficial to employ this method in real-time SHM applications (van der Horst et al., 2013).

On the other hand, van der Horst et al. (2013) proposed a technique based on wireless monitoring as an application of SHM for marine structures. They indicated that the implementation of networks of wireless sensors can effectively enable the detection of fatigue cracks on a structure, even though it has some disadvantages such as a lack of robust connectivity, inadequate data rates, etc. It was concluded that the conventional methods for detecting cracks and recent techniques for monitoring crack propagation can be combined in order to increase the sensitivity and efficiency of the SHM.

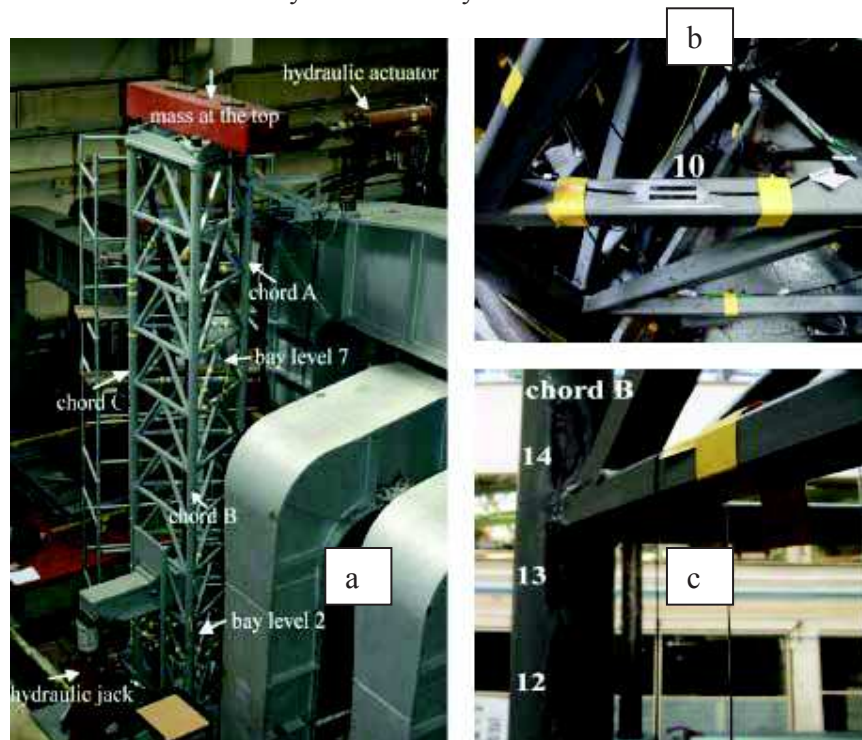


Figure 20. Laboratory experiments: a) the offshore platform leg model b) sensor with steel carrier, c) sensors without steel carriers.

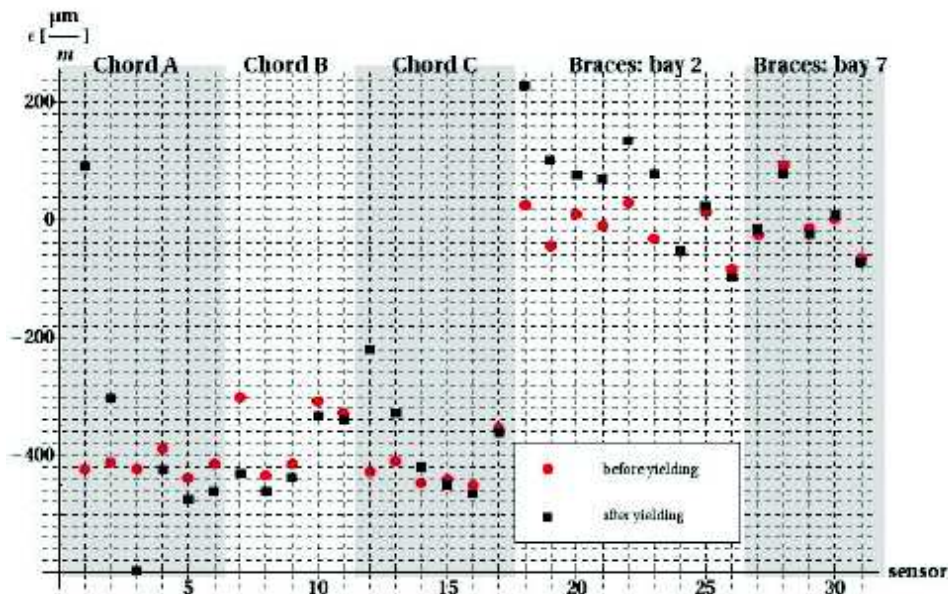


Figure 21. Mechanical strains before and after yielding of undamaged model.

3.4.3 Inspection and Maintenance

The structural strength of ships is a key issue that affects the safety of crew, economic costs and pollution of the environment. The required structural management and safety of ships can be achieved by performing appropriate inspections at the right intervals and repairing the defects that are identified. Chao et al. (2013) indicated that a vision system based on the laser measurement system (LMS), which is a new sensor to accurately calculate distances of the target in an arc section, can be used for bulk ship inspection. Their study concluded that ship loaders can achieve the bulk cargo loading operation automatically based on the inspection data calculated by using LMS scanners and the architecture of this operation is illustrated in Figure 22.

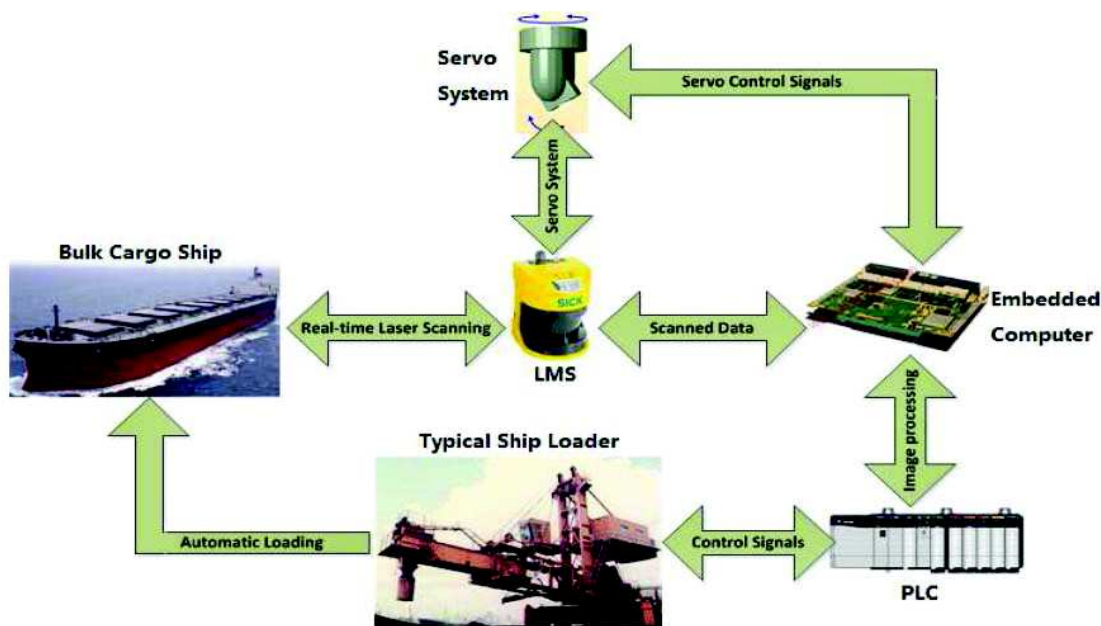


Figure 22. The Architecture of the Automatic Ship Loader.

The importance of using autonomous underwater vehicles has recently increased in the inspection of ships’ hulls and marine structures after the more challenging application of robotics has emerged. Hover

et al. (2012) have built and applied navigation algorithms that can control the hovering autonomous underwater vehicle (HUAV) in order to achieve full imaging coverage of hull structures in high resolution, and with better simultaneous localization and mapping processes.

Today's structural reliability applications have had a great impact on the determination of inspection and maintenance planning. The assessment of structural strength by using probabilistic techniques is one of the most popular structural reliability applications. The target of this method is to calculate the failure probability of the system by evaluating a reliability index for the assumed scenarios. Câmara and Cyrino (2012) developed a statistical model of hull structure containing the effects of fatigue and corrosion. Based on the developed model, time-dependent reliability of the hull structure is calculated by using Monte Carlo Simulation. Figure 23 illustrates the probability of failure change versus operation time for their considered model. It was concluded that maintenance/inspection time, which should be done around 7.5 years of operation for the considered model, can be arranged by using target reliability.

A powerful fast integration technique based on the first order reliability methods was adopted by (Zayed et al., 2013a, b) to calculate the structural reliability of ship hulls. Guo et al. (2012) used the Latin Hypercube Sampling (LHS) method with Monte Carlo Simulation in order to determine the failure probability level for corroded aging tankers. The probability distribution of each variable is divided into non-overlapping segments and a value for each variable can randomly be generated from each segment in the LHS procedure, so that the total variety of the distribution is sampled more evenly and steadily. This study concluded that LHS is mainly more accurate than conventional Monte Carlo direct sampling during the simulation. Structural Health Monitoring (SHM) data obtained from sensors was used by Zhu and Frangopol (2013) to improve the accuracy and redundancy of reliability assessments of ship cross-sections.

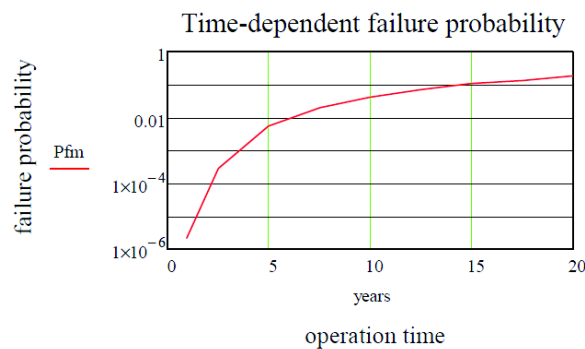


Figure 23. Failure probability in relation to operation time.

Li et al. (2012a) introduced a hull structure information integration model that can be used in mobile devices in order to record the data during the inspection process, and therefore transferring these data is much easier than using conventional ways. Lee et al. (2013) suggested a radio-frequency identification device (RFID, which can be applied to cloud technology, for an effective maintenance/inspection operation. It was proposed that RFID can be used to identify correct data and save these data accurately via a cloud system, thus if RFID is used during the inspection process, it will improve the efficiency of maintenance operations.

3.5 Composites

Coronado et al. (2012) studied the influence of temperature on the static and fatigue resistance of a carbon-fibre epoxy composite, which is a material commonly used in aerospace and naval applications specifically because of its low weight. According to the authors, whilst fatigue in metals can be studied in terms of crack nucleation and propagation, fatigue in composites may result in a more complex phenomenon, where multiple damage mechanisms nucleate, grow and interact (e.g. fibre breakage, fibre-matrix debonding, delamination and matrix cracking). The fracture mechanics of these materials resulting from static loading are currently the subject of extensive research. On the otherhand, few studies have focused on dynamic loadings and the influence of temperature. Coronado et al. (2012) used the data reduction method called the Modified Beam Theory (MBT) method to calculate the interlaminar fracture toughness in mode I resulting from their experiments. As seen from Figure 24, the fracture energy necessary to initiate delamination increases with the increment of temperature and decreases with the increment of the number of fatigue cycles.

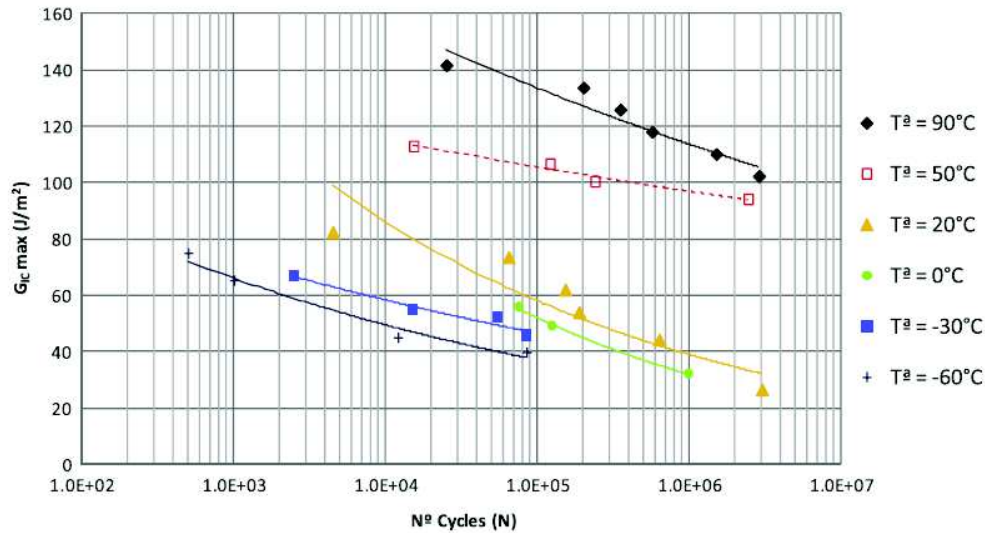


Figure 24. Delamination fatigue curves at different temperatures.

Vina et al. (2011), conducted a similar study on a different composite material: glass fibre reinforced polypropylene. According to the authors, the tensile strength of the material decreases with the increment of temperature, as well as its fatigue life (Figure 25).

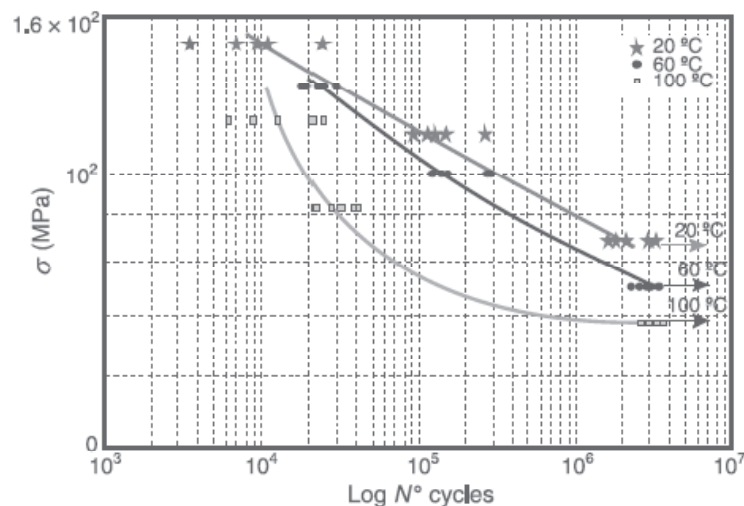


Figure 25. Results of fatigue tests (Vina et al., 2011).

An interesting finding of this study is represented by the non-linear shape of the fatigue fitting curve corresponding to a temperature of 100°C. This change in behaviour of the material was explained by the fact that the material is preparing to change from its viscoelastic temperature zone to its viscous temperature zone.

4. FATIGUE ASSESSMENT METHODS

Generally speaking, ship- and offshore structures can be classified as stiffened (curved) panel-, truss-, or frame assemblies consisting of shells, plates, profiles, tubular members and castings. Arc-welding, the commonly applied joining technique, introduces notches at the weld toe and, depending on the weld penetration level, notches at the weld root as well. Since notches have been identified as fatigue sensitive locations and ship and offshore structures typically contain a $O(10^3)$ [m] weld seam, particular attention is paid to (arc-)welded joints and V-shaped notches. Different assessment methods have been developed over time and will be discussed.

Fatigue assessment requires defining the Fatigue Loads, Strength and Damage accumulating rule. IACS (2014) defines the calculation of fatigue loading in a direct calculation (spectral approach) and describes the assumption of service conditions used to define the Equivalent Design Wave simplified approach which is used in rules to check fatigue criteria by analytical formulae.

Derbanne et al. (2011) analysed the effect of different probability levels of rule-based loads on the fatigue damage. The sensitivity of the Weibull shape parameter on long-term distribution has been studied. It has been observed that while the shape parameter is unity, the 10^{-2} probability level of rule-based loads has less sensitivity to the final fatigue damage. Based on this study it has been concluded that the Bureau Veritas (BV) rule for fatigue assessment will be updated from the existing 10^{-5} probability level to the 10^{-2} probability level.

4.1 Overview

As in the report of the ISSC 2012 TC III.2 only a brief overview of newly developed fatigue assessment methods was presented, it was decided this time to pay more attention to this subject. Actually, several approaches and methodologies have been and continue to be proposed in the literature dealing with a wide range of cases of ships and offshore structures and more in general with welded structures. It seemed interesting, therefore, to propose an updated overview offering a categorization of approaches based on the type of parameter believed to govern the fatigue phenomena, but having also in mind their complexity and application limits that were well described by Figure 1 of the ISSC 2012 TC III.2 report.

Noticeable advancements in fatigue assessment approaches of welded joints using local approaches, have appeared in recent years since the publication of the well-known book on the subject by Radaj et al. (2006). These same authors recently published a review of recent developments in local concepts of fatigue assessment of welded joints that can be seen as an appendix to the original book (Radaj et al., 2009b). Fricke (2014) outlines the most recent developments and future challenges in fatigue strength assessment of welded joints, pointing out the links among different approaches.

A new book by Radaj and Vormwald (2013) reviews and explains advanced methods of brittle fracture and fatigue assessment, looking at them even more locally than before as they move from the generalized Neuber (1968) concept of fictitious notch rounding (FNR) to explain methods based on the stress intensity factor (SIF) and on the energy density concepts, finally touching upon the crack propagation approach based on both linear elastic and elasto-plastic fracture mechanics principles.

Traditional approaches to fatigue assessment are based on simplified structural analyses and fatigue tests of standard structural details. The well-known nominal stress approach is still widely applied and provides consistent results in several practical cases, even if the trend is more and more towards local approaches.

Local stress approaches were introduced decades ago for tubular joints of offshore structures in the hot spot stress fashion and their applications to plated structures is nowadays mainly based on finite element (FE) models of relatively large parts of the structure, refined according to well established regulations, limiting their application to specific cases. These methods are now referred to as structural or geometric stress approaches.

The effective notch stress approach has recently been regulated by Fricke et al. (2008) and is nowadays commonly applied by the marine industry, even if not actually included in classification societies' rules for ship construction. Indeed, recent rules, such as the IACS Common Structural Rules, apply the structural stress approach in as far as the notch stress is obtained by a stress concentration factor, rather than FE analysis simulating the weld seam effect, while the effective notch stress approach is more common in the offshore field.

Local approaches should be able to avoid long lasting tests of specific structural details as required by the nominal stress approach. However, results are not always conservative and sometimes are largely over-conservative, depending on the loading and geometry of the structural detail and applied approaches. It is noted that often fatigue assessments carried out by different local approaches, even when based on the same principle, are not consistent. It appears that not only the method (e.g. structural stress can be evaluated using different techniques such as surface stresses extrapolation, through-thickness stress linearization, stress at critical distances from hot spot, etc.) but also the FE analysis has an influence on the final result.

Indeed, the trend towards local approaches to assess the fatigue strength of structural details is still in progress and methodologies for fatigue strength assessment of welded structures are becoming more and more local while new ones are continuing to appear in the literature. Since computational tools are continuously being advanced, fatigue assessment approaches proposed several decades ago have now become applicable in everyday engineering practice.

In general, test results in terms of S-N curves do not clearly distinguish between crack initiation and complete failure; rather a parameter that is believed to govern the phenomenon is considered and associated with the fatigue strength of the structure, i.e. to the cycles to failure, without distinguishing

between different propagation phases (Schijve, 2012, 2014). However, the crack propagation approach is still felt to be not suitable or sufficiently reliable for basic design, rather it is commonly applied for failure analysis and detailed assessments of in-service structures, especially in the oil and gas industry.

Fatigue strength assessment approaches are categorised below on the basis of the parameter believed to govern the fatigue strength behaviour. Figure 26 proposes an improvement to the well-known overview of fatigue assessment approaches given by Radaj et al. (2006) in order to provide a clear summary of first principles on which the approaches are based. Actually, the parameter believed to govern fatigue failure is shared by several different variants within the approach category; each approach has specific application limits. The idea is, therefore, to provide a guideline for design engineers and at the same time to present an overview of the fatigue assessment approaches recently proposed in the literature.

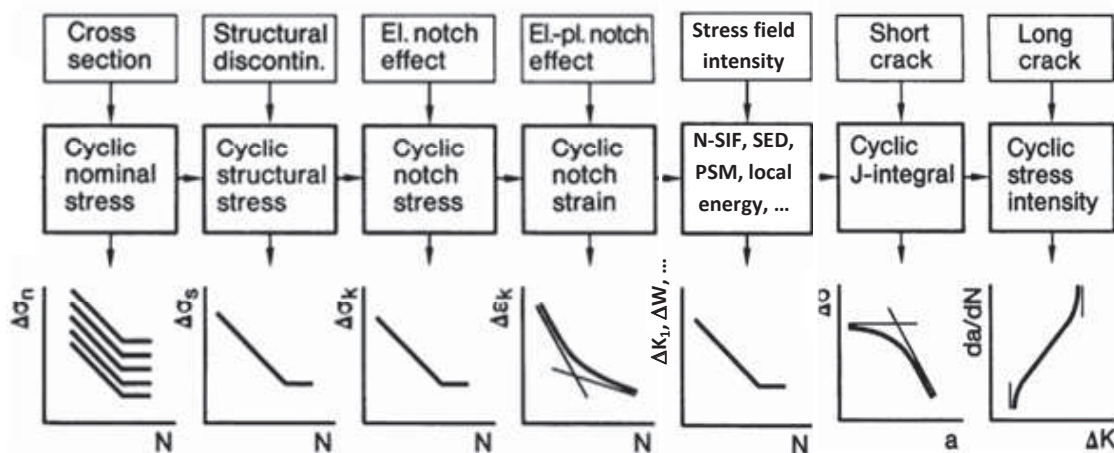


Figure 26. Overview of fatigue assessment approaches, adapted from Radaj et al. (2006).

In summary, several local approaches have been developed in the last 20-30 years in addition to the nominal stress approach, which is based on the stress in a component resolved using general theories and disregarding all local stress raising effects of the welded joint. They are generally categorized as:

- Structural stress approaches, based on the structural (or geometric) stress at the hot spot that includes all stress raising effects of a structural detail, excluding all stress concentrations due to the local weld seam profile itself;
- Notch stress approaches, based on the effective notch stress, i.e. the total stress in the notch, obtained assuming linear-elastic material behaviour, generally replacing in the calculations the actual weld seam profile by an effective one to account for the scatter of weld shape irregularities as well as for the plastic material behaviour of the notch root;
- Notch strain approaches, based on the notch strain instead of notch stress and considering the elasto-plastic behaviour of the material occurring in the notch, thus overcoming at the root the problem of the unrealistically high stress values obtained by the notch stress approach but not removing the need for rather complex calculations to obtain the stress and strain at the notch root;
- Crack propagation approaches, evaluating the crack growth up to failure, according to the fracture mechanics model, i.e. the fatigue strength is related to the stress intensity factor range by the well-known Paris-Erdogan law, provided that an initial crack is assumed to exist in the welded detail and is propagated by each applied loading cycle in a stable way.

The fatigue phenomena in welded structures are far more complex than the existing descriptions and are controlled by what occurs in the area surrounding the weld notch, therefore involving many other geometrical and material parameters not included in the current approaches. Indeed, every approach has its own features and applicability limits while a unified approach seems rather far from current practice.

Among the others, there is a new category of promising fatigue assessment approaches based on the concept of notch stress intensity, explicitly accounting for the singularity of the stress field at the notch tip without a fictitious description of it (see section 4.2.3). Such approaches can be regarded as in between the notch stress or notch strain based approaches and the rather more complex crack propagation approaches. Hence, they can provide the link for a unified approach to fatigue assessment.

4.2 Fatigue damage models

The following advancements have been developed in recent years:

4.2.1 Stress based concepts

Effective notch stress concept: Notches typically introduce stress concentrations reducing the fatigue strength and fatigue life time, but not to the extent of the linear elastic notch stress increase $K_t \cdot \Delta\sigma$. The effective stress concentration often turns out to be smaller. Adopting a microstructural support hypothesis, the influence of the notch stress gradient is included by averaging the notch stress along the (presumed) crack path over a material-characteristic micro-structural length ρ^* . The real weld toe and weld root notch radius ρ is artificially enlarged by employing a fictitious component $\rho_f = s \cdot \rho^*$ to obtain an effective one $\rho_e = \rho + \rho_f$ and the corresponding notch stress of the original geometry (Radaj et al., 2009a; Fricke, 2013); an intact geometry parameter. However, a real weld seam is somehow curved and anything but simple, e.g. ρ is widely scattered meaning the statistical weld volume effect has to be incorporated. Using the effective notch radius $\rho_e = \rho(\mu, \sigma) + s \cdot \rho^*$, the effective notch stress range becomes: $\Delta\sigma_e = K_f \cdot \Delta\sigma = K_t(\rho_e) \cdot \Delta\sigma$. The statistical component, however, is often left in the fatigue resistance data scatter. The support factor s depends predominantly on the loading mode (uni-axial, , multi-axial), level of constraint (plane stress; plane strain), notch angle ($2\alpha = (5\pi/4, 2\pi)$) for respectively idealized weld toe- and weld root notches) and notch shape (blunt hyperbolic, root hole or blunt circular for weld toe notches; elliptic, key-hole or U-hole for weld root notches) and last but not least the adopted strength criterion (e.g. von Mises). Plateau values are in the range (1, 10) Radaj and Vormwald (2013) and (Radaj et al., 2013).

The microstructural length ρ^* is typically obtained in an implicit way. Using fatigue test data, S_e - N curve parameters can be estimated. Assuming the data correlation is at maximum for the correct ρ^* , its most likely value can be found in (Zhang et al., 2012a; Zhang, 2012). Although ρ^* is a material characteristic parameter, the HAZ and weld material, the effects of respectively the weld toe and weld root notch are ignored. In an engineering approach, the most likely ρ_e value can be obtained directly as well, meaning average (ρ_r, ρ_f) contributions are involved.

For engineering applications, one fatigue resistance curve related to one reference radius $\rho_r = \rho_e = 1$ [mm] has been defined (for both steel and aluminium weld toe and weld root notches) because of the simplifications (concerning notch angle, elasto-plasticity, notch acuity, etc.) with respect to the original concept. The reference radius $\rho_r = 1$ [mm] is restricted to plate thickness $t_p \geq 5$ [mm] because of cross-sectional weakening (weld root notches). Strengthening of weld toe notches is ignored. In both cases structural stress corrections should be applied. Concerning notch shape, root notches are obviously critical and classified as conservative (e.g. key-hole) and non-conservative (U-hole) as noticed in a Round Robin (Fricke et al., 2013a), although the main criterion should be that the adopted shape, as used to obtain the fatigue resistance curve, and the one used for the fatigue assessment, are in agreement. Note that only the absolute notch acuity has been taken into account. It is proposed to be replaced by a relative one (Schijve, 2012), although—at least for weld toe notches—the plate thickness seems a better solution than a weld leg length.

The case $t_p < 5$ [mm], $\rho_r = 0.05$ [mm] has been adopted based on a completely different hypothesis, i.e. the relationship between the stress intensity factor and notch stress as well as crack tip blunting. At the same time, it is a compromise with respect to FE modelling and the calculation of a reasonable local stress component (Sonsino et al., 2012).

Battelle structural stress concept: Assuming the fatigue life time of welded joints is predominantly related to (micro-) crack growth because of the welding process induced flaws, the stress intensity factor K_I has been adopted to obtain a damage tolerant equivalent stress parameter, i.e. a through-thickness criterion (Selvakumar and Hong, 2013).

The through-thickness weld notch stress distribution has been bi-linearised, and is related to a relatively mesh-insensitive linear far field stress distribution ($\Delta\sigma_s, r_s$) and has been used to approximate the crack tip wake field, i.e. to obtain a blend stress intensity factor weight function $Y_n Y_f$ including the notch and far field contribution. However, the bi-linearisation induced transition at $0.1t_p$ is valid for low weld load carrying levels only; for increasing ones the notch affected region should be increased. The stress intensity K_I however shows singular behaviour for $a \rightarrow 0$ and cannot be explained as a higher order effect.

The notch and far field related stress intensities have been translated into a two-stage crack growth model, a modified Paris equation. Notch plasticity has been assumed, i.e. the (anomalous) crack growth behaviour is non-monotonic. Integration yields an equivalent stress parameter. The adopted initial defect

size is based on crack growth integral convergence—a result of the assumed notch plasticity. The crack growth integral $I(r_s)$ has been approximated using a polynomial formulation. It is applicable to monotonic weld notch stress distributions only ($r_s > 0$) and is based on a single edge crack formulation. For this reason, only half the plate thickness has been considered to obtain the structural stress for WJs showing symmetry with respect to half the plate thickness as adopted—although significantly weld load carrying—in a Round Robin (Fricke et al., 2013a). ASME implemented the BSS concept for fatigue design. Its structural strain equivalent has recently been proposed (Dong et al., 2014).

4.2.2 *Strain concepts*

Most marine and offshore structures are designed such that the nominal strains remain elastic; however, stress concentrations often cause plastic strains to develop in the vicinity of notches. The strain-based methods, i.e. Coffin-Manson equation and its modified forms accounting for mean stress effects (i.e. the Morrow, Manson-Halford and Smith-Watson-Topper equations) are often used to predict the crack initiation at notches (Chen and Wang, 2012; Wang et al., 2014).

Chen and Wang (2012) proposed an approach to determine the minimum allowable size of a crack-stopping hole, in which the Morrow, Manson-Halford and Smith-Watson-Topper equations are used for low-cycle fatigue analysis. Gladyski and Fatemi (2013) investigated the notch effects on the axial and torsion fatigue behaviours of low carbon steel and found that the Coffin-Manson equation, with the use of the effective strain obtained from Neuber's rule, results in poor correlation of the fatigue life data of smooth and notched specimens under axial and torsion loadings. Karakas (2013) investigated three types of welded joints with regard to their fatigue strength based on the Smith-Watson-Topper equation, accounting for the mean stress effects and the reference notch radius concept. His study showed that the mean stress effects on fatigue strength were described properly by calculating the elastic-plastic deformations in weld toes and roots and by evaluating them using the Smith-Watson-Topper equation. Gates and Fatemi (2014) investigated the effects of notches on multiaxial fatigue behaviour of thin-walled tubular 2024-T3 aluminium specimens with a circular transverse hole. Constant amplitude fully reversed axial, torsion, and in-phase and 90° out-of-phase axial-torsion tests were performed under load control. The results showed that the local strain approach using Neuber's rule with the fatigue notch factor K_f was able to correlate axial and torsion data for both smooth and notched specimens in the low-cycle fatigue regime. The use of the elastic stress concentration factor K_t in Neuber's rule resulted in overly conservative life predictions.

The strain-based methods were also applied for probabilistic fatigue analysis. Based on the Morrow equation, Lorén and Svensson (2012) performed a second moment reliability evaluation and Monte Carlo simulations for a welded structure to investigate the variability of the fatigue life. Zhu et al. (2013) applied the Smith-Watson-Topper equation and Bayesian framework to perform a probabilistic low-cycle fatigue life prediction of aircraft turbine disk alloys and the results showed the prediction of fatigue life agrees well with the experimental data. Correia et al. (2013) proposed a local unified probabilistic approach to model both crack initiation and crack propagation of a notched rectangular plate with the use of the Coffin-Manson and Smith-Watson-Topper equations. The results showed that there is a good agreement between predictions and experimental data.

The strain-based methods have also been accepted by industry standards as useful methods for predicting the fatigue life of a notched component. The American Society for Testing and Materials (ASTM) and the Society of Automotive Engineers (SAE) have published procedures and practices for performing strain-controlled tests and predicting fatigue lives based on the test data.

Although strain-based methods have been widely applied to predict the crack initiation of a notched component in the low-cycle fatigue regime, there are still some weaknesses in these methods:

- Some effects considered in strain-based methods, i.e. mean stress effects and notch size effects, are still empirical in nature;
- Further studies still need to be conducted to improve the strain-based methods for predicting the crack initiation of a notched component under variable amplitude loading;
- The constants used in strain-based methods depend on the condition of the specimens tested. There is still no defined way to account for differences in surface finish, plating, surface treatment, etc.

4.2.3 *Notch-intensity factor, -integral and -energy density concepts*

A few methods linking fracture mechanics concepts with more traditional stress based approaches were recently revived, moving forward from the generalised Neuber concept of Fictitious Notch Rounding (Radaj et al., 2013; Zappalorto and Lazzarin, 2014; Radaj and Vormwald, 2013) and looking at

parameters describing the singular stress field at the notch tip; the Notch Stress Intensity Factor (N-SIF) concept, first introduced by Williams in 1952, is in fact the basis for various fatigue assessment approaches ranging from the N-SIF approach itself, to the Strain Energy and Strain Energy Density (SED) concepts, to the Peak Stress Method (PSM).

In some cases such approaches are able to explicitly account for the very local plastic behaviour of the material and may consider either sharp or blunt notches, despite in the latter cases analytical formulae are by far the more complex. The bridge linking a novel version of the effective notch stress approach with the N-SIF concepts has been recently explained by Zhang et al. (2012a).

The literature review presented in Rizzo (2011) reports the fundamentals of the most recently proposed N-SIF based approaches in view of their application in the shipping industry.

A research group in the University of Padua has mostly developed such methods in recent years and one of the most promising features for the marine industry is the possibility of automatically implementing them in finite element sub-modelling techniques, capable to transfer appropriate boundary conditions from large and coarse shell element models to smaller and refined solid element models.

N-SIF based methods promise to overcome the need for extensive and dedicated fatigue experiments and of validations based on component failures and in-service experience, even if it should be admitted that developments are still necessary in two directions: on the one side Wöhler curves for such approaches are still to be fully developed and/or validated for their application in the ship and offshore field, on the other side no guidelines exist for the implementation of novel, N-SIF based, fatigue assessment approaches, rather only research papers were presented in the literature dealing with simplified and mostly two-dimensional geometries.

The N-SIF based approaches are relatively young and therefore their application is not widespread. Very few references were found dealing with ship and offshore structures despite the methods appearing to be quite promising and few independent applications have been carried out other than those by the researchers most involved in the development of such approaches.

The most suitable approach evolving from the N-SIF method, and applicable to ship and offshore structures, is that based on the strain energy density (SED) in a volume. Feltz et al. (2010) and Fischer et al. (2010) compared the SED results with experimental data of lap joints and cover plates; the crack propagation approach was applied as well. Two-dimensional finite element models were used and some preliminary analyses were carried out showing general agreement with experimental data but also some discrepancies because of the three-dimensional stress fields. Fischer et al. (2011a) analysed the finite element evaluation of SED and highlighted some differences depending on the element type and shape.

Fischer et al. (2011b) presented the application to a very typical yet still challenging case, the hopper knuckle, building a solid elements sub-model surrounded by a larger shell element model, hence considering a complex three-dimensional stress field. Overly-conservative results were generally found.

Later another method based on the N-SIF concept was proposed allowing relatively straightforward fatigue assessments of welded joints if well calibrated in advance: the Peak Stress Method (PSM) actually largely simplifies the estimate of N-SIF when using particular elements and meshes. Applications to ship structures were found in (Fischer et al., 2013; Fischer et al., 2015; Cosso et al., 2014).

The above mentioned approaches seem to overcome the difficulties introduced by other local fatigue assessment approaches, including several different effects not considered by other methods. For example, observing that an energy parameter is in principle a function of all loading modes, particularly the SED criterion can be successfully used to estimate fatigue strength of welded details even if subjected to multiaxial fatigue loading. However, N-SIF based approaches are not yet recognised as a procedure for fatigue life assessment in the various industrial fields nor were they agreed to be included in any regulation or standard.

4.2.4 *Confidence and reliability*

The determination of S-N curves is associated with large scatter (DNV GP RP 0005, 2014). Parameters in S-N curves are often regressed from fatigue tests under constant amplitude loads. While stress responses in ship and offshore structures are often variable amplitude random loads, in particular for larger and fast container ships, fatigue contribution due to high frequency loads has attracted a great deal of attention. Agerskov (2000) tested welded steel plate specimens with longitudinal attachments under variable amplitude loads using three typical offshore load spectra: broad band, narrow band, and a modified Pierson-Moscowitz wave spectrum with broad band character, see Figure 27. A significant difference was indicated by the test series between constant amplitude and variable amplitude fatigue test results. It concluded that for broad-banded random loads, the Miner fatigue accumulation value of 1/3–1/2 should be used corresponding to fatigue failure.

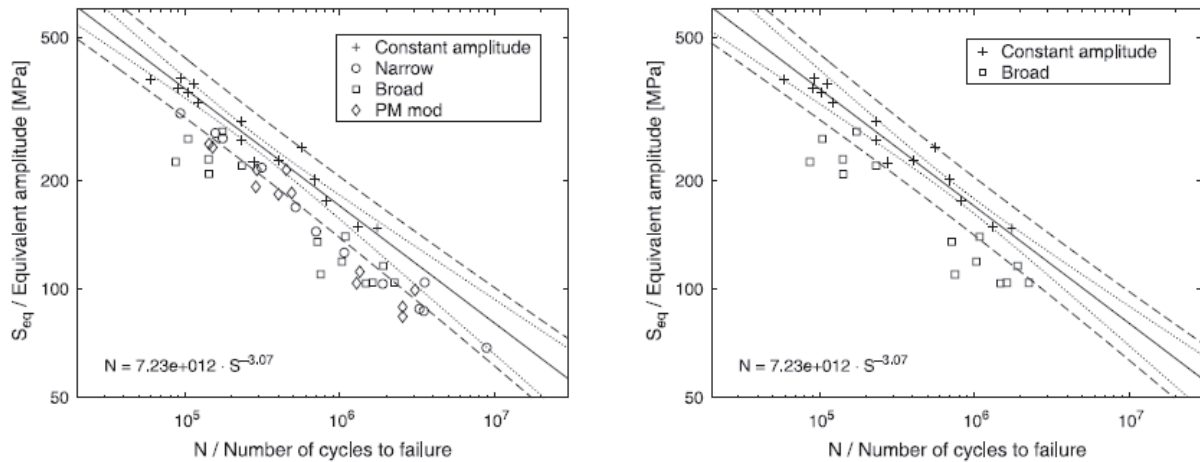


Figure 27. Fatigue test results under constant amplitude loads and variable amplitude loads of different spectra.

Osawa et al. (2013) developed fatigue tests using superimposed vibrations with a special testing machine powered by two exciters. The preliminary test results illustrated that using the simple envelope counting method can give a good prediction of the fatigue life. In order to simulate the low-frequency wave loading and higher frequent whipping stresses, Fricke and Paetzold (2014) created the stress signals by using two superimposed sinusoidal functions with different frequencies for the fatigue tests. Full-scale measurements of stress histories on a Panamax container ship, containing typical whipping events, were applied for the fatigue test of the specimen with double-sided transverse stiffeners. Based on the fatigue tests, a simple method was proposed to take into account the whipping signals by multiplying a factor of the maximum increase of wave-induced stress ranges due to whipping by the cumulative damage caused by wave-induced stress ranges.

Due to the time, expense and difficulties associated with fatigue testing many researches have devoted attention to the development of methods to consider the S-N parameter scatter, using a limited number of tests or currently available test results for practical fatigue estimations. Ronold and Lotsberg (2012) showed how to estimate characteristic S-N curves with confidence when the amount of data is limited. The confidence level in estimating the characteristic value of cycle numbers to failure from limited data was established to be able to maintain the same safety level under an infinite number of fatigue tests. The results provided a new way to optimize fatigue design and may form a useful corrigendum to existing recommendations for given confidence levels for the estimation of S-N curves.

Based on existing fatigue test data, some methods were developed to consider S-N scatter for more reliable fatigue assessment. Johannesson et al. (2005) proposed using the equivalent stress for the regression of S-N parameters by the maximum likelihood method. It was then applied to estimate fatigue damage caused by random loads. The features and usefulness of this method were demonstrated from fatigue test data by Agerskov (2000). In addition to the scatter of S-N parameters from the data, Mao et al. (2010) employed the Cornell safety index to account for the uncertainty from encountered sea environments for ship structures. The procedure was validated by a full-scale measurement of a container ship.

Some statistical techniques were also used to investigate the fatigue test database in order to find a probabilistic way to describe the relation between stress cycles and fatigue failure. Recent fatigue tests have explored the gigacycle fatigue properties of materials. The results indicated the introduction of modifications to the conventional statistical fatigue life models characterized by a single fatigue failure mechanism and a fatigue limit, because specimens may fail even if the applied stress value is smaller than the conventional fatigue limit. Paolino et al. (2013) presented a unified fatigue model using random variables to describe (knee points) transition stresses between two failure mechanisms. This model is able to account for different failure mechanisms and the possible presence of the fatigue limit. Angelo and Nussbaumer (2013) also pointed out that disregarding run-out data and arbitrarily fixing the fatigue limit at 10^7 cycles is unrealistic. A random fatigue limit model may be used to overcome this aspect, but only for the test results with an existence of fatigue limit. While for S-N test results without a fatigue limit, this paper proposed an alternative four-parameter fatigue limit asymptote model based on the hypothesis that S-N curves have an oblique asymptote in the high cycle fatigue region ($N > 10^7$). In the model, the parameters of median curve and stress range-dependent standard deviation represent the randomness of the fatigue life.

By making use of the “Database on fatigue strength of Metallic Materials” published by the Society of Materials Science Japan, Mukoyama et al. (2014) identified the correlations between the regression parameters of S-N parameters and static mechanical properties (tensile strength) of material. Based on the correlation, a statistical estimation method of the S-N curve was developed for iron and structural steels in terms of their tensile strength. Pedersen et al. (2013) also collected a fatigue test database from public literature to investigate the thickness effect for the fatigue assessment of transverse butt joints. The test data were taken to compare with the thickness correction according to the IIW recommendations and most other codes/guidelines; it was concluded that these codes/guidelines are very conservative for fatigue estimation of butt joints.

4.3 Fracture mechanics models

The trend in the ship and offshore building industry is to construct ever bigger structures by means of their size and as a result, strength of material must be satisfied under several loading scenarios. Apart from strength, toughness of material has become an important issue for big structures and both must have acceptable limits. Unfortunately, the attainment of both of these properties is not a simple issue and there are several studies on this subject. Ritchie (2011) indicated strength-toughness relationships for several engineering materials (Figure 28) including new state-of-the-art materials, i.e. metallic glasses, metallic-glass composites, as well as future trends of materials (indicated as a white arrow in Figure 28). In this study, it is concluded that both of these properties are related to several length scales, i.e. nano to macro scale, and one should consider the effect of different length scales on material behaviour.

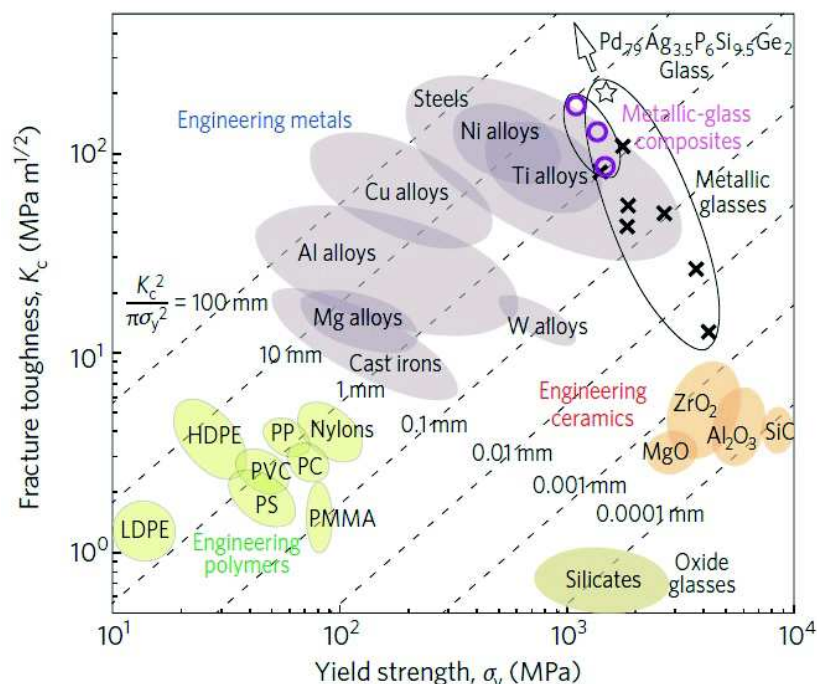


Figure 28. Conflicts of Strength versus Toughness (Ritchie, 2011).

Constructing ever bigger ship structures leads to the application of thicker steel plates in the shipbuilding industry. Several attempts have been undertaken in order to gain both strength and toughness of shipbuilding materials, especially for thick steel plates. In January 2013, the International Association of Classification Societies (IACS, 2013) released a new rule, the so-called “Requirement for Use of Extremely Thick Steel Plates”. In this documentation, several requirements and recommendations are highlighted for the use of extremely thick steel plates, i.e. between 50 mm and 100 mm, concerning brittle fracture toughness and brittle crack arrestability.

There are several parameters describing the fracture toughness of materials, such as energy release rate (G), stress intensity factor (K), J integral, crack tip opening displacement (CTOD) and crack tip opening angle (CTOA). These parameters are related to material behaviour which can be linear elastic, non-linear elastic or elastic-plastic. While measuring and evaluating these parameters, proper test methods must be adopted. A detailed research reviewing these issues from past to state-of-the-art developments has been undertaken by Zhu and Joyce (2012). Their review is based on the American Society for Testing and Materials (ASTM) standards. Usually fracture tests give too conservative results when compared with actual

structures. For this reason, Bayley and Aucoin (2013) examined the fracture behaviour of welded single edge notched tension specimens using constraints and loading conditions encountered by ship structures in service. They examined large scale samples of hull structural material. They developed a crack mouth opening displacement (CMOD)–CTOD transfer function utilizing the Finite Element Method (FE) simulations of these samples and this led to the determination of fracture toughness values. So, fracture toughness values of non-standardised tests specimens can also be determined using the same procedure. On the other hand, while measuring fracture toughness values of thick steel plates, large test specimens and a testing machine, with significantly large expenditures, are necessary. This issue was addressed by Yajima et al. (2011) who used a small sized centre-notched tension test specimen using steel plate thickness as the specimen width. They accomplished evaluating the fracture toughness of 70mm thick steel plate using this specimen.

The relationship between the microstructure of weld joints and fracture toughness was investigated by Leng et al. (2012). They performed several experiments including the CTOD test, metallographic analysis and fracture surface analysis on high strength, low alloy steel S335G10+N, which is suitable for marine structures. Welded joints are subjected to different thermal cycles and experience crystallization and solid transformation, which lead to heterogeneity. Samples from weld position (WP), fusion line (FL) and fusion line plus 2mm (FL+2) are used in experiments. In their study, average grain sizes of samples were measured and compared with CTOD values that are listed in Tables 1 and 2. It was observed that average grain size distribution is in agreement with CTOD values. The larger the CTOD, the smaller the average grain size will be.

Table 1. CTOD Values.

Crack position	WP	WP	WP	FL	FL	FL	FL+2	FL+2	FL+2
Specimen	S3553	S3554	S3557	S3556	S35510	S35511	S3551	S3552	S3559
δ_u (mm)	0.583	0.455	0.623	0.596	0.531	-	-	0.837	0.714
δ_m (mm)	-	-	-	-	-	0.889	0.925	-	-
Mean value(mm)	0.554			0.672			0.825		

Table 2. Average grain sizes.

Sample Number	S3557B	S3556B	S3559B
Average Grain Size	9.39	8.40	7.85

In fracture mechanics, crack arrest toughness (K_a) has also become an important parameter to determine the failure characteristics of materials, along with crack initiation toughness (K_c). After crack initiation takes place, it is important to arrest its propagation in order to prevent failure or fracture of the related structure. In the fatigue study field, crack arrest toughness and/or crack retardation effects are also investigated for failure characteristics of structures under several variations of loads, i.e. sea loadings. An et al. (2014) investigated crack arrest fracture toughness (K_{Ia}) characteristics of thick steel base material and its heat-input weld for 50 mm thick high strength shipbuilding steel and concluded that K_{Ia} is a linear function of temperature. In their experiments, while base material (BM) satisfied IACS (2013) rule, this was not the case for the weld material. In addition, they obtained a straight crack propagation path along the fusion line (FL) of weld and that is why investigation into the material properties of the path, i.e. grain size, hardness, Charpy impact energy, was carried out; they found that localised degradation of materials' strength and toughness in the impact notch region of the experimental setup can be the cause of disparities. Note that it is also important to obtain satisfactory fracture toughness values for weld joints of ship structures. Moon et al. (2013) carried out several experiments to obtain CTOD values of API 2W Gr.50 steel at welds and their heat affected zone (HAZ) using two types of welding: submerged arc welding (SAW) and flux cored arc welding (FCAW). Apart from the utilisation of crack initiation and arrest toughness, crack tip opening displacement (CTOD) is a commonly used parameter for evaluating fracture toughness of structures in fracture mechanics. It can be related to the J integral using the plastic constraint factor, m (Equation 2).

$$J = m \cdot \sigma_y \cdot \delta \quad (2)$$

where δ is the CTOD value. From several experiments using two types of welding Moon et al. (2013) concluded that a plastic constraint factor based on the ASTM standard, E1820, does not include the effect of weld process and it is too conservative. They also carried out Charpy impact and hardness tests of

SAW and FCAW welding processes and compared them with each other. They concluded that CTOD values have similar tendencies to impact energy and hardness results.

A comprehensive research study has been made by the Japan Ship Technology Research Association (JSTRA) to prevent failure in large container ships and the results are published by Sumi et al. (2013). They mainly focused on the initiation of brittle crack, fatigue crack growth under several sea loading conditions and investigated crack arrest designs in the deck structure of large container ships for a thickness range of 50 – 75mm steel plates. It is emphasized that allowable initial defects in the weld joints can grow in critical sizes and may cause brittle fracture. They also referred to guidelines published by ClassNK on Brittle Crack Arrest Design for countermeasures of brittle crack propagation. It has also been shown that the most reliable method to prevent crack propagation along welded joints is a weld line shift, as shown in Figure 29.

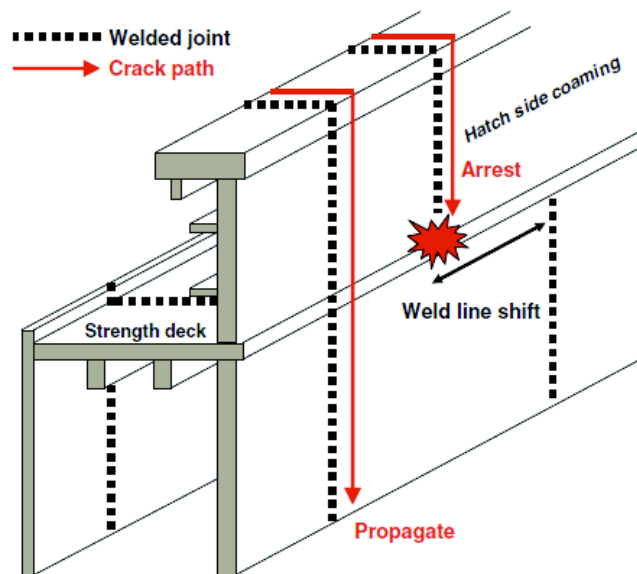


Figure 29. Concept of weld line shift (Sumi et al., 2013).

A more detailed research on fatigue crack growth has been undertaken by Sumi (2014), considering the same locations and thickness ranges of container ships. In this study, fatigue crack growth was simulated using two types of model, 1) crack growth model based on ΔK_{RP} and simple crack growth model, the so-called Paris-Elber law, and 2) a random sequence of clustered loading, the so-called storm model. Fatigue lives of ΔK_{RP} criterion were found to be 2–3 times longer than the simple method, because retardation and acceleration effects cannot be considered by the latter model which does not properly take into account the increase in plastic wake (Figure 30). Crack growth model based on ΔK_{RP} is basically defined by Equation 3; please refer to Toyosada et al. (2004) for a more detailed discussion.

$$da / dN = C (\Delta K_{RP})^m \tag{3}$$

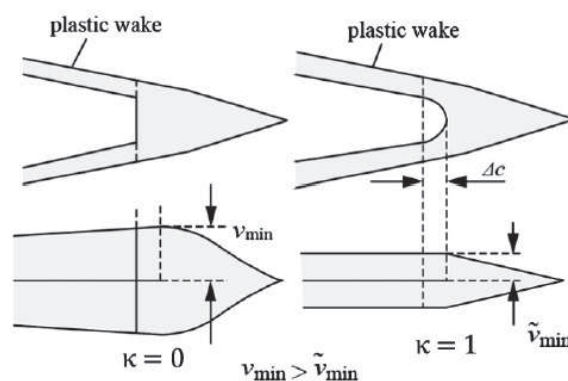


Figure 30. Formation of plastic wake during fatigue crack growth (Sumi, 2014).

In the same paper by Sumi (2014), the effect of slamming-induced whipping stress on fatigue crack growth is also investigated since the longer marine structures mean more slamming-induced vibratory stresses considering their flexible bodies. It is concluded that M-series specimens may be used in order to estimate fatigue crack propagation life under whipping stress. But still further research is needed in this area.

Quéméner et al. (2013b) made a fatigue crack evaluation of stiffened plate longitudinal elements located at the bottom and deck regions of ships where critical bending stresses occur. First, critical crack lengths were evaluated for extreme bending moments which represent the fracture resistance of members based on actual CTOD values and these critical lengths correspond to the fatigue life of each component for which fatigue crack propagation becomes unstable. Another fatigue crack evaluation study for longitudinal elements of ship structures has been undertaken by (Mao, 2014; Mao and Ringsberg, 2013). They considered an effective method for fatigue crack propagation which is based on the narrow band spectral fatigue method and is validated by full scale measurements of a 2800 TEU container ship. In general, ships are subjected to several cyclic loads during their service life and it is hard to expect an occurrence frequency of these loads. Additionally, other uncertainties such as residual stresses from manufacturing, corrosion, weld defects etc. can also cause difficulties in fatigue analysis. So it is highly probable that fatigue cracks may occur earlier than expected. Due to the different approaches that are applied for fatigue strength assessment of ship structures, Fricke et al. (2012) performed several tests using two types of structure, i.e. web frame corners as well as the intersection between longitudinal and transverse web frames, under several loading conditions and all available techniques were applied to models as far as possible. They investigated both large and small scale specimens experimentally and numerically. In their analysis, fabrication-related conditions, welding induced pre-deformations and residual stresses were all included. At the end, they summarized the strength behaviours of the chosen complex welded structures.

Mechanical properties of materials such as fracture toughness, strength, fatigue life can be improved with several techniques. In this respect, Rubio-González et al. (2011) studied duplex stainless steels which are used in different fields including the ship industry. These steels have high strength and excellent fracture toughness as well as high corrosion resistance. They investigated the relatively new laser shock processing (LSP) technique and its effect on mechanical properties of these steels. It was already known that the LSP technique, especially, increases fatigue crack initiation life and reduces the fatigue growth rate of materials. Their work confirmed that the application of LSP on 2205 duplex steel improved fatigue properties and no effect has been found on micro-hardness and microstructure of material but an improvement in fracture toughness was reported. Kim et al. (2012a) studied the mechanical properties of adhesive joints which are used to join stainless steel sheets. Stainless steel sheets have been used at a cryogenic temperature of -150°C for their relatively high mechanical and low coefficient of thermal expansion (CTE) properties in the containment system of liquefied natural gas (LNG) ships. However, adhesives of steel sheets become quite brittle at that temperature and need to be reinforced to improve fracture toughness values. In this study the film-type epoxy adhesive was reinforced with randomly oriented aramid fibre mats. As fracture toughness values are influenced by mechanical properties as well as thermal residual stresses, both properties are investigated. It was found that aramid fibres could reduce the thermal residual stresses between the stainless steel and adhesive layer. The optimum volume fraction of the aramid fibre mats was found to be 16.3% from the double cantilever beam (DCB) tests of the adhesive joint. It was concluded that the adhesive reinforced with aramid fibre mat has a higher load-carrying capacity and fracture toughness at a cryogenic temperature of -150°C than those of other choices, such as polyester or glass fibre mats. An LNG ship's containment system is mainly composed of dual barriers and insulation board. The insulation board must be reliable against leakage of LNG and have a high thermal insulation performance. The reliability of insulation board, considering sufficient fracture toughness at a cryogenic temperature of -163°C , was studied by Yu et al. (2013). Conventionally, the polyurethane foam (PUF) reinforced with glass fibre (RPUF) is used for insulation board to increase fracture toughness. This implementation not only increases costs but also decreases thermal insulation characteristics. As a result the volume fraction of glass fibre is restricted to less than 0.5% and sufficient fracture toughness is uncertain. This uncertainty can possibly lead to crack propagation in insulation board and induce leakage of LNG. Cracks usually initiate and propagate as a result of local tensile stress concentrations due to the temperature change. In this study, the crack resistance of insulation board increased with the reinforcement of glass fibre polymer composite in selective areas which have high stress concentrations. Mainly glass fibre reinforcement sustains high thermal stresses by its high stiffness property. The tensile failure strengths of both a conventional RPUF system and glass composite reinforcement were measured and the safety factor of the latter is calculated as

42% higher than the former by Equation 4 below:

$$\text{Safety factor} = \frac{\text{Failure strength of insulation board}}{\text{Average thermal stress on insulation board}} \tag{4}$$

4.3.1 Crack growth rate model

A very important engineering method used to predict fatigue crack growth is still based on Paris law. A number of modifications to the Paris law have been proposed in recent years to account for different fatigue phenomena such as load sequence effect, load ratio effect, specimen size effect, environmental effect etc., especially load sequence effect. Ship structures are subjected to complex variable amplitude loading (VAL) stress-time histories during their service lives. As a result, many modifications to crack growth rate models are focused on a particular loading mode, such as the retardation effect resulting from the applied peak tensile overload cycles.

Iranpour and Taheri, 2013, 2014 validated the effectiveness of some of the commonly used analytical crack growth models for estimating the fatigue life of the material under the VAL stress-time history using the Willenborg retardation approach, combined with the Walker fatigue model, which has proved to be non-conservative, thus undesirable for design purposes. The differences seen in the prediction of the fatigue life by the use of the widely used Willenborg retardation model, would provide an incentive to researchers to further investigate the influence of the loading effect. Chen et al. (2012) proposed an improved crack growth rate model expressed by Equations (5)–(6) to consider the effect of variable amplitude loading by modifying the crack closure level based on the concept of partial crack closure due to crack-tip plasticity, as shown in Figure 31, which can explain the phenomena of retardation due to overload and the tiny acceleration due to underload.

$$\frac{da}{dN} = \frac{A(K_{\max} - \Phi K_{\text{op}} - \Delta K_{\text{effth}})^m}{1 - \left(\frac{K_{\max}}{K_C}\right)^n} \tag{5}$$

$$\text{where } \Phi = \begin{cases} \left(\frac{a_{\text{OL}} + r_{\text{OL}} - r_{\text{yi}} - r_{\text{UL}}}{a_i}\right)^\gamma & a_{\text{OL}} \leq a_i \leq a_{\text{OL}} + r_{\text{OL}} - r_{\text{yi}} - r_{\text{UL}} \\ 1 & a_i > a_{\text{OL}} + r_{\text{OL}} - r_{\text{yi}} - r_{\text{UL}} \end{cases} \tag{6}$$

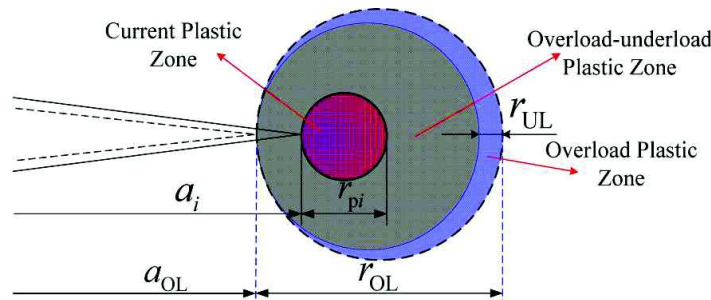


Figure 31. Schematic representation of modifying plastic zone sizes to account for the effect of underload following overload.

Abdullah et al. (2012) tested the applicability of a unified two-parameter fatigue crack growth model for high-low sequence loading conditions and identified some uncertainty parameters to evaluate the prediction accuracy of the model. Dai et al. (2013) proposed a plasticity-corrected stress intensity factor to describe the effects of overload on the fatigue crack growth in ductile materials. From the use of this new crack driving force parameter, a theoretical correlation of the Paris law with crack tip plastic zone is established, which can describe fairly well the effects of the crack length and different loading variables, including the applied stress intensity factor range, load ratio, overload extent and overload number, on the overload retardation. Liu et al. (2013) discussed a new formula under single overload and evaluated the residual life under single overload by adopting a dynamic coefficient mechanics model. Silitonga et al. (2014) pursued a numerical method based on a cohesive zone model aimed at simulating fatigue crack growth as well as crack growth retardation due to an overload. Zhan et al. (2014) proposed a new approximate model for predicting the crack growth rate which can condense the stable crack propagation stage curves for non-zero stress ratios to that for $R = 0$ in a narrow band. By using the new approximate

model, the obtained material constants corresponding to $R = 0$ can be further and widely used for different loading amplitude ratios. All the above mentioned new modified models in recently published literatures are verified by experimental data to some extent.

However, almost all existing fatigue prediction models using fracture mechanics have a reversal-based approach (or cycle-based formulation). However, for most engineering structures, load history is usually very complex and far from being regularly cycled. The conversion from random load history to cyclic load sequence (such as the cycle counting technique) introduces additional complexities and uncertainties in fatigue damage modelling. And the cycle-based approach makes it impossible to continue reducing the time scale for more fundamental investigation since the smallest time scale is one cycle, as shown in Figure 32 (Lu and Liu, 2010). It is also observed that crack growth is not uniformly distributed within a loading cycle and only happens during a small portion of the loading path. Multiple mechanisms exist within one cyclic loading, which is not able to be captured using the classical cycle-based approaches (Zhang and Liu, 2012). The recently developed small time scale fatigue crack growth model can be expressed as follows:

$$da(t) = \frac{ctg\theta}{2} d\delta = Cd\delta(t) \quad (7)$$

where, $C = \frac{ctg\theta}{2}$, δ is CTOD, and θ is the crack tip opening angle (CTOA).

The crack length at any arbitrary time can be calculated via direct time integration as,

$$\int_t^{t+\Delta t} \frac{1}{C\lambda a} \frac{da}{dt} = \int_t^{t+\Delta t} \frac{2\sigma}{1-C\lambda\sigma^2} \frac{d\sigma}{dt} \quad (8)$$

where, λ is redefined as $\lambda = \frac{3\pi}{8E\sigma_y}$ so as to include the hardening effect.

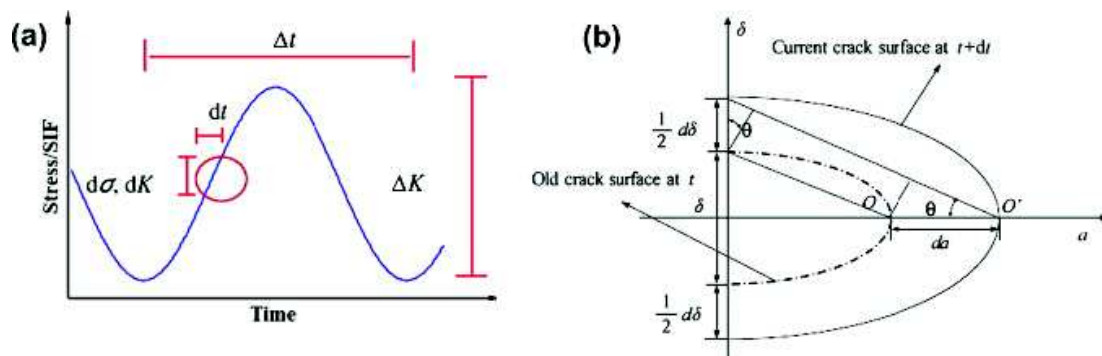


Figure 32. Schematic illustration of the small time scale crack growth model: (a) difference in time scales of the small time scale model and the cycle-based approach; (b) Geometric relationship between crack growth and CTOD (Lu and Liu, 2010; Zhang and Liu, 2012).

4.3.2 Crack growth assessment

Crack path prediction is one of the bases in the remaining life assessment of structures when considering crack growth, crack arrest and the design of critical details. In the past, the crack growth simulation has usually been based on a predefined path. In the last five decades, there have been substantial advances in the understanding and prediction both of the macroscopic aspects of crack paths, largely through developments in fracture mechanics, and in the application of modern computers and microscopes. The papers presented at the International Conference on Crack Paths (CP 2009) show that understanding of crack paths is increasing (Pook, 2013). Judt and Ricoeur (2013) present numerical methods used for predicting crack paths in technical structures, based on the theory of linear elastic fracture mechanics. A precise FE-mesh technique is required, as shown in Figure 33. Several crack extension criteria have been proposed in the past decades to describe crack paths under mixed mode loading conditions, such as maximum principal stress criterion and the minimum extension of the core plastic zone criterion. The crack path is mainly affected by loading conditions, structural details, residual stress distributions and material microstructural features, such as unavoidable inhomogeneities when the conditions of crack initiation and crack growth under fatigue loading have to be evaluated (Brighenti et al., 2012; Sumi and Okawa, 2013). So, in complex conditions, the propagation path was unknown, the accuracy of simulation was decreased and the application of fracture simulation was limited (Chen and Chen, 2012). However, with the development of computational techniques, some researchers developed algorithms to simulate three-dimensional crack growth more precisely under non-proportional mixed-mode loading based on linear elastic fracture mechanics, e.g. Yang and Vormwald (2013). In recent years, (Sumi and Okawa,

2013; Sumi, 2013; Sumi et al., 2013) continuously introduced the computational simulation methods developed for multiple fatigue cracks propagating in a three-dimensional stiffened panel structure used in ships, by taking into account the effects of weld, complicated stress distributions at three-dimensional structural joints, and structural redundancy.

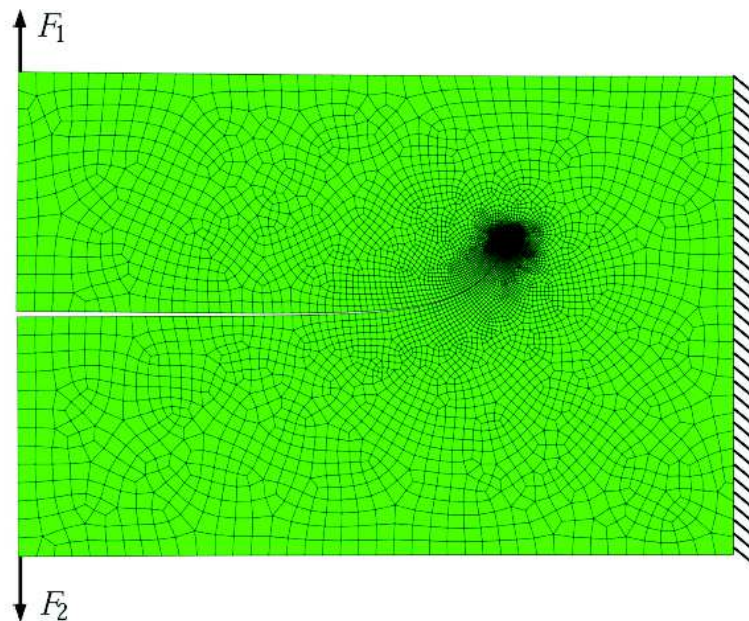


Figure 33. FE-mesh of the grown curved crack shown in a deformed configuration.

Multiple crack identification plays an important role in the vibration-based crack identification of structures. Complex engineering structures with multiple cracks are difficult to simulate accurately. A traditional crack detection method of a single crack is difficult to be used in a multiple crack diagnosis (Li et al., 2013a). Some research efforts in recent years have focused on numerical technique developments on multiple crack initiation and propagation. Kim et al. (2012b) proposed an extended finite element method to be applied to predict lifetime under constant amplitude cyclic loadings of fatigue tests on several multiple site damage specimens. The numerical results were compared to testing data by using Forman and NASGROW fatigue equations. Holländer et al. (2012) developed an advanced numerical algorithm to analyse the multiple crack growth at each crack simulation step automatically in combination with a numerical crack path simulation. The additional crack initiated during the crack growth process is considered in a fully automatic analysis. Oliveira and Leonel (2013) applied a boundary element method to model multiple crack propagation in two-dimensional domains. An interactive scheme is proposed in order to predict the crack growth path using maximum circumferential stress criteria and the crack length increment by using a displacement correlation technique at each load step. The scheme proposed by them is proved to be accurate enough to simulate localisation and coalescence phenomena. Li et al. (2013a) presented a three-step-meshing method for the multiple cracks identification in structures. The multiple cracks quantitative diagnosis process can be successful with an accurate and reasonably finite element structural model whose calculated values of natural frequency agree well with the measured values. Judt and Ricoeur (2013) present numerical methods used for predicting crack paths in technical structures based on the theory of linear elastic fracture mechanics in combination with a smart re-meshing algorithm. Shi et al. (2013) used an extended meshless method, based on partition of unity to simulate multiple cracks, which has a higher computational efficiency and precision compared with the modified intrinsic enriched meshless method. Similar work on meshfree methods to simulate multiple crack growth and coalescence, has been undertaken by Barbier and Petrinic (2013). Pang and Chew (2014) presented an algorithm for multiple surface cracks originating from weld toes. All these efforts are compared with experimental findings to show their accuracy and efficiency, which can provide the basis for further application.

4.3.3 Fracture mechanics based fatigue evaluation of ship structures

Present ship building rules follow the S-N curve approach to evaluate the fatigue damage at identified locations while the use of a fracture mechanics approach has yet to receive due attention. Feng et al. (2012) calculated the crack growth using Paris law on the basis of simulating the fatigue stress

history of ship structures and calculating the stress intensity factors in random sea states. Doshi and Vhanmane (2013) have done some work aimed at exploring the prospect of fatigue evaluation of ship structure detail, such as the connection of the longitudinal stiffener with the transverse web frame, using the fracture mechanics technique. The study is performed on weld details at the mid-ship of an oil tanker vessel. Paris law, combined with model parameters reported by others, are used. Randomness in the crack size, crack growth model parameters and loads has been considered and the results are thus presented within a probabilistic framework using Monte Carlo simulations. It is observed that the fracture mechanics based fatigue life predictions are in good agreement and conservative compared to the predictions using the S-N curves, as given in the common structural rules. Bardetsky (2013) analysed the progressive structural failure caused by cracks emanating from the damaged area by using a procedure for predicting the crack propagation under sea wave loading and based on Paris law combined with a finite element model to calculate the stress intensity factor. The procedure for the estimation of the crack propagation is implemented for a typical modern 170,000 DWT bulk carrier in full load condition. Quéméner et al. (2013a) investigate the fracture failure of ship longitudinal members, constituted of a stiffener and its attached plate, in which a crack has propagated by fatigue from either the stiffener flange or fillet weld. The study employs the failure assessment diagram methodology to assess the conditions of failure at the crack tip, which enables determining critical fatigue crack lengths corresponding to the maximum longitudinal stresses derived from extreme loads. Zilakos et al. (2013) established a common base for evaluating difference crack arrest technologies following the guidelines proposed by the CSR based on the Paris law.

To sum up the recent research work, fracture mechanics based methods have attracted attention but the footsteps stop in the Paris law. More progress has been made on the crack growth theory which requires more research work for application in the fatigue life assessment of ship structures.

4.4 Rules, standards & guidance

4.4.1 Ship rules

Harmonized Common Structural Rules (CSR-H)

Some of the highlights of CSR-H in comparison with CSR-OT and CSR-BC are as follows:

1. *Loads*: CSR-H uses the Equivalent Design Wave (EDW) load approach, which is similar to CSR-BC; however, CSR-OT uses the envelope load approach. Oblique Sea (OS) load cases are included in CSR-H but are not considered in CSR-BC and CSR-OT.
2. *Probability level*: In both CSR-BC & CSR-OT, the probability level of 10^{-4} is used for fatigue load calculation; however, in CSR-H the 10^{-2} probability level is used. This change in level of probability is because loads at this probability level have maximum contribution to damage, and fatigue life shows less sensitivity with the Weibull shape parameter.
3. *Details to be assessed using very fine mesh analysis*: In the case of CSR-OT, only the hopper knuckle connection is considered for fatigue assessment by using very fine mesh analysis, but in CSR-H some more details are considered (e.g. connection of lower stool to inner bottom plating, etc.)
4. *Fatigue assessment by screening*: This method is newly introduced in CSR-H; in this method fine mesh analysis with 50 mm mesh size at given locations is carried out and the obtained stress is multiplied by a stress magnification factor (SMF), to obtain the hot spot stress. This stress is used to determine fatigue life. This type of fatigue screening is not available in both CSR-OT & CSR-BC.
5. *Reference stress for hot spot stress calculation*: CSR-H uses principal stress within $\pm 45^\circ$ as well as outside $\pm 45^\circ$ with respect to normal to the weld. Stress obtained outside $\pm 45^\circ$ is multiplied with factor 0.9, to take into account the effect of the S-N curve. The maximum stress range out of the two is chosen for fatigue life calculation. CSR-OT uses stress normal to the weld and CSR-BC uses principal stress within $\pm 45^\circ$ with respect to normal to the weld.
6. *Calculation of stress range*: In CSR-H, stress range and mean stress, for a particular loading condition are calculated using individual stress components for load cases i_1 and i_2 . However in CSR-BC, the stress range and mean stress are calculated using principal stress in individual load cases i_1 and i_2 . CSR-OT uses stress combination factors for the calculation of stress range.
7. *Fatigue assessment at stiffener end connections*: The nominal stress approach is used in CSR-OT, and the notch stress approach in CSR-BC. In CSR-H, the hot spot stress approach is used for fatigue assessment at stiffener end connections.

8. *Stress due to relative displacement:* In CSR-BC and CSR-OT, two separate approaches are used to calculate stress due to relative displacement. These individual approaches are kept as they are for bulk carriers and oil tankers, in CSR-H.
9. *Special procedure for web stiffened cruciform joints:* In CSR-H, a special procedure has been introduced (considering bending effect) for hot spot stress calculations for web stiffened cruciform joints. In CSR-BC, for the assessment of stress in a cruciform connection, stress correction factor λ is used, which is based on the angle between intersecting plates. CSR-OT uses stress normal to the weld.
10. *Corrosive environment consideration:* CSR-BC and CSR-OT use factors f_{coat} and f_{SN} respectively to take into account the effect of corrosion. However CSR-H uses two different S-N curves to calculate individual damages (in air, in corrosive environment), and finally added to obtain fatigue life.
11. *Thickness correction:* CSR-BC uses thickness correction factor f_{thick} which is a function of thickness of the member. In CSR-OT, thickness effect is included in the type of S-N curve used. CSR-H uses factor f_{thick} , for the correction of thickness effect; this factor is a function of thickness of member and the attachment types.

Fatigue assessment of ship structures–DNV guideline

This Classification Note is intended to give a general background for the rule requirements for fatigue control of ship structures, and to provide detailed recommendations for such control.

In the DNV GP RP 0005 (2014) version the requirements are aligned with DNV Ship rules and IACS CSR-H rules for specific details. In addition improved formulations and less conservative approaches for details with limited damage experience have been included.

Fatigue assessment of ship structures–ABS guideline

ABS (2012) is an update of ABS (2009) which has introduced a new guideline to provide supplementary requirements for the application of higher-strength, thick steel plates, i.e. greater than 51 mm, within the structure of large container carriers. The requirements given in the guideline are based on extensive experience with the design, construction and in-service performance of large and ultra large container carriers.

When the hull girder strength is designed to the rules' minimum requirements, the accompanying effects of higher-strength thick steel plates are largely associated with higher stress levels and reduced fatigue and fracture strength characteristics. In the upper flange of the hull structure, wave-induced fatigue damage of the thick plated weld connections is absolutely critical. As a countermeasure, the fatigue behaviour of these weld connections is to be extensively evaluated to avoid crack initiation. Satisfactory fatigue and fracture characteristics are to be attained from improvements in structural design measures, steel materials, welding consumables, welding procedures and post-weld enhancements.

In this guideline, special attention is provided for the butt welds and hatch corners of upper flanges for the high strength thick steel plates of H40 or H47 grade steel. In order to minimise the fatigue failures of thick plates in the container ship, the rules recommend the construction procedures, weld treatment methods and fatigue design procedures specific to the thick plates. The guideline also incorporates the effect of springing and whipping on the fatigue strength of upper flange of hull structure. ABS (2012) pays special attention to fracture avoidance, particularly by using inserted plates as crack arrestors.

Fatigue assessment of ship structures–LR rule

As part of the Lloyd's Register (LR) ShipRight design and construction procedures, LR has developed a fatigue design assessment procedure, ShipRight FDA ICE (2010), to assess the fatigue damage of ship structure induced by ice loads for ships navigating in ice covered regions.

The ShipRight FDA ICE assessment procedure examines ship-ice interaction loads, ice-load impact frequency, ice-load distribution, structural responses and the fatigue behaviour of hull structures in cold temperatures, including associated fatigue responses. The fatigue-response assessment is determined for different winter conditions and ice thicknesses on typical routes for winter trade.

Zhang et al. (2011) presented the salient features of the Ship Right FDA ICE guideline. It is explained by the authors that compared to non-ice classed ships, ice classed ships have increased scantlings to strengthen the hull structure against ice loads; it is normally expected that ice classed ships would have fewer cracks and fractures due to fatigue. The data analysis, however, shows the opposite, which implies that cracking of the hull structure caused by cyclic ice loading during ships' navigating in ice regions is an important phenomenon that warrants investigation and assessment in the structural design of the ships.

Fatigue assessment of ship structures–GL rule

GL (2012) introduced guideline for the fatigue analysis of racing yacht keels. The method of calculating dynamic stress amplitudes and fatigue calculations at keel connections are described in the rule. The rule is applicable for fatigue analysis of Yachts with a canting keel as well as those with a fixed keel.

GL (2013) introduced a guideline to assess the high frequency hull girder response of container ships. This guideline was established to aid the designer in assessing the effects of hull girder fatigue loads caused by the high frequency response of the ship's structure. It comprises a semi-empirical approach based on the results from the measurement campaigns as well as on collected damage data from the fleet of container ships, currently classed by Germanischer Lloyd. The method used reflects all kinds of hull girder vibrations, including whipping and springing. These high frequency loads are transferred to any considered container ship as a function of averaged rule slamming pressures which are considered to comprise parameters important for high frequency ship response.

In GL (2014) the thickness effect for fatigue strength was updated. Now as well as the geometrical notch effect, the requirement comprises a consideration of the allowable axial misalignment. Finally, for butt welds with standard quality (FAT80) a moderate thickness exponent of only 0.1 is required.

Fatigue assessment of ship structures–BV rule

BV NR 583 (2012) is dedicated to long term loading calculation when springing or whipping is prone to occur. Fatigue is concerned both for linear quasi-static and dynamic fatigue damage, and non-linear fatigue assessment including whipping. Quasi-static and linear dynamic assessment may be carried out by a spectral analysis, when non-linear fatigue needs a time domain analysis.

BV NR 483 (2011) is dedicated to Naval ship design. Fatigue rules are very similar to rules applicable to merchant ships but due to specific operating conditions, naval ship loads are different, e.g. longitudinal bending moment depends on the characteristic Froude number, and may be corrected by a factor taking into account dynamic loads due to bow flare impact.

IACS URS 3

These unified requirements deal with the use of extremely thick steel plates, mainly on container ships. It is intended to define either structural arrangements or material properties leading to stopping a sudden break propagating, starting from an undetected defect. It is applicable for thick plates such as container ships' decks and for higher tensile steels.

4.4.2 Design codes for Offshore Structures

DNV (Fatigue Design of Offshore Steel Structures)

DNV GP RP 0005 (2014) deals with the fatigue design of offshore structures. Fatigue assessment can be carried out based on the S-N curve approach or fracture mechanics approach. In the present version of the code, the stress concentration factors for tubular butt weld connections due to eccentricities (due to the change in thickness or misalignments) have been updated. Stress concentration factors have also been updated for members of equal thickness.

Recommendations for applicable S-N curves at the inside of tubular joints and S-N curves for piles have been added. In addition a section on thickness effect for butt welds and cruciform joints has been added and the thickness exponent for S-N class C and C1 has been modified.

DNV RP-C206 (Fatigue Methodology of Offshore Ships)

DNV RP-C206 (2012) has moved design fatigue factors and details to be assessed to DNV OS-C102 (2012). Criteria related to initial fatigue assessment are updated (stress concentration factor k_g).

ABS (Fatigue Assessment of Offshore Structures)

ABS (2013) (fatigue) has updated requirements related to the benefits due to grinding, in the case of the tubular intersection connections. The use of grinding is allowed, and the requirements for the same are specified. A benefit factor of '2' is also applicable in the case of ultrasonic/hammer peening providing suitable documentation is provided.

BV NR593 Ship Conversion into Surface Offshore Units and Redeployment of Surface Offshore Units

BV NR 593 (2012) is dedicated to the assessment of converted marine structures. Fatigue assessment involves both fatigue due to operation before conversion and expected fatigue after conversion.

Evaluation of fatigue due to operation before conversion may take advantage of the knowledge of actual loading conditions. Within the standard, repaired details are considered as having a damage corresponding to their actual life.

BV NR578 Rules for the classification of Tension Leg Platforms (TLPs)

BV NR 578 (2012) is dedicated to the assessment of TLP fatigue requirements involving both hull and Tendon Leg Systems (TLSs). Depending on the linearity of loading, spectral analysis is proposed, or time domain analysis is required. When appropriate, deterministic analysis is accepted. Fracture mechanics are also considered as an alternative approach.

BS 7910

BS 7910 (2013) is intended to justify the ability of structures to resist loading, by considering different failure modes such as fatigue but mainly concentrating on crack propagation and unstable cracks. BS 7910 is currently used to assess, on offshore structures, the ability to postpone repairs when cracks are discovered during inspection. It has been updated from BS:2005, adding annexes on NDT and corrosion. It has been drastically modified for the analysis of unstable fracture mechanics using FITNET and R6 results.

The fracture strength reference has been shifted from critical CTOD to critical Stress Intensity Factor (K_{mat}). The effect of the residual stress contribution to the stress intensity factor has been reanalysed, and total stress intensity factor now involves three components: one dealing with tension stresses, another dealing with bending, the last one corresponding to a residual stress, stress intensity factor based on a design residual stress distribution. For a crack length greater than the thickness of the structure, it results in a less conservative approach than in the 2005 revision. A procedure has been developed to avoid an over-conservatism related to shallow crack effect (constraint effect).

4.4.3 IIW recommendation

Document IIW (2013c) XIII-2460-13 is an IIW document following Document XIII-2151-r4/XV-1254-r4 dealing with the fatigue of welded and cut structures or components. In particular, this document provides procedures to check fatigue life according to nominal stress, structural stress or effective notch stress analysis. In addition, with this last document, a crack propagation procedure is developed, and a background document has been drafted for traceability reasons.

Document IIW (2013a) XIII-2301r3-13 is an incomplete draft to Guideline Weld quality; in relation to fatigue strength it reanalyses the current welding quality standards in order to clarify the criteria dealing with fatigue performances. The quality criteria are ranked according to their sensitivity to fatigue life with respect to the weld design. Considerations are provided for the inspection methods and the consequences on fatigue strength confidence.

Document IIW XIII-2380r3-11/XV-1383r3-11 provides a comprehensive description of methods to analyse fatigue strength in the weld bead commonly called root crack fatigue. Up to now this analysis is not explicitly considered in ship rules, but implicitly through the requirements of minimum weld throat. With the higher strength characteristic of modern steels, the relevance of these requirements have to be examined.

4.4.4 ISO Standards

ISO/TR 14345:2012 (2012) is guidance on the best practices for fatigue testing under constant or variable amplitude loading, including specimen selection, e.g. measurement of radius at weld toe, monitoring of testing itself and data treatment of testing results to obtain a fatigue strength including data sheet. This ISO document has been developed as Document XIII-2140-6 within the IIW framework.

ISO 12110-1:2013 (2013) and ISO 12110-2:2013 (2013) deal with variable amplitude load testing. The documents in addition to describing the overall test parameters focus on methods for cycle counting and signal reconstruction.

Although different counting methods are enumerated, the second part of ISO 12110 focuses on rain flow counting and provides numerical examples allowing assessment of the software using the rain flow method.

4.5 Acceptance criteria

Traditionally, the acceptance criteria for the high-cycle fatigue strength assessment of a structural component are established based on the design fatigue life and the applied safety factor. If the calculated fatigue life exceeds the design life divided by the applied safety factor, the fatigue strength of the

component is considered to meet the design requirements. Otherwise, the component should be redesigned to satisfy the requirements.

As for the assessment of fracture resistance, the so-called Failure Assessment Diagram (FAD) (API RP 579-1/ASME FFS-1, 2007; BS 7910, 2013) is normally performed based on the principles of fracture mechanics. Typically, the vertical axis of the FAD represents a ratio of the applied conditions to the conditions required to cause fracture and the ratio of the applied load to that required to cause plastic collapse is plotted on the horizontal axis. Fracture mechanics analysis for a crack provides either the coordinates of an assessment point or a locus of points. These positions are compared with a defined assessment line to determine the acceptability of the crack.

Recently, the acceptance criteria were also developed for fatigue and fracture assessment under extreme environmental loading. This development was triggered by the unexpected large number of cracks observed in many platforms in the Gulf of Mexico after hurricanes passed. API RP 2T (2010) recommended a so-called “single event fatigue” analysis, in which components that are susceptible to low-cycle/high-stress fatigue should also be analysed to assess fatigue damage during a rare/extreme event that may be of extended duration, such as a 48-hour rise and fall of a 100-year storm. Analyses have found that fatigue damage during such a rare/extreme event may be comparable or even higher than high cycle fatigue accumulation over the service life.

Chen et al. (2012) developed acceptance criteria to determine the minimum allowable size of a crack-stopping hole. The limiting condition of this stopping hole is that no new crack would initiate from it when the structure is subject to a storm with a return period of one year or longer. The time to initiate a new crack at a crack-stopping hole was predicted based on the low-cycle fatigue analysis. A safety factor of 3 was selected such that the predicted crack re-initiation time would be 3 times longer than the time needed for the cracked structure to sail to a repair facility.

4.6 Measurement techniques

4.6.1 Crack growth and propagation

Conventional experimental techniques, such as strain gauge, photo elasticity and more interferometry, have been used to determine stress intensity factors (SIFs) during recent decades. Although these techniques have greatly improved the accuracy of SIF measurement, they also have some limitations. For example, the angular and radial locations of strain gauges are complicated to determine when measuring the SIF near the crack tip region. Sarangi et al. (2013) conducted experiments to determine the optimal strain gauge locations, and results showed that highly accurate values of SIFs can be obtained if the strain gauges are placed at the optimal locations. Chakraborty and Murthy (2014) proposed a new single strain gauge technique for accurate determination of mode I SIF in orthotropic composite materials. Their research also demonstrated the existence of reasonable strain gauge locations.

In the last few years, digital image correlation (DIC) techniques have become increasingly popular due to their simplicity and effectiveness. Pataky et al. (2012) developed an anisotropic least-squares regression algorithm using displacements from DIC to find the effective SIFs, including KI, KII and T-stress. They studied the effects of anisotropy during mixed mode fatigue crack growth in single crystal 316L stainless steel, and determined crack tip plastic zones using an anisotropic yield criterion. Strains in the plastic zone obtained from DIC showed a dependence on the crystallography and load ratio. Crack tip slip irreversibility was also measured and showed an increasing trend with increasing crack length. In parallel, Zhang and He (2012) investigated the determination of the mixed-mode SIFs using the DIC method. Experiments were performed on an edge fatigue cracked aluminium specimen and the full-field displacements around the crack-tip region of the test sample were calculated using DIC, and then the SIFs associated with unavoidable rigid-body displacement motion were calculated from the experimental data. A coarse-fine searching method was developed to determine the crack tip location. This proposed technique is validated by comparing it with the theoretical results of SIF, which show DIC to be a practical and effective tool for full-field deformation and SIF measurement.

For small fatigue cracks (physical size of the order of 500 μm), Lachambre et al. (2014) utilized X-ray tomography to monitor the initiation and growth of a 3-D fatigue crack in a nodular cast iron sample, and SIF values along the curved crack front were extracted from displacement fields by digital volume correlation (DVC) technique. The obtained results of SIF were in agreement with analytical calculations and showed variations: larger values of SIF were found close to the sample surface, which was attributed to a higher level of closure compared to the bulk of the specimen. However, the presented method is limited by the relatively large size of the nodules.

In addition, Shlyannikov and Zakharov (2014) investigated the fatigue crack growth behaviour in the elastic-plastic stress fields; the distributions of the governing parameter of elastic-plastic stress fields, the In-factor, have been determined in various specimens. Biaxial and mixed mode fatigue crack propagation tests have also been carried out on cruciform and compact tension shear specimens, and discrepancies in fatigue crack growth rate have been observed in various multiaxial loading conditions. The experimental results provided the opportunity to explore the suggestion that multiaxial fatigue crack propagation may be governed more strongly by the plastic SIF than the magnitude of the elastic SIFs alone. Both the In-factor and T-stress are used as the main parameters of the elastic-plastic SIF, which is sensitive to the in-plane and out-of-plane constraint effects.

4.6.2 Fatigue

By using DIC and electron backscatter diffraction (EBSD) techniques, Carroll et al. (2013) presented the sub-grain level full field plastic strain accumulation, near a growing fatigue crack, measurement results for the first time. In these experiments, inhomogeneities were observed in the strain field behind the crack tip in both macro- and micro-scales which suggests the necessity for using crystal plasticity models to capture an accurate fatigue behaviour.

By following a different approach, Rethore et al. (2012) performed *in situ* fatigue experiments using a tomograph. In order to extract displacement fields and crack geometry from images, digital volume correlation was utilized. As part of post-processing, crack front positions and stress intensity factor ranges were obtained which were used to extract local Paris law coefficients.

Temperature change can also be used as a good fatigue damage indicator. Wang et al. (2010) developed a Quantitative Thermographic Method to assess the residual fatigue life and perform non-linear stress measurement. The technique allows obtaining several fatigue parameters including fatigue limit, S-N curve and residual fatigue life. Furthermore, in-depth analysis of stress concentration zones was done by using lock-in thermography. Moreover, Amiri and Khonsari (2012) proposed a technique for the estimation of remaining fatigue life (RFL) by using the slope of the temperature rise as a function of time. By using the thermography technique, their results showed that as the materials age, the slope of the temperature increases.

For very high cycle regime conditions, Stanzl-Tschegg (2014) investigated the characterization of the fatigue properties of materials and components at a very high cycle fatigue regime. It was concluded that ultrasonic machines are the most suitable for characterization in these cases. The main advantages of ultrasonic machines are time and energy saving, no need for water cooling equipment, low maintenance costs and low noise. As an example, Heinz et al. (2013) performed ultrasonic fatigue tests for the very high cycle fatigue regime up to 10^{10} cycles. Moreover, they used 3-Dimensional laser scanning vibrometry to investigate the oscillation behaviour of the specimens in different fatigue states and to perform non-contact strain measurements during ultrasonic fatigue loading. Furthermore, Müller and Sander (2013) also used an ultrasonic fatigue testing system for a very high cycle regime to investigate the effect of variable amplitude loading. The potential drop technique was also utilized to quantify crack growth in conjunction with an optical microscope for surface crack measurement.

There are three different available techniques to measure slip during fretting fatigue experiments; clip gauge, Wittkowsky and DIC. Clip gauge technique characteristically captures a significant amount of elastic deformation of the surrounding material since it measures the slip remotely. This problem is eliminated in the Wittkowsky technique. However, this approach suffers from calibration inaccuracies. The DIC technique developed by De Pauw et al. (2014) allows measuring global slip closer to the contact region while eliminating the effect of elastic deformations. Moreover, Meriaux et al. (2010) developed a dual-actuator fatigue set-up which is capable of separating the fatigue and the fretting load. The test set-up contains a potential drop technique device in order to accurately detect crack nucleation and propagation. The technique allows detection of cracks as small as $50\mu\text{m}$ in size.

The analysis of experimental data is of paramount importance. Full-scale component fatigue tests are complex and several effects should be accounted for in order to apply such results to fatigue assessment procedures, for example: scale effects, fabrication imperfections and defects, environmental conditions, loading conditions, etc. Notable examples are provided in (Kim et al., 2010; Rother and Rudolph, 2011; Fricke et al., 2012; Li et al., 2013b; Fricke and Feltz, 2013). The Benchmarking study reported in this document is also an example illustrating the complexities of component testing and interpretation of results.

Validation of assessment approaches with experimental data need particular care and often data available in literature are not complete and sufficient for the intended purpose. Often, component testing carried out in

past years does not distinguish clearly the crack initiation and/or the failure criteria making it rather difficult to use such data for comparison of newly proposed methods.

4.6.3 Material properties

The principal material properties required for fatigue and fracture mechanics analysis include modulus of elasticity, E , yield strength, σ_y , tensile strength, σ_u , constants C and m in Paris law, fracture toughness data (K_{Ic} , J values, and crack tip opening displacement, CTOD), n' , cyclic strain hardening exponent, b , fatigue exponent, c , fatigue ductility exponent, K' , cyclic strength coefficient, σ_f' , fatigue strength coefficient, ϵ_f' , fatigue ductility coefficient, etc.

E , σ_y , and σ_u can be determined from the tests in terms of standards, e.g. (BS EN ISO 6892-1 Metallic materials, 2009; BS EN ISO 6892-2 Metallic materials, 2011; ASTM Standard E8 / E8M-13a, 2013; ASTM Standard E111-04, 2010), etc., σ_y is to be taken as either the lower yield or the 0.2% proof strength depending on the material type. The constants C and m in Paris' law may be determined from the tests according to standards, e.g., ASTM Standard ASTM E647-13a (2013), BS ISO 12108 Metallic materials (2012), etc. The constants C and m also depend on the material and the applied conditions, including environment and cyclic frequency. K_{Ic} , J values, and CTOD can be determined from the tests in accordance with standards, e.g. ASME E399, BS EN ISO 15653 Metallic materials (2010), etc. n' , b , c , K' , σ_f' , and ϵ_f' can be determined from the tests provided in standards, e.g. ASTM Standard E606 / E606M-12 (2012), BS 7270 Metallic materials (2006), ISO 12106 (2003), etc.

4.6.4 Fracture toughness

Fracture toughness is considered to be one of the key input material properties for fatigue life assessment based on fracture mechanics. In recent years, there have been some new developments on this topic. Many researchers studied the fracture toughness under different temperatures and for different components. For example, Ganesh et al. (2014) studied the initial fracture toughness (J0.2) and critical crack tip opening displacement fracture toughness values of laser rapid manufactured structures. The fracture toughness is usually obtained by using laboratory size specimens that meet certain requirements. This represents a major challenge due to the pronounced effect of the specimen size on the mechanical and fracture properties. Fatigue pre-cracking of the specimens, in order to obtain sharp crack, is one of the standard procedure conditions to determine the plane strain fracture toughness, which is a costly and time consuming process. Then some researchers tried to find the relationship between the fracture toughness value and other material or structural properties. Pettinà et al. (2014) presented a virtual testing tool with a fracture toughness determination module to estimate fracture toughness vs. specimen thickness. It is realized from transforming the simple tensile tests of the material. Mourad et al. (2013) investigated the effect of specimen notch radius r and specimen size (thickness B and ligament b) on the apparent fracture toughness $K_{Ic,app}$ and verified the equations for predicting the apparent toughness by comparing with tests, as shown in Figure 34. Two models have also been found in this research work to reasonably predict the apparent fracture toughness $K_{Ic,app}$ values, one of which can be expressed by:

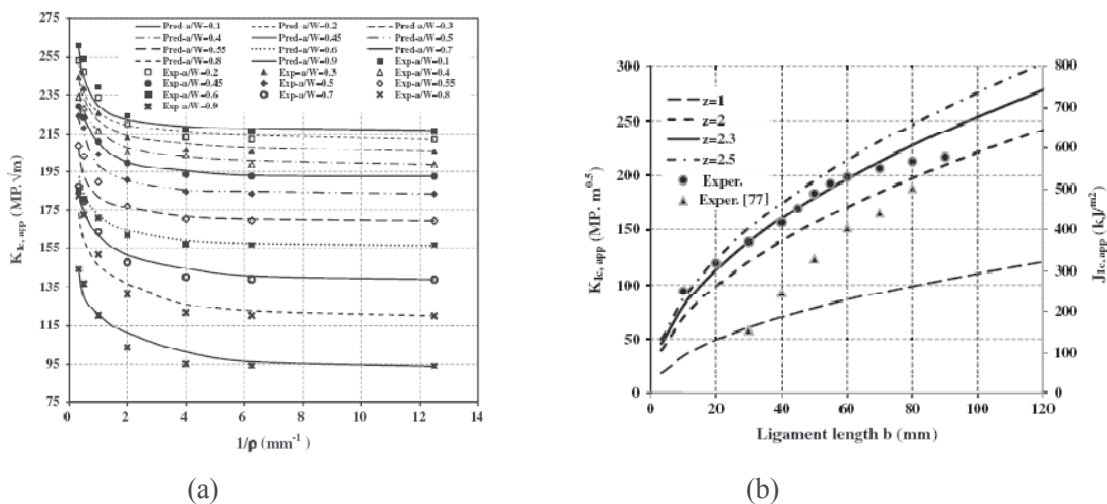


Figure 34. (a) The apparent critical fracture toughness $K_{Ic,app}$ as a function of the ligament length b and compared with experimental results (J_{Ic} vs. b for $q = 0.05$ mm); (b) Predicted $K_{Ic,app}$ compared with the experimental data.

$$K_{l,app} = K_{lc,app} + (P_{max} / B\sqrt{W}) \cdot e^{-(r_p/\rho)} \cdot f(a/W) \quad (9)$$

where B is the specimen thickness, W is the specimen width, P_{max} is the maximum load and $K_{lc,app}$ and m are two constants, $f(a/W)$ is the geometry factor, r_p is the plastic zone size. The two constants $K_{lc,app}$ and m can be determined by testing two specimens with different ρ .

5. BENCHMARKING STUDY

Increasing needs to have higher payload-to-structural weight ratio have increased the need to study lightweight, structural solutions in ships. This is especially important in ships where structural weight is a significant part of the displacement, e.g. passenger ships. The previous committee Horn et al. (2012a) carried out a benchmark investigation on the bulkhead structures of passenger ships and focused on the fatigue damage assessment under multi-axial stresses. Another way to reduce weight is to decrease the plate thickness of the passenger decks within the superstructure. However, this requires design around the minimum plate thickness requirement of 5mm, set typically by the classification societies. Thus, the starting point of this Benchmarking study is the discussion of the previous committee work on plate thickness effect (Horn et al., 2012a). The issue was raised by the official discussor, Bacicchi, who stated that recent experimental work has shown an increasing trend of fatigue strength for decreasing plate thickness in the thickness range of $t = 5\text{mm}$ to $t = 20\text{mm}$. The question was commented upon by Professor Fricke who stated that at thicknesses around 5mm, the fatigue strength actually shows a decreasing trend based on recent experimental findings. Since 2012, fatigue tests have been carried out in the range from 3mm to 6mm (Fricke et al., 2013a; Fricke and Feltz, 2013; Lillemäe et al., 2012; Remes and Fricke, 2014) in the large EU-project BESST (Breakthrough in European Ship and Shipbuilding Technologies) involving all the major European shipyards. Their experimental evidence has been provided to complement this discussion, and is described below to identify the limitations for the Benchmarking study.

Typically welding processes are developed by butt- and T-joint welding experiments to optimize the welding parameters and weld geometry, and mechanical properties. A dog-bone specimen is commonly used in fatigue tests during this process; see Figure 35. Lillemäe et al. (2012) showed that both the shape and magnitude of the welding-induced initial imperfections have a large impact on the fatigue strength of the thin and slender butt-welded specimens. When the shape and geometrical non-linearity were taken into account, the test specimen straightening was properly modelled. Their investigation showed that in this case the fatigue strength defined, based on notch or structural stress, corresponds to that of the thicker plates. They also showed that the relationship between structural and notch stress is constant; thus the emphasis should be put on the structural stress and how it develops during straightening. Fricke et al. (2013a) extended these findings for larger experimental sets of both butt and fillet welds. They also noted that the slope issue needs further investigations as the normally used slope of $m = 3$ results in non-conservative fatigue strength in comparison to design curves. The slope of $m = 5$ gave a better agreement between the test results and existing design curve. A slope of '5' is also recommended by Sonsino et al. (2010) for thin plates below $t = 5\text{mm}$. Remes and Fricke (2014), using structural stress assessment and different stress extrapolation strategies showed that there is no beneficial plate thickness effect if the butt and T-joints of 3–4 mm and 6–8 mm specimens are compared. However, they also showed that the weld quality and especially the undercuts have a significant impact on the strength of thin-plates, especially in the high-cycle domain. They further showed that accounting for undercuts and carrying out the stress extrapolation through the thickness and using geometrically non-linear analysis would result in smaller scatter in the predicted fatigue life and proposed that the influence of undercuts be taken into account in FEM modelling emphasising the role of specimen shape.

Based on these observations, this Committee decided to focus on the assessment of structural stresses in thin slender specimens. Altogether, seven parties using ten different approaches contributed to the Benchmarking study.

5.1 Problem Statement

A dog-bone specimen was selected for this Benchmarking study. The specimen represents the average geometry of 10 specimens produced by arc welding (Lillemäe et al., 2012). The specimen is curved and the geometry is shown in Figure 35. It has a length of $L = 250\text{ mm}$, width varies from $B = 50\text{ mm}$ at the ends to $B = 20\text{ mm}$ at the middle. The radius of $R = 160\text{ mm}$ defines the dog bone shape where the curved shape is also given in terms of coordinates, weld details and load and boundary conditions.

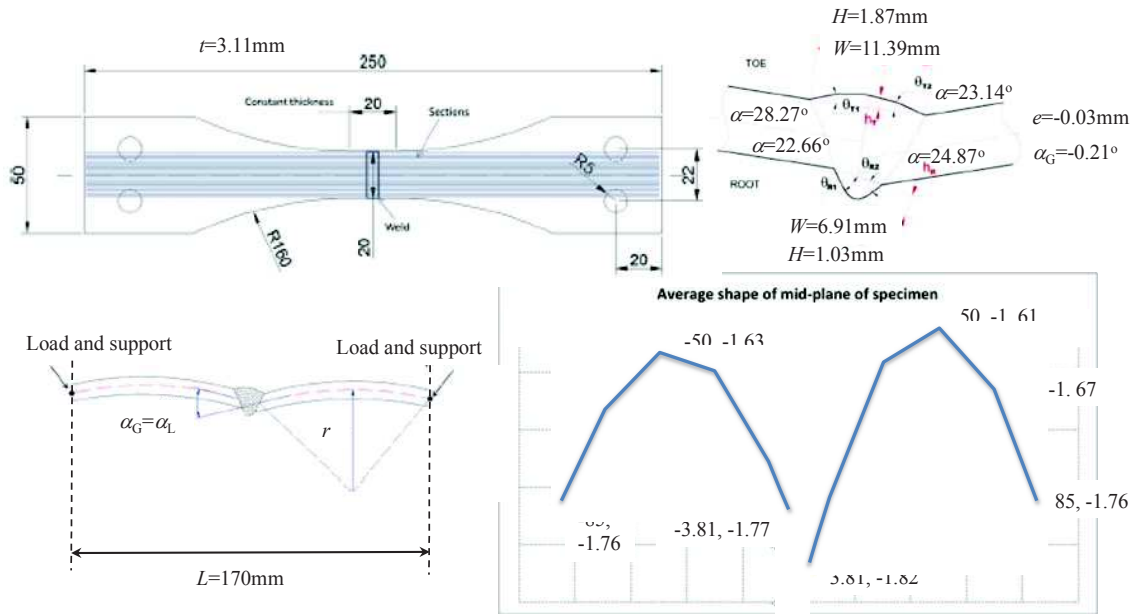


Figure 35. The “dog-bone” specimen.

This kind of specimen is typically assessed using stress-based fatigue assessment methods. The peak stress at the weld notch, σ_{notch} ; see Equation 9, is needed for fatigue assessment. This can be obtained using a notch stress approach where the shape of the specimen and the weld is modelled explicitly. However, the approach suffers from considerable modelling efforts, thus structural stress, σ_{HS} , and nominal stress, σ_{nom} , can also be used as input for the fatigue assessment. In the case of the structural stress method, the notch stress can be approximated using calculated structural stress, σ_{HS} , and notch factor, K_w . In the case of the nominal stress method, the same is obtained by replacing, structural stress with the product of nominal stress, σ_{nom} , by the stress magnification, k_m ; i.e.,

$$\sigma_{Notch} = \sigma_{Nom} \cdot k_m \cdot K_w = \sigma_{HS} \cdot K_w, \tag{10}$$

An objective of the Benchmarking Study is to understand the range of predicted k_m values when different analysis approaches are used. Special emphasis is put on the influence of geometrical non-linearity.

The specimen is exposed to tensile loading with a load ratio of $R = 0$ and a nominal stress level of $\sigma_{nom} = 30\text{--}200\text{MPa}$. Both ends of the specimen are free to rotate around the y-axis, i.e., the secondary bending effect due to clamping is neglected. The distance between the load introduction points is 170 mm while the entire length is 250 mm. During the fatigue test, the specimen straightens. The material is steel with $E = 206\text{GPa}$, $\sigma_y = 355\text{MPa}$ and $\nu = 0.3$.

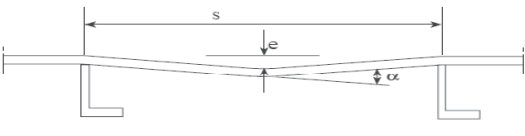
5.2 Analytical Methods

The stress concentration factors were obtained according to the following codes.

- DNV (2003)– Classification Note No. 30.7 Fatigue Assessment of Ship Structures February 2003, taking into account the effects of axial and angular misalignment, multiplying these and using the initial, undeformed shape to define k_m ,
- RINA Rules (2014) for the classification of ships, 2014 edition, taking into account the effects of axial misalignment only and using the initial, undeformed shape to define k_m ,
- IIW (2013b) Fatigue Recommendations IIW-doc. XIII-2460-13/XV-1440-13 (rev. April 2013) taking into account the effects of axial and angular misalignment and using the deformed shape to define k_m .

It is worth noting that IIW recommendations account for the reduction of angular misalignment due to acting membrane stress. RINA Rules are not specifically suited for the assessment of butt joints of tensioned plates and even less of very thin plates rather the focus is on ship structural details.

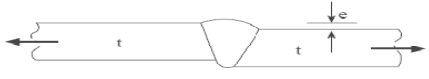
DNV

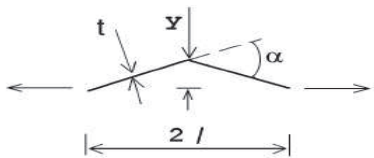
Geometry	K-factor
<p>10.4.a</p>  <p>Default: $e = 6 \text{ mm}$</p>	<p>Angular mismatch in joints between flat plates results in additional stresses at the butt weld and the stiffener</p> $K_{\alpha} = 1 + \frac{\lambda}{4} \alpha \frac{s}{t}$ <p>where: $\lambda = 6$ for pinned ends $\lambda = 3$ for fixed ends α = angular mismatch in radians s = plate width t = plate thickness</p>

RINA

Geometry	K_{α}
<p>Axial misalignment between flat plates</p> 	$1 + \frac{3(m - m_0)}{t}$

IIW

<p>10.4.e Welding from one side</p>  <p>Default: $e = 0.15 t$.</p>	<p>Welding from one side is not recommended in areas prone to fatigue due to sensitivity of workmanship and fabrication</p> $K_g = 1.0$ <p>Default value: $K_w = 2.2$</p> $K_{\alpha} = 1 + \frac{3e}{t}$ <p>K_{α} from 10.4.a</p>
--	---

<p>4</p>	<p>Angular misalignment between flat plates</p>  <div style="display: flex; justify-content: space-between;"> <div data-bbox="853 1444 1404 1948"> <p>Assuming fixed ends:</p> <p>with $\beta = \frac{2l}{t} \sqrt{\frac{3\sigma_m}{E}}$</p> $k_m = 1 + \frac{3y}{t} \frac{\tanh(\beta/2)}{\beta/2}$ <p>altern.: $k_m = 1 + \frac{3}{2} \frac{\alpha \cdot l}{t} \frac{\tanh(\beta/2)}{\beta/2}$</p> <p>assuming pinned ends:</p> $k_m = 1 + \frac{6y}{t} \frac{\tanh(\beta)}{\beta}$ <p>altern.: $k_m = 1 + \frac{3\alpha \cdot l}{t} \frac{\tanh(\beta)}{\beta}$</p> </div> <div data-bbox="311 1971 1388 2049"> <p>The tanh correction allows for reduction of angular misalignment due to the straightening of the joint under tensile loading. It is always ≤ 1 and it is conservative to ignore it.</p> </div> </div>
----------	---

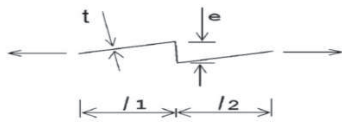
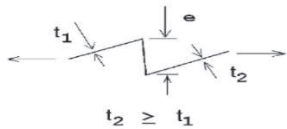
#	TYPE OF MISALIGNMENT	
1	<p>Axial misalignment between flat plates</p> 	$k_m = 1 + \lambda \cdot \frac{e \cdot l_1}{t(l_1 + l_2)}$
	<p>λ is dependent on restraint, $\lambda=6$ for unrestrained joints. For remotely loaded joints assume $l_1=l_2$.</p>	
2	<p>Axial misalignment between flat plates of differing thickness</p> 	$k_m = 1 + \frac{6e}{t_1} \cdot \frac{t_1^n}{t_1^n + t_2^n}$

Figure 36. Assumptions of the various analytical approaches by DNV, RINA and IIW.

5.3 Numerical analysis using FEM

As indicated by Fricke et al. (2013a) and Remes and Fricke (2014), the weld shape and straightening are important factors when defining the k_m -factor in thin-plates, and therefore, they need to be modelled properly. An accurate scheme is to use fine 3D-solid elements to model the weld and specimen shape based on geometrical measurements see Figure 37 (A). However, this scheme is very time consuming and is seldom used in practice. Often, simplifications are made in modelling of geometry.

As determining the straightening k_m value is complex, simplifications can be done by: excluding the dog-bone or curved shape and using plane strain or plane stress assumption (Figure 37 (B)); excluding the weld and considering only the curved specimen shape (Figure 37 (C)) or simplifying the weld shape and using shell elements (Figure 37 (D)).

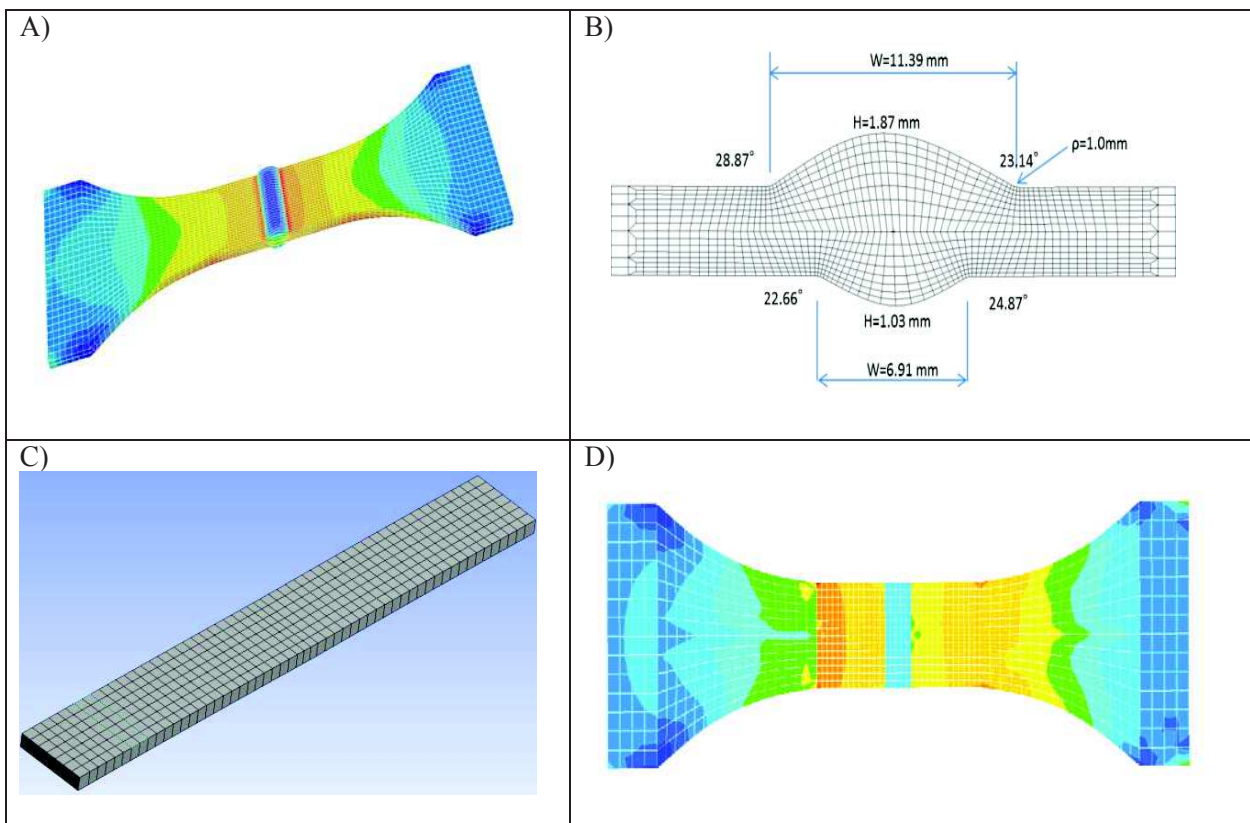


Figure 37. Various FE-modelling schemes. A) Full 3D-solid, B) 2D-plane strain or plane stress, C) Simplified 3D-solid and D) Shell element mesh.

The analyses utilised here employed various approaches to extract k_m values from the solid element results. Basically, the total stress concentration factor, K , was derived with FEA. The fixed K_w values were obtained from the rules. The k_m values were then calculated according to Eq. (9). The results are given in *Italic font* in Table 3. The k_w values vary from 1.46 to 1.50 (Anthes et al., 1993; DNV, 2003). Similarly, in three cases, the k_m factor is obtained by linear surface interpolation at $x=0.4t$ and $x=1.0t$ or $x=0.5t$ and $x=1.5t$. This with the total stress concentration factor, K , gave in turn the K_w factor.

Table 3. Calculated notch stress values and fatigue parameters for different nominal stress levels. The k_w -values given in *italic font* are taken from rules. The element length is denoted by L_e and plate thickness by t .

Analysis	Code	Mesh type	Geometry	K_w -calculation	Nominal Stress	K_w -values		K_m -values	
						Linear	Non-linear	Linear	Non-linear
Analytical	DNV CN30.7	-	Straight plates, separately angular and axial misalignment	Rules	30	<i>1,46</i>	-	1,41	-
					100				
					200				
Analytical	IIW, XIII-2460-13/XV-1440-13	-	Straight plates, separately angular and axial misalignment	Rules	30	<i>1,60</i>	-	1,03	1,26
					100				1,17
					200				1,13
Analytical	RINA Rules 2014 Pt. B, Sect.4 Para 3.3.	-	Straight plates, axial misalignment	Rules	30	<i>2,33</i>	-	1,03	-
					100				
					200				
FEM	DNV CN30.7 & Sesam	A) 8-node Hex, $L_e=t/4$	Fully modeled	Rules	30	<i>1,50</i>	-	1,13	-
					100				
					200				
FEM	Ansys	A) 8-node Hex, $L_e=0.01\text{mm}$, radius 0.05mm	Half modeled	FEM	30	-	-	1,15	-
					100				
					200				
FEM	Abaqus	B) 8-node plane strain, $L_e=0.07\text{mm}$	Transverse section only	FEM	30	<i>1,44</i>	<i>1,64</i>	1,30	1,10
					100		<i>1,62</i>		1,14
					200		<i>1,62</i>		1,15
FEM	DNV CN30.7 & Sesam	D) 4-node Quad $L_e=t/2$	Fully modeled, $t_{\text{weld}}=2t$	Rules	30	<i>1,50</i>	-	1,10	-
					100				
					200				
FEM	Ansys	C) 20-node Hex, $L_e=t$	Plate strip, weld excluded	Anthes et al. (1993)	30	<i>1,46</i>	-	1,11	1,16
					100				1,20
					200				1,20
FEM	Ansys	A) 20-node Hex, $L_e=t/5$	Fully modeled	Not computed	30	-	-	1,09	1,08
					100				1,07
					200				
FEM	Abaqus	B) 8-node plane stress, $L_e=0.01\text{mm}$	Transverse section only	FEM	30	-	1,63	-	1,19
					100		1,64		1,15
					200		1,65		1,13

5.4 Results

As Table 3 indicates, the linear 3D-solid element models without any geometrical modifications gives $k_m = 1.09$ – 1.15 using the surface extrapolation; this means a deviation of 5.5%. The difference is due to the modelling of the weld toe radius, the smaller radius causing a higher k_m . When only plate strip is modelled (without modelling of the weld), the k_m value falls to this range with $k_m=1.11$. When K_w is taken from the rules and k_m is derived from the total stress concentration value using Eq. (9) the $k_m = 1.10$ – 1.13 . So the values are again within the range. The 2D-plane strain model gives $k_m=1.30$; the difference is due to plane strain assumption. From the comparison between the linear 3D-solid results ($L_e = t/4$) and shell element results, with equivalent weld modelled with twice the base plate thickness, the results indicate that the k_m values are, 1.10 and 1.13, respectively. Analytical results by IIW and RINA give the same, un-conservative results of $k_m=1.03$ while DNV gives a much more conservative result of $k_m=1.41$. It should be noted that different fatigue analysis methods use very different assumptions, and a direct comparison of k_m may not be relevant. It should also be noted that the way the clamp length is determined has an effect. For example, when s changes from 210mm to 170mm, see Figure 35, the calculated k_m reduces from 1.41 to 1.34.

When the analysis is carried out with geometrical non-linearity, the k_m value decreases from $k_{m,30\text{MPa}}=1.19$ to $k_{m,200\text{MPa}}=1.13$. Thus, the straightening causes 5.3% decrease in non-linear range k_m value when nominal stress is increased from 30MPa to 200MPa. In the case that the curved shape is not modelled, the weld is not

considered to be in the middle of the specimen and/or weld toe extrapolation is used for k_m while failure occurs on the root, the k_m values can have an unphysical increasing trend; see values $k_{m,30MPa} = 1.16$ to $k_{m,200MPa} = 1.20$ and $k_{m,30MPa} = 1.10$ to $k_{m,200MPa} = 1.15$. The analytical equation of IIW also predicts a decreasing trend; however, the decrease is stronger than in FE-analyses. It should be noted that this equation does not account for a curved shape.

5.5 Discussion & Benchmarking Study Conclusions

The comparison of the FE-results shows that the assumption made in modelling can cause relatively moderate deviation of the predicted stress state from that observed in the specimen. Therefore, special attention should be put on the accuracy of the modelling of the geometry, discretization and analysis type. Even for a single, simple dog-bone geometry, the different stress assessment methods show significant scatter. It should also be noted that this specimen had relatively moderate deformations and in practice higher amplitudes and different shapes can occur within specimen series, causing even higher scatter.

The highest and lowest k_m values observed were 1.41 and 1.03, respectively. Both were observed in analytical methods. None of the analytical methods were able to model the effects of curved shape properly thus, there is a need to update the design equations to account for the shapes observed in thin specimens. In the case of solid elements in 3D or 2D, the problem becomes far more complicated, depending on the method by which the k_m value is being determined. In some cases the k_m value is determined from the total stress concentration factor using rule value for weld factor, K_w . The values used in this investigation ranged from $K_w=1.46$ (Anthes et al., 1993) to $K_w=1.5$ given for example by the DNV (2003) rules (CN30.7). However, as noted by IIW, Maddox and Fricke (2008) both the structural hot spot stress and the effective notch stress at a weld toe need to be checked. A minimum value of $K_w=1.6$ is recommended for welds with high weld toe radius for design purposes. The non-linear analyses based on plane stress and plane strain values indicate that the K_w value is 1.62-1.65. Linear analysis gives lower $K_w=1.44$ and thus higher $k_m=1.30$. Thus, it is recommended to follow the IIW proposal.

In practical analysis of ship structures, the curvature occurs in two directions. This means that the stresses are being redistributed within the panels, and that the stiffeners carry more loading (Eggert et al., 2012; Fricke and Feltz, 2013; Lillemäe et al., 2013, 2014b). As Eggert et al. (2012) pointed out, the consequence is that the fatigue damage can also occur along the stiffeners that are parallel to loading direction. Lillemäe et al. (2013) in turn stated that the curvature in two directions reduces the influence of straightening considerably. This can lead to false conclusions on the dog-bone results on a panel level as there are compensating effects; see also Fricke and Feltz (2013). When decks are considerably distorted, the redistribution of stresses also happens between various decks of the superstructure. The study did not consider variation of the specimen geometry. As Fricke et al. (2013a) and Remes and Fricke (2014) show, this causes additional scatter, which needs to be incorporated into the analysis of test results. Considering the fact that the slope of the S-N curve has been shown to vary between $m=3$ and $m=5$, this means that the sensitivity of modelling the specimens is of utmost important. Considering these facts, one recommendation is that large-scale tests should be carried out where the surrounding structure is included to consider properly the stress redistribution, initial imperfections and residual stresses. This would allow conclusions on what kind of impact these shapes have on the panel and, further, to the entire hull.

6. SUMMARY & CONCLUSIONS

This report is the latest update in the long series of ISSC Fatigue & Fracture Technical Committee reports and as highlighted earlier is not meant to be a stand-alone report rather than to build on the accumulated knowledge reported previously. However, we have structured the report in a manner to make it accessible to the relatively new researcher and designer. We therefore included Section 2 which summarised approaches and methodologies to ship and offshore structure design, setting out some basic terminology and characteristics of most structures in the marine environment e.g. damage tolerance which may not necessarily be familiar to those accustomed to other application areas. Readers will have appreciated the emphasis on uncertainty and reliability, including inspection and maintenance through the life-cycle. Marine structures are subject to stochastic loading and corrosion processes meaning that an “absolute” determination of “remaining life” is always impossible but offshore and marine engineers use probabilistic models coupled with safety factors to ensure acceptable confidence in calculated levels of structural integrity.

Section 3 considered factors influencing fatigue and fracture categorised under “Resistance”, “Materials”, “Loading” and “Complex Stresses” including multiaxial aspects. The section then developed the concepts of Structural Integrity and Life-cycle management addressing fabrication and repair and Inspection and Maintenance. It was seen that significant activity has taken place during the review period, probably the

greatest emphasis has been the urgent need for more component testing results to better validate models. Section 4 presented a brief overview of the recent developments in fatigue and fracture assessment methods, as well as an update of rules, standards & guidelines. Measurement techniques were also reviewed and the latest experimental results available concerning fatigue, crack growth resistance and material properties were presented and reviewed.

The main conclusion from benchmark study is that as we move to very thin decks the work by the committee on ultimate strength analysis of ships starts to approach the work of this committee. The main reason is that the analysis requires large deflection plate theory, but instead of looking at the average load-end-shortening behaviour, we have to look at details of the stress distribution. This is theory. In practise the shape is far more complex that the theory is capable to model properly. Thus, we need full-scale data in terms of actual measured shapes and residual stresses of the thin deck structures. Such data should be exposed to new benchmarking exercise so that we can extend this to practical application. The Committee's benchmarking study reveals moderate deviations in predicted stress state as a result of modelling techniques and assumptions.

Overall the report highlights a highly active subject area which has developed significantly to address growing trends in the industry for weight saving and cost efficiencies during fabrication and maintenance. These drivers demand more of materials and our understanding of them in order to model accurately progressive through-life failure mechanisms.

REFERENCES

- Abdullah, N. N., Hafezi, M. H. & Abdullah, S. 2012. High-Low Sequence Loading Effect on the Crack Growth Rate using UniGrow Model. *In: Oechsner, A., Da Silva, L. F. M. & Altenbach, H. (eds.) Materials with Complex Behaviour II*. Springer Berlin Heidelberg, 647–660.
- ABS 2009. Application of Higher-Strength Hull Structural Thick Steel Plates in Container Carriers. American Bureau of Shipping.
- ABS 2012. Application of Higher-Strength Hull Structural Thick Steel Plates in Container Carriers. American Bureau of Shipping.
- ABS 2013. Fatigue assessment of offshore structures. American Bureau of Shipping.
- Agerskov, H. 2000. Fatigue in steel structures under random loading. *Journal of Constructional Steel Research*, 53, 283–305.
- Aihara, S., Shibanuma, K. & Namegawa, T. 2014. Numerical Simulation of Brittle Crack Propagation and Arrest in Steels Considering Shear-Lip Formation. *ISOPE*, Volume 4
- Akselsen, O. M. & Østby, Ø. 2014. Evaluation of Welding Consumables for Application down to -60°C . *ISOPE*, Volume 4.
- Alvaro, A., Akselsen, O. M., Ren, X. & Kane, A. Fundamental Aspects of Fatigue of Steel in Arctic Applications. Proceedings of the Twenty-fourth International Ocean and Polar Engineering Conference, June 2014 Busan, Korea. 15–20.
- Amiri, M. & Khonsari, M. M. 2012. Nondestructive estimation of remaining fatigue life: Thermography technique. *Journal of Failure Analysis and Prevention*, 12, 683–688.
- An, G. B., Woo, W. & Park, J.-U. 2014. Brittle crack-arrest fracture toughness in a high heat-input thick steel weld. *International Journal of Fracture*, 185, 179–185.
- Andersen, I. M. & Jensen, J. J. Hull girder fatigue damage estimations of a large container vessel by spectral analysis. PRADS, 2013. 557–565.
- Andreikiv, O. E. & Hembara, O. V. 2013. Influence of Soil Corrosion and Transported Products on the Service Life of Welded Joints of Oil and Gas Pipelines. *Materials Science*, 49, 52–58.
- Anes, V., Reis, L., Li, B., Fonte, M. & De Freitas, M. 2013. New approach for analysis of complex multiaxial loading paths. *International Journal of Fatigue*, 62, 21–33.
- Angelo, L. D. & Nussbaumer, A. 2013. Reconsideration of standard S-N curves for welded components using maximum likelihood based fatigue models with and without fatigue limit. *International Institute of Welding*, WG1–163.
- Anthes, R. J., Köttgen, V. B. & Seeger, T. 1993. Stress Concentration Factors for Butt and Cruciform Joint. *Schweißen und Schneiden*, 45, 685–688.
- API RP 2t 2010. Recommended practice for planning, designing, and constructing tension leg platforms. The American Petroleum Institute.
- API RP 579–1/ASME FFS-1 2007. Fitness-for-service. The American Society of Mechanical Engineers and the American Petroleum.
- Araújo, J. A., Dantas, A. P., Castro, F. C., Mamiya, E. N. & Ferreira, J. L. A. 2011. On the characterization of the critical plane with a simple and fast alternative measure of the shear stress amplitude in multiaxial fatigue. *International Journal of Fatigue*, 33, 1092–1100.
- ASTM Standard ASTM E647–13a 2013. Standard test method for measurement of fatigue crack growth rates. West Conshohocken, USA: ASTM International, DOI: 10.1520/E0647.
- ASTM Standard E8 / E8m–13a 2013. Standard Test Methods for Tension Testing of Metallic Materials. West Conshohocken, USA: ASTM International, DOI: 10.1520/E0008_E0008M.

- ASTM Standard E111–04 2010. Standard test method for Young's modulus, tangent modulus, and chord modulus. DOI: 10.1520/E0111–04R10.
- ASTM Standard E606 / E606m–12 2012. Standard test method for strain-controlled fatigue testing. West Conshohocken, USA: ASTM International, DOI: 10.1520/E0606_E0606M-12.
- Azevedo, J., Infante, V., Quintino, L. & Dos Santos, J. 2014. Fatigue Behavior of Friction Stir Welded Steel Joints. *Advanced Materials Research*, 891–892, 1488–1493.
- Barbier, E. & Petrinic, N. 2013. Multiple Crack Growth and Coalescence in Meshfree Methods with Adistance Function-Based Enriched Kernel. *Key Engineering Materials*, 560, 37–60.
- Bardetsky, A. 2013. Fracture mechanics approach to assess the progressive structural failure of a damaged ship. *Collision and Grounding of Ships and Offshore Structures*, 77.
- Bayley, C. & Aucoin, N. 2013. Fracture testing of welded single edge notch tensile specimens. *Engineering Fracture Mechanics*, 102, 257–270.
- Bertoglio, C., Gaggero, S., Rizzo, C. M. & Viviani, M. Fatigue strength assessment of propellers by means of weakly coupled CFD and FEM analyses. OMAE, Proc.s of the 33rd Int. Conf. on Ocean, Offshore and Arctic Engineering, June 2014 San Francisco: CA. 246–55.
- Bertoglio, C., Gaggero, S., Rizzo, C. M., Viviani, M., Vaccaro, C. & Conti, F. Improvements in fatigue strength assessment of marine propellers. MARSTRUCT, Proc.s of the 5th Int. Conf. on Marine Structures, March 24–27 2015 Southampton: UK.
- Brighenti, R., Carpinteri, A., Spagnoli, A. & Scorza, D. 2012. Crack path dependence on inhomogeneities of material microstructure. *Frattura e Integrità Strutturale*, 20.
- BS 7270 Metallic Materials 2006. Constant amplitude strain controlled axial fatigue. Method of test. London: British Standard Institute.
- BS 7910 2013. Guide to methods for assessing the acceptability of flaws in metallic structures. London: British Standard Institute.
- BS EN ISO 6892–1 Metallic Materials 2009. Tensile testing. Method of test at ambient temperature. London: British Standard Institute.
- BS EN ISO 6892–2 Metallic Materials 2011. Tensile testing. Method of test at elevated temperature. London: British Standard Institute.
- BS EN ISO 15653 Metallic Materials 2010. Method of test for the determination of quasistatic fracture toughness of welds London: British Standard Institute.
- BS ISO 12108 Metallic Materials 2012. Fatigue testing. Fatigue crack growth method. London: British Standard Institute.
- BV NR 483 2011. RNS PartB Rules for the Classification of Naval Ships. Bureau Veritas.
- BV NR 578 2012. Rules for the Classification of Tension Leg Platforms. Bureau Veritas.
- BV NR 583 2012. Whipping and Springing Assessment. Bureau Veritas.
- BV NR 593 2012. Ship Conversion into Surface Offshore Units and REdeployment of Surface Offshore Units. Bureau Veritas.
- Câmara, M. C. & Cyrino, J. C. R. Structural Reliability Applications in Design and Maintenance Planning of Ships Subjected to Fatigue and Corrosion. ASME 2012 31st International Conference on Ocean, Offshore and Arctic Engineering, 2012. American Society of Mechanical Engineers, 503–514.
- Carroll, J. D., Abuzaid, W., Lambros, J. & Sehitoglu, H. 2013. High resolution digital image correlation measurements of strain accumulation in fatigue crack growth. *International Journal of Fatigue*, 57, 140–150.
- Chakraborty, D. & Murthy, K. S. R. K. 2014. A new single strain gage technique for the accurate determination of mode I stress intensity factor in orthotropic composite materials. *Engineering Fracture Mechanics*, 124–125, 142–154.
- Chao, M., Haiwei, L., Ning, Z. & Yang, S. 2013. A Ship Cargo Hold Inspection Approach Using Laser Vision Systems. *TELKOMNIKA Indones. J. Electr. Eng*, 11, 330–337.
- Chen, F., Wang, F. & Cui, W. 2012. Fatigue life prediction of engineering structures subjected to variable amplitude loading using the improved crack growth rate model. *Fatigue & Fracture of Engineering Materials & Structures*, 35, 278–290.
- Chen, G. H. & Chen, L. J. 2012. Solution-dependent path crack propagation simulation and its application. *Pressure Vessel Technology*, 29, 36–40, (in Chinese).
- Chen, N. Z. & Wang, G. Low-cycle fatigue and a rational method for determining the size of a crack-stopping hole. Proceedings of the First International Conference on Performance-based and Life-cycle Structural Engineering, 2012 Hong Kong, China. 1895–1903.
- Choudhary, B. K., Samuel, E. I., Sainath, G., Christopher, J. & Mathew, M. D. 2013. Influence of Temperature and Strain Rate on Tensile Deformation and Fracture Behaviour of P92 Ferritic Steel. *Metallurgical and Materials Transactions A*, 44, 4979–4992.
- Choung, J., Nam, W., Noh, M.-H., Lee, J.-Y. & Shim, S. 2014. Impact Bending Tests and Simulations of an High Strength Steel FH32 for Arctic Marine Structures. *ISOPE*.
- Coronado, P., Argüelles, A., Viña, J., Mollón, V. & Viña, I. 2012. Influence of Temperature on a Carbon-Fibre Epoxy Composite Subjected to Static and Fatigue Loading Under Mode-I Delamination. *International Journal of Solids and Structures*, 49, 2934–2940.
- Correia, J. a. F. O., De Jesus, A. M. P. & Fernández-Canteli, A. 2013. Local unified probabilistic model for fatigue crack initiation and propagation: application to a notched geometry. *Engineering Structures*, 52, 394–407.

- Cosso, G. L., Rizzo, C. M. & Servetto, C. 2014. Fitness for service assessment of defected welded structural details by experimental evaluation of the fatigue resistance S-N curve. *IIW doc. XIII-2536-14*. Paris: International Institute of Welding.
- Dai, P., Li, S. & Li, Z. 2013. The effects of overload on the fatigue crack growth in ductile materials predicted by plasticity-corrected stress intensity factor. *Engineering Fracture Mechanics*, 111, 26–37.
- De Baere, K., Verstraelen, H., Rigo, P., Van Passel, S., Lenaerts, S. & Potters, G. 2013. Study on alternative approaches to corrosion protection of ballast tanks using an economic model. *Mar. Struct.*, 32, 1–17.
- De Pauw, J., De Waele, W., Hojjati-Talemi, R. & De Baets, P. 2014. On the use of digital image correlation for slip measurement during coupon scale fretting fatigue experiments. *International Journal of Solids and Structures*, 51, 3058–3066.
- Derbanne, F. R., De Hauteclouque, G. & Chen, X. B. Evaluation of Rule-Based Fatigue Design Loads Associated at a New Probability Level. Proceedings of the Twenty-first International Offshore and Polar Engineering Conference, 2011 Maui, Hawaii, USA. 19–24.
- DNV 2003. Classification Notes, No. 30. Fatigue assessment of ship structures. 7.
- DNV Gp Rp 0005 2014. Fatigue Design of Offshore Steel Structures. Det Norske Veritas.
- DNV Os-C102 2012. Structural Design of Offshore Ships. Det Norske Veritas.
- DNV Rp-C206 2012. Fatigue Methodology of Offshore Ships. Det Norske Veritas.
- Doerk, O., Fricke, W. & Von Selle, H. Validation of Different Fatigue Assessment Approaches for Thick Plate Structures Made of High Tensile Strength Steel YP47. Proceedings of the Twenty-second International Offshore and Polar Engineering Conference, 2012 Rhodes, Greece.
- Dong, P., Pei, X., Xing, S. & Kim, M. H. 2014. A structural strain method for low-cycle fatigue evaluation of welded components. *Int. J. of Pressure Vessels and Piping*, 119, 39–51.
- Doring, R., Hoffmeyer, J., Seeger, T. & Vormwald, M. 2006. Short fatigue crack growth under nonproportional multiaxial elastic–plastic strains. *International Journal of Fatigue*, 28, 972–982.
- Doshi, K. & Vhanmane, S. 2013. Probabilistic fracture mechanics based fatigue evaluation of ship structural details. *Ocean Engineering*, 61, 26–38.
- Eggert, L., Fricke, W. & Paetzhold, H. 2012. Fatigue strength of thin-plated block joints with typical shipbuilding imperfections. *Welding in the World*, 56.
- Fatemi, A. & Shamsaei, N. 2011. Multiaxial fatigue: An overview and some approximation models for life estimation. *International Journal of Fatigue*, 33, 948–958.
- Feltz, O., Fischer, C. & Fricke, W. Fatigue assessment of weld toe and root cracks with the notch stress intensity factor and crack propagation approach. Proc. 11th Int. Symp. on Practical Design of Ships and Other Floating Structures (PRADS), 2010 Rio de Janeiro, Brazil.
- Feng, G., Cao, J., Ren, H. & Li, H. The Fatigue Crack Propagation of the Ship Structures in Random Sea States. ASME, 31st International Conference on Ocean, Offshore and Arctic Engineering, July 2012. American Society of Mechanical Engineers, 39–44.
- Fischer, C., Düster, A. & Fricke, W. Different finite element refinement strategies for the computation of the strain energy density in a welded joint. Proc. MARSTRUCT 2011 Congress, 2011a Hamburg, Germany.
- Fischer, C., Feltz, O., Fricke, W. & Lazzarin, P. 2010. Application of the Notch stress intensity and crack propagation approaches to weld toe and root fatigue. *IIW-Doc. XIII-2337-10/XV-1354-10*. Paris: International Institute of Welding.
- Fischer, C., Fricke, W., Meneghetti, G. & Rizzo, C. M. Fatigue strength assessment of HP stiffener joints with fillet-welded attachments using the peak stress method. In: Brinkmann, B. & Wriggers, P., eds. Proc.s of the fifth Conference on Computational Methods in Marine Engineering (MARINE 2013), 2013 Germany. 660–669.
- Fischer, C., Rizzo, C. M. & Fricke, W. 2011b. Fatigue assessment of hopper knuckles according to N-SIF based approaches. In: Rizzuto & Guedes Soares, C. (eds.) *Sustainable Maritime Transportation and Exploitation of Sea Resources*. London: Taylor & Francis Group.
- Fischer, C., Rizzo, C. M. & Fricke, W. Fatigue Assessment of Joints at Bulb Profiles by Local Approaches. MARSTRUCT Proc.s of the 5th Int. Conf. on Marine Structures, March 24–27 2015 Southampton. UK Fitness-for-service', (2007) The American Society of Mechanical Engineers and the American Petroleum API RP 579–1/ASME FFS-1.
- Fremy, F., Pommier, S., Poncelet, M., Raka, B., Galenne, E., Courtin, S. & Roux, J.-C. L. 2013. Load path effect on fatigue crack propagation in I+II+III mixed mode conditions - Part 1: Experimental investigations. *International Journal of Fatigue*.
- Fricke, W. 2013. IIW guideline for the assessment of weld root fatigue. *Welding in the World*, 57, 753–791.
- Fricke, W. 2014. Recent developments and future challenges in fatigue strength assessment of welded joints. *Proc IMechE Part C: J Mechanical Engineering Science*, DOI : 10.1177/0954406214550015.
- Fricke, W., Bollero, A., Chirica, I., Garbatov, Y., Jancart, F., Kahl, A., Remes, H., Rizzo, C. M., Von Selle, H., Urban, A. & Wei, L. 2008. Round Robin Study on Structural Hot-Spot and Effective Notch Stress Analysis. *Ship and Offshore Structures* 3, 335–345.
- Fricke, W., Codda, M., Feltz, O., Garbatov, Y., Remes, H., Risso, G., Rizzo, C. M. & Romanoff, J. 2013a. Round robin study on local stress and fatigue assessment of lap joints and doubler plates. *Ship and Offshore Structures*, 8, 621–627.
- Fricke, W. & Feltz, O. 2013. Consideration of influence factors between small-scale specimens and large components on the fatigue strength of thin-plated block joints in shipbuilding. *Fatigue & Fracture of Engineering Materials & Structures*, 36, 1223–1231.

- Fricke, W. & Paetzold, H. 2012. Experimental Investigation of the Effect of Whipping Stresses on the Fatigue Life of Ships. *Proc. Intl. Marine Design Conf. IMDC'2012*, 3, 3 – 10.
- Fricke, W. & Paetzold, H. 2014. Effect of whipping stresses on the fatigue damage of ship structures. *Weld World*, 58, 261–268.
- Fricke, W., Remes, H., Feltz, O., Lillemäe, I., Tchuindjang, D., Reinert, T., Nevierov, A., Sichermann, W., Brinkmann, M., Kontkanen, T., Bohlmann, B. & Molter, L. Fatigue strength of laser-welded thin plate ship structures based on nominal and structural hot-spot stress approach. Analysis and Design of Marine Structures - Proceedings of the 4th International Conference on Marine Structures, MARSTRUCT, 2013b. 249–254.
- Fricke, W., Von Lilienfeld-Toal, A. & Paetzold, H. 2012. Fatigue strength investigations of welded details of stiffened plate structures in steel ships. *International Journal of Fatigue*, 34, 17–26.
- Fukasawa, T. & Mukai, K. 2014. On the effects of hull-girder vibration upon fatigue strength of a Post-Panamax container ship disaggregated by short-term sea state. *Int. J. Nav. Archit. Ocean Eng*, 6, 431–441.
- Ganesh, P., Kaul, R., Sasikala, G., Kumar, H., Venugopal, S., Tiwari, P. & Kukreja, L. M. 2014. Fatigue Crack Propagation and Fracture Toughness of Laser Rapid Manufactured Structures of AISI 316L Stainless Steel. *Metallography, Microstructure, and Analysis*, 3, 36–45.
- Gates, N. & Fatemi, A. 2014. Notched fatigue behavior and stress analysis under multiaxial states of stress. *International Journal of Fatigue*, 67, 2–14, <http://dx.doi.org/10.1016/j.ijfatigue>.
- GL 2012. Guidelines for the Structural Design of Racing Yachts Greater than 24m. Hamburg: Germanischer Lloyd.
- GL 2013. Guidelines to Assess High-Frequency Hull Girder Response of Containerships. Hamburg: Germanischer Lloyd.
- GL 2014. Rules for Classification and Construction, I – Ship Technology, Part 1 – Sea-Going Ships, Chapter 1–Hull Structures. Hamburg: Germanischer Lloyd.
- Gladskyi, M. & Fatemi, A. 2013. Notched fatigue behavior including load sequence effects under axial and torsional loadings. *International Journal of Fatigue*, 55, 43–53.
- Gotoh, K., Matsuda, K. & Kitamura, O. Numerical Simulation of Fatigue Crack Propagation under Superposed Loading Histories with Two Different Frequencies. *Proc. Hydroelasticity in Marine Technology*, 2012. 287–297.
- Guo, J., Wang, G., Perakis, A. N. & Ivanov, L. 2012. A study on reliability-based inspection planning – Application to deck plate thickness measurement of aging tankers. *Mar. Struct.*, 25, 85–106.
- Haagensen, P. & Maddox, S. 2013. IIW recommendations on methods for improving the fatigue lives of welded joints. Cambridge: Woodhead Publishing Ltd. International Institute of Welding, Paris.
- Haagensen, P. J., Larsen, J. E. & Vårdal, O. T. 2014. Long Term Effectiveness of Life Extension Methodologies Applied to Offshore Structures. *Procedia Materials Science*, 3, 2187–2194.
- Han, D. K., Jung, H. G., Kim, K. Y. & Kim, S. J. 2013. Effect of Heat Treatment on Hydrogen Diffusion and Hydrogen Induced Cracking Behavior of Process Pipe Steel in Sour Environment. *ISOPE*, 4.
- Harksen, S., Lischewski, I., Schneider, A., Schmidt, T. & Mahn, D. 2013. A Modern Methodology of Materials Development for High Toughness Seamless Line Pipe Products for Offshore Applications. *ISOPE*, 4.
- Hauge, M. & Østby, E. Fracture Integrity of Arctic Structures—How to Determine Characteristic Fracture Toughness for Engineering Critical Assessment. The Twenty-third International Offshore and Polar Engineering Conference, June 2013. International Society of Offshore and Polar Engineers.
- Heinz, S., Balle, F., Wagner, G. & Eifler, D. 2013. Analysis of fatigue properties and failure mechanisms of Ti6Al4V in the very high cycle fatigue regime using ultrasonic technology and 3D laser scanning vibrometry. *Ultrasonics*, 53, 1433–1440.
- Hobbacher, A. 2009. Recommendations for Fatigue Design of Welded Joints and Components. *IIW doc, Welding Research Council Bulletin 520*, 1823–07.
- Holländer, D., Wünsche, M., Henkel, S. & Theilig, H. 2012. Numerical Simulation of Multiple Fatigue Crack Growth with Additional Crack Initiation. *Key Engineering Materials*, 488, 444–447.
- Horn, A., Aihara, S., Andersen, M., Biot, M., Bohlmann, B., Van Der Cammen, J., Choi, B. K., Garbatov, Y., Mishra, B., Qian, X., Remes, H., Ringsberg, J., Samanta, A., Wang, D. & Zhang, S. Committee III.2 Fatigue and Fracture. Proceedings of the 18th International Ships and Offshore Structures Congress, September 9–13 2012a Rostock, Germany.
- Horn, A. M., Østby, E., Hauge, M. & Aubert, J. M. Robust material qualification for Arctic applications. *Proc. 22nd Intl Ocean & Polar Eng Conf*, 2012b Greece. ISOPE, volume 4, available at www.isopec.org.
- Hover, F. S., Eustice, R. M., Kim, A., Englot, B., Johannsson, H., Kaess, M. & Leonard, J. J. 2012. Advanced perception, navigation and planning for autonomous in-water ship hull inspection. *Int. J. Rob. Res*, 31, 1445–1464.
- Huang, W. 2013. The Rain-Flow Estimate of Fatigue Damage of Combined High and Low Frequency Load Effects. *ASME, 32nd International Conference on Ocean, Offshore and Arctic Engineering (OMAE2013)*. American Society of Mechanical Engineers.
- IACS 2013. Requirements for Use of Extremely Thick Steel Plates.
- IACS 2014. Technical Background for Equivalent Design Waves (EDW) for Fatigue Loads.
- IIW 2013a. Draft for Development: IIW guidelines on weld quality in relationship to fatigue strength, IIW-doc. XIII-2301r3–13.
- IIW 2013b. Fatigue Recommendations, IIW-doc. XIII-2460–13/XV-1440–13 rev. (April 2013).
- IIW 2013c. Recommendation for Fatigue Design of Welded Joints and Components, IIW-doc. -2460–13.
- Ince, A. & Glinka, G. 2014. A generalized fatigue damage parameter for multiaxial fatigue life prediction under proportional and non-proportional loadings. *Int. J. of Fatigue*, 62, 34–41.

- Iranpour, M. & Taheri, F. 2013. Influence of the Peak Tensile Overload Cycles on the Fatigue Crack Growth of Aluminum Alloy Under Spectrum Loading. *Journal of Materials Engineering and Performance*, 22, 3490–3499.
- Iranpour, M. & Taheri, F. 2014. Analytical and computational investigation into the influence of the compressive stress cycles on crack growth under variable amplitude loading using CTOD. *Fatigue & Fracture of Engineering Materials & Structures*, 37, 645–658.
- ISO 12106 2003. Metallic materials- Fatigue testing. Strain control axial fatigue method. International Organization for Standardization.
- ISO 12110-1:2013 2013. Metallic materials -- Fatigue testing -- Variable amplitude fatigue testing -- General principles, test method and reporting requirements. International Organization for Standardization.
- ISO 12110-2:2013 2013. Metallic materials --Fatigue testing -- Variable amplitude fatigue testing -- Cycle counting and related data reduction methods. International Organization for Standardization.
- ISO/TR 14345:2012 2012. Fatigue --Fatigue testing of welded components --Guidance. International Organization for Standardization.
- Itoh, T., Sakane, M. & Ohsuga, K. 2013. Multiaxial low cycle fatigue life under non-proportional loading. *International Journal of Pressure Vessels and Piping*, 110, 50–56.
- Itoh, T. & Yang, T. 2011. Material dependence of multiaxial low cycle fatigue lives under non-proportional loading. *International Journal of Fatigue*, 33, 1025–1031.
- Johannesson, P., Svensson, T. & Maré, J. D. 2005. Fatigue life prediction based on variable amplitude tests – methodology. *International Journal of Fatigue*, 27, 954–965.
- Jonsson, B., Dobmann, G., Hobbacher, A., Kassner, M. & Marquis, G. 2013. IIW-XIII-2510–13 IIW Guidelines on weld quality in relationship to fatigue strength.
- Judt, P. & Ricoeur, A. 2013. Efficient simulation of crack growth in multiple-crack systems considering internal boundaries and interfaces. *In ICF13*.
- Karakas, O. 2013. Consideration of mean-stress effects on fatigue life of welded magnesium joints by the application of the Smith-Watson-Topper and reference radius concepts. *International Journal of Fatigue*, 49, 1–17.
- Kim, J. G., Hwang, Y. J., Yoon, S. H. & Lee, D. G. 2012a. Improvement of the fracture toughness of adhesively bonded stainless steel joints with aramid fibers at cryogenic temperatures. *Composite Structures*, 94, 2982–2989.
- Kim, J. H., Chau Dinh, T., Zi, G. & Kong, J. S. 2012b. The effect of compression stresses, stress level and stress order on fatigue crack growth of multiple site damage. *Fatigue & Fracture of Engineering Materials & Structures*, 35, 903–917.
- Kim, M. H., Kang, S. W., Kim, J. H., Kim, K. W., Kang, J. K. & Heo, J. H. 2010. An experimental study on the fatigue strength assessment of longi-web connections in ship structures using structural stress. *International Journal of Fatigue*, 32, 318–329.
- Kim, Y. W., Lee, J. M., Kim, M. H., Noh, B. J., Sung, H. J., Ando, R. & Matsumoto, T. An Experimental Study for Fatigue Performance of 7% Nickel Steels for Type B LNG Carriers. ASME 2014 33rd International Conference on Ocean, Offshore and Arctic Engineering, 2014. American Society of Mechanical Engineers.
- Kirkhope, K. J., Bell, R., Caron, L., Basu, R. I. & Ma, K.-T. 1999a. Weld detail fatigue life improvement techniques. Part 1: review. *Marine Structures*, 12, 447–474.
- Kirkhope, K. J., Bell, R., Caron, L., Basu, R. I. & Ma, K.-T. 1999b. Weld detail fatigue life improvement techniques. Part 2: application to ship structures. *Marine Structures*, 12, 477–496.
- Köder, T. 2015. *On the Fatigue Strength of Thin-Plated Ship Structures*. Ph.D. Thesis, University of Southern Denmark.
- Lachambre, J., Réthoré, J., Weck, A. & Buffiere, J. Y. 2014. Extraction of stress intensity factors for 3D small fatigue cracks using digital volume correlation and X-ray tomography. *International Journal of Fatigue*, 71, 3–10.
- Lee, J.-M., Lee, K.-H. & Kim, D.-S. 2013. Cloud-Based RF-Inspection for Ship Maintenance. *Int. J. Distrib. Sens. Networks*, 2013, 1–8.
- Leng, S. W., Miao, Z. M., Qiu, F. X., Niu, L. N. & Miao, T. 2012. Analysis of the Relationship between CTOD Toughness and Micromechanism of Marine Steel Weld Joints. *Applied Mechanics of Materials*, 117–119, 1867–1873.
- Li, B., Chen, X. & He, Z. 2013a. Three-steps-meshing based multiple crack identification for structures and its experimental studies. *Chinese Journal of Mechanical Engineering*, 26, 400–405.
- Li, J., Zhang, Z. P., Sun, Q. & Li, C. W. 2011. Multiaxial fatigue life prediction for various metallic materials based on the critical plane approach. *International Journal of Fatigue*, 33, 90–101.
- Li, K., Chen, M. & Lin, Y. 2012a. Research on marine structure inspection support system on mobile device platform. *J. Shanghai Jiaotong Univ*, 17, 70–75.
- Li, X. D., Wang, X. S., Ren, H. H., Chen, Y. L. & Mu, Z. T. 2012b. Effect of Prior Corrosion State on the Fatigue Small Cracking Behavior of 6151–T6 Aluminum Alloy. *Corrosion Science*, 55, 26–33.
- Li, Z., Ringsberg, J. W. & Storhaug, G. 2013b. Time-domain fatigue assessment of ship side-shell structures. *International Journal of Fatigue*, 55, 276–290.
- Lieser, M. J. & Xu, J. 2010. Composites and the Future of Society: Preventing a Legacy of Costly Corrosion with Modern Materials. [Accessed 26th March 2014]. Available from: http://www.ocvreinforcements.com/pdf/library/CSB_Corrosion_White_Paper_Sept_10_10_English.pdf.
- Lillemäe, I. 2014. *Influence of Initial Distortion on the Fatigue Assessment of Thin Ship Deck Structure*. Ph.D. Thesis, Aalto University.

- Lillemäe, I., Lammi, H., Molter, L. & Remes, H. 2012. Fatigue strength of welded butt joints in thin and slender specimens. *International Journal of Fatigue*, 44, 98–106.
- Lillemäe, I., Remes, H. & Romanoff, J. 2013. Influence of initial distortion on the structural stress in 3 mm thick stiffened panels. *Thin-Walled Structures*, 72, 121–127.
- Lillemäe, I., Remes, H. & Romanoff, J. Fatigue assessment of large thin-walled structures with initial distortions. Proceedings of the 11th International Fatigue Congress, March 2–7 2014a Melbourne, Australia. Presented on Advanced Materials Research, 123–129.
- Lillemäe, I., Remes, H. & Romanoff, J. 2014b. Influence of initial distortion of 3 mm thin superstructure decks on hull girder response for fatigue assessment. *Marine Structures*, 37, 203–218.
- Liu, Z. F., Gu, L. X. & Xu, Z. Y. 2013. Fatigue Crack Propagation Prediction under Single Overload Variable Loading. *Applied Mechanics and Materials*, 275, 215–219.
- Lorén, S. & Svensson, T. 2012. Second moment reliability evaluation vs. Monte Carlo simulations for weld fatigue strength. *Quality and Reliability Engineering International*, 28, 887–896.
- Lu, Z. Z. & Liu, Y. M. 2010. Small time scale fatigue crack growth analysis. *International Journal of Fatigue*, 32, 1306–1321.
- Maddox, S. J. & Fricke, W. 2008. Guideline for the Fatigue Assessment by Notch Stress Analysis for Welded Structures, IIW-Doc. XIII-2240r1–08/XV-1289r1–08.
- Mao, W. 2014. Development of a Spectral Method and a Statistical Wave Model for Crack Propagation Prediction in Ship Structures. *Journal of ship research*, 58, 106–116.
- Mao, W., Li, Z., Ogeman, V. & Ringsberg, J. W. 2015. A Regression and Beam Theory based Approach for Fatigue Assessment of Container Structures including Bending and Torsion Contributions. *Marine structures*, in press.
- Mao, W. & Ringsberg, J. W. Analysis of Fatigue Crack Initiation and Propagation in Ship Structures. 2013 Proceedings of the Thirteenth International Conference on Fracture (ICF13). 10.
- Mao, W., Rychlik, I. & Storhaug, G. 2010. Safety index of fatigue failure for ship structure details. *Journal of Ship Research*, 54, 197–208.
- Marciniak, Z., Rozumek, D. & Macha, E. 2013. Verification of fatigue critical plane position according to variance and damage accumulation methods under multiaxial loading. *International Journal of Fatigue*, 58, 84–93.
- Marquis, G. & Barsoum, Z. 2013. A guideline for fatigue strength improvement of high strength steel welded structures using high frequency mechanical impact treatment. *Procedia Engineering*, 66, 98–107.
- Marquis, G., Mikkola, E., Yildirim, H. C. & Barsoum, Z. 2013. Fatigue Strength Improvement of Steel Structures by HFMI: Proposed Fatigue Assessment Guidelines. *Welding in the World*, 57, 803–822.
- Matsubara, G. & Nishio, K. 2013. Multiaxial high-cycle fatigue criterion considering crack initiation and non-propagation. *International Journal of Fatigue*, 47, 222–231.
- Matsuda, K. & Gotoh, K. 2013. Numerical Simulation of Fatigue Crack Propagation Under Simulated Whipping Loading Arising in Hull Structures. *OMAE2013–10985*.
- Meriaux, J., Fouvry, S., Kubiak, K. J. & Deyber, S. 2010. Characterization of crack nucleation in TA6V under fretting-fatigue loading using potential drop technique. *International Journal of Fatigue*, 32, 1658–1668.
- Mikkola, E., Dore, M. & Khurshid, M. 2013. Fatigue strength of HFMI treated structures under high R-ratio and variable amplitude loading. *Procedia Engineering*, 66, 161–170.
- Molter, L. 2013. *Fatigue strength of laser hybrid weld seams in ship construction*. Ph.D. Thesis, University of Southern Denmark.
- Moon, D. H., Lee, J. S., Lee, J. M. & Kim, M. H. 2013. Estimation of Constraint Factor on the Relationship Between J Integral and CTOD for Offshore Structural Steel Weldments. *Materials Technology; Ocean Space Utilization*, 3, V003T03A023.
- Moore, P. & Nicholas, J. The Effect of Inclusions on the Fracture Toughness of Local Brittle Zones in the HAZ of Girth Welded Line Pipe. *OMAE*, 2013. 10729.
- Mourad, A. H. I., El-Domiatiy, A. & Chao, Y. J. 2013. Fracture toughness prediction of low alloy steel as a function of specimen notch root radius and size constraints. *Engineering Fracture Mechanics*, 103, 79–93.
- Mukoyama, K., Hanaki, K., Okada, K., Sakaida, A., Sugeta, A., Nishikawa, I., Ueno, A. & Sakai, T. 2014. A Study on Estimation of S-N curves for Structural Steels Based on Their Static Mechanical Properties. *Advanced Materials Research*, 891–892, 1639–1644.
- Müller, T. & Sander, M. 2013. On the use of ultrasonic fatigue testing technique – variable amplitude loadings and crack growth monitoring. *Ultrasonics*, 53, 1417–1424.
- Murakami, Y., Takeuchi, Y. & Kazukuni Hase, K. 2013. Development of YP460 Class Steel Plate with Excellent Brittle Crack Arrestability for Large Container Ships. *ISOPE*, Volume 4.
- Murawski, L., Ostachowicz, W., Opoka, S., Mieloszyk, M. & Majewska, K. 2012. Practical Application of Monitoring System Based on Optical Sensors for Marine Constructions. *Key Eng. Materials*, 518, 261–270.
- Nakashima, K., Hase, K., Endo, S., Eto, T., Fukai, H. & Shiomi, H. Development of YP390MPa Steel Plate for Shipbuilding with Superior Low Temperature Toughness for Large Heat Input Welding. The Twenty-fourth International Ocean and Polar Engineering Conference, August 2014. International Society of Offshore and Polar Engineers.
- Nash, I. 2013. The Production and Testing of MEIDP Line-Pipe for 3500m Application. *ISOPE* Volume 4.
- Neuber, H. 1968. Über die Berücksichtigung der Spannungskonzentration bei Festigkeitsberechnungen. *Konstruktion*, 20, 245–251.

- Nielsen, U. D., Jensen, J., Pedersen, J., Preben, T. & Ito, Y. 2011. Onboard monitoring of fatigue damage rates in the hull girder. *Marine Structures*, 24, 182–206.
- Noban, M., Jahed, H., Ibrahim, E. & Ince, A. 2012. Load path sensitivity and fatigue life estimation of 30CrNiMo8HH. *International Journal of Fatigue*, 37, 123–133.
- Oliveira, H. L. & Leonel, E. D. 2013. Dual BEM Formulation Applied to Analysis of Multiple Crack Propagation. *Key Engineering Materials*, 560, 99–106.
- Osawa, N., Nakamura, T., Yamamoto, N. & Sawamura, J. Development of a new fatigue testing machine for high frequency fatigue damage assessment. ASME 2013 32nd International Conference on Ocean, Offshore and Arctic Engineering (OMAE), 2013. American Society of Mechanical Engineers.
- Østby, E., Akselsen, O. M. & Kristensen, T. A. Monitoring of Cleavage Microcrack Arrest in Weld Thermal Simulated Microstructures by Means of Acoustic Emission. Proceedings of the Twenty-third International Offshore and Polar Engineering Conference, 2013a Anchorage, Alaska.
- Østby, E., Horn, A. M., Hauge, M. & Akselsen, O. M. Fracture Mechanics Design Criteria for Low Temperature Applications of Steel Weldments. Proceedings of the twenty-third International Offshore and Polar Engineering Conference, 2013b Anchorage, Alaska.
- Pang, J. H. L. & Chew, Y. X. 2014. Fatigue Crack Growth and Coalescence Algorithm Starting from Multiple Surface Cracks. *Advanced Materials Research*, 891, 1003–1008.
- Paolino, D. S., Chiandussi, G. & Rosetto, M. 2013. A unified statistical model for S-N fatigue curves: probabilistic definition. *Fatigue and Fracture of Engineering Materials & Structures*, 36, 187–201.
- Pataky, G. J., Sangid, M. D., Sehitoglu, H., Hamilton, R. F., Maier, H. J. & Sofronis, P. 2012. Full field measurements of anisotropic stress intensity factor ranges in fatigue. *Engineering Fracture Mechanics*, 94, 13–28.
- Pedersen, M. M., Andersen, J. G. & Ólafsson, Ó. M. 2013. Investigation of the thickness effect for butt welded joints. IIW, WG1, 154–12.
- Pettinà, M., Farahmand, B., Berto, F. & Abdi, F. 2014. Virtual testing for fracture toughness, fatigue crack growth and fatigue life data estimation of metallic components. *Key Engineering Materials*, 577, 177–180.
- Polezhayeva, H., Maddox, S. J., Howarth, D. & Robinson, A. Fatigue Testing to Identify Effect of Mean Stress on Fatigue Strength of Welded Joints in Ship Structures. The Twenty-third International Offshore and Polar Engineering Conference., 2013. International Society of Offshore and Polar Engineers.
- Pook, L. P. 2013. Fifty years of crack path research. *In CP2009*.
- Quéméner, Y., Huang, C.-H. & Lee, C.-F. 2013a. Assessment of Critical Fatigue Crack Length Considering the Fracture Failure of Ship Longitudinal Members. *The 27th Asian-Pacific Technical Exchange and Advisory Meeting on Marine Structures (TEAM2013)* Keelung, Taiwan.
- Quéméner, Y., Huang, C.-H. & Lee, C.-F. 2013b. Fracture Resistance of Ship Longitudinal Members Including Fatigue Crack. *Structures, Safety and Reliability*, 2a, V02AT02A026.
- Radaj, D., Lazzarin, P. & Berto, F. 2009a. Fatigue assessment of welded joints under slit-parallel loading based on strain energy density or notch rounding. *Int. J. Fatigue*, 31, 1490–1504.
- Radaj, D., Lazzarin, P. & Berto, F. 2013. Generalised Neuber concept of fictitious notch rounding. *Int. J. of Fatigue*, 51, 105–115.
- Radaj, D., Sonsino, C. M. & Fricke, W. 2006. *Fatigue assessment of welded joints by local approaches* Cambridge, Woodhead Publishing Ltd.
- Radaj, D., Sonsino, C. M. & Fricke, W. 2009b. Recent developments in local concepts of fatigue assessment of welded joints. *International Journal of Fatigue*, 31, 2–11.
- Radaj, D. & Vormwald, M. 2013. *Advanced Methods of Fatigue Assessment*, Springer.
- Remes, H. & Fricke, W. 2014. Influencing factors on fatigue strength of welded thin plates based on structural stress assessment. *Welding in the World*, 58, 915–923.
- Renaud, M., De Lorgeril, E., Boutillier, J. B. & Gerad, L. Fatigue and weather on ultra large containerships. Proceedings of the PRADS2013, 2013. 384–394.
- Rethore, J., Limodin, N., Buffiere, J.-Y., Roux, S. & Hild, F. 2012. Three-dimensional analysis of fatigue crack propagation using X-Ray tomography, digital volume correlation and extended finite element simulations. *Procedia IUTAM*, 4, 151–158.
- RINA Rules 2014. Pt.B, Ch.7, Sect.4, Para 3.3 and Tables 7 and 9.
- Ritchie, R. O. 2011. The conflicts between strength and toughness. *Nature Materials*, 10, 817–822.
- Rizzo, C. M. 2011. Application of advanced notch stress approaches to assess fatigue strength of ship structural details: literature review, Report 655. Germany: Schriftenreihe Schiffbau, Technische Universität.
- Ronold, K. O. & Lotsberg, I. 2012. On the estimation of characteristic S-N curves with confidence. *Marine Structures*, 27, 29–44.
- Rother, K. & Rudolph, J. 2011. Fatigue assessment of welded structures: practical aspects for stress analysis and fatigue assessment. *Fatigue & Fracture of Engineering Materials & Structures*, 34, 177–204.
- Rozumek, D. & Marciniak, Z. 2012. The investigation of crack growth in specimens with rectangular cross-sections under out-of-phase bending and torsional loading. *International Journal of Fatigue*, 39, 81–87.
- Rubio-González, C., Felix-Martinez, C., Gomez-Rosas, G., Ocaña, J. L., Morales, M. & Porro, J. A. 2011. Effect of laser shock processing on fatigue crack growth of duplex stainless steel. *Material Science and Engineering A*, 528, 914–919.
- Sahu, J. K., Gupta, R. K., Swaminathan, J., Paulose, N. & Mannan, S. L. 2013. Influence of Hot Corrosion on Low Cycle Fatigue Behaviour of Nickel Base Superalloy SU 263. *International Journal of Fatigue*, 51, 68–73.

- Sarangi, H., Murthy, K. S. R. K. & Chakraborty, D. 2013. Experimental verification of optimal strain gage locations for the accurate determination of mode I stress intensity factors. *Engineering Fracture Mechanics*, 110, 189–200.
- Schaumann, P., Raba, A. & Lochte-Holtgreven, S. Load Sequence Effects in the Fatigue Design of Welded Spatial Tubular Joints in Jackets. The Twenty-second International Offshore and Polar Engineering Conference, 2012. International Society of Offshore and Polar Engineers.
- Schijve, J. 2012. Fatigue predictions of welded joints and the effective notch stress concept. *Int. J. of Fatigue*, 45, 31–38.
- Schijve, J. 2014. The significance of fatigue crack initiation for predictions of the fatigue limit of specimens and structures. *International Journal of Fatigue*, 61, 39–45.
- Selvakumar, P. & Hong, J. K. 2013. Robust mesh insensitive structural stress method for fatigue analysis of welded structures. *Procedia Engineering*, 55, 374–379.
- Shamsaei, N. & Fatemi, A. 2009. Effect of hardness on multiaxial fatigue behaviour and some simple approximations for steels. *Fatigue & Fracture of Engineering Materials & Structures*, 32, 631–646.
- Shamsaei, N. & Fatemi, A. 2010. Effect of microstructure and hardness on non-proportional cyclic hardening coefficient and predictions. *Materials Science and Engineering: A*, 527, 3015–3024.
- Shamsaei, N. & Fatemi, A. 2014. Small fatigue crack growth under multiaxial stresses. *International Journal of Fatigue*, 58, 126–135.
- Shamsaei, N., Fatemi, A. & Socie, D. F. 2010a. Multiaxial cyclic deformation and non-proportional hardening employing discriminating load paths. *International Journal of Plasticity*, 26, 1680–1701.
- Shamsaei, N., Gladskyi, M., Panasovskiy, K., Shukaev, S. & Fatemi, A. 2010b. Multiaxial fatigue of titanium including step loading and load path alteration and sequence effects. *International Journal of Fatigue*, 32, 1862–1874.
- Shi, J., Ma, W. & Li, N. 2013. Extended meshless method based on partition of unity for solving multiple crack problems. *Meccanica*, 48, 2263–2270.
- Shlyannikov, V. N. & Zakharov, A. P. 2014. Multiaxial crack growth rate under variable T-stress. *Engineering Fracture Mechanics*, 123, 86–99.
- Sielski, R. A. 2012. Ship Structural Health Monitoring Research at the Office of Naval Research. *JOM: The Journal of The Minerals, Metals & Materials Society*, 64, 823–827.
- Silitonga, S., Maljaars, J., Soetens, F. & Snijder, H. H. 2014. Numerical Simulation of Fatigue Crack Growth Rate and Crack Retardation due to an Overload Using a Cohesive Zone Model. *Advanced Materials Research*, 891, 777–783.
- Slobodyan, Z. V., Kyryliv, V. I., Mahladyuk, L. A. & Kupovych, R. B. 2009. Influence of the Inhibitor Treatment on the Corrosion Resistance of Different Zones of Welded Joints. *Materials Science*, 45, 136–139.
- Sonsino, C. M., Bruder, T. & Baumgartner, J. 2010. S-N lines for welded thin joints – suggested slopes and FAT values for applying the notch stress concept with various reference radii. *Welding in the World*, 54, 375–392.
- Sonsino, C. M., Fricke, W., De Bruyne, F., Hoppe, A., Ahmadi, A. & Zhang, G. 2012. Notch stress concepts for the fatigue assessment of welded joints – background and applications. *Int. J. of Fatigue*, 34, 2–16.
- Stanzl-Tschegg, S. 2014. Very high cycle fatigue measurement techniques. *International Journal of Fatigue*, 60, 2–17.
- Sumi, Y. 2013. Computational crack path prediction for ship structural details. *In FCP2003*.
- Sumi, Y. 2014. Fatigue crack propagation in marine structures under seaway loading. *International Journal of Fatigue*, 58, 218–224.
- Sumi, Y. & Okawa, T. 2013. Crack Paths from Weld Details in Three-dimensional Plate Structures. *In CP2006*.
- Sumi, Y., Yajima, H., Toyosada, M., Yoshikawa, T., Aihara, S., Gotoh, K., Ogawa, Y., Matsumoto, T., Hirota, K., Hirasawa, H., Toyoda, M. & Morikage, Y. 2013. Fracture control of extremely thick welded steel plates applied to the deck structure of large container ships. *Journal of Marine Science and Technology*, 18, 497–514.
- Suominen, L., Khurshid, M. & Parantainen, J. 2013. Residual stresses in welded components following post-weld treatment methods. *Procedia Engineering*, 66, 181–191.
- Thévenet, D., Ghanameh, M. F. & Zeghloul, A. 2013. Fatigue strength assessment of tubular welded joints by an alternative structural stress approach. *International Journal of Fatigue*, 51, 74–82.
- Toyosada, M., Gotoh, K. & Niwa, T. 2004. Fatigue crack propagation for a through thickness crack: a crack propagation law considering cyclic plasticity near the crack tip. *International Journal of Fatigue*, 26, 983–992.
- Tronskar, J. P. & Andresen, V. Avoiding Local Brittle Zones in Offshore Pipeline Girth Welds for Reeling Installation Involving Large Plastic Strain. ASME 2013 32nd International Conference on Ocean, Offshore and Arctic Engineering (OMAE), June 2013. American Society of Mechanical Engineers, 11094.
- Van Der Horst, M. P., Kaminski, M. L. & Puik, E. Methods for Sensing and Monitoring Fatigue Cracks and Their Applicability for Marine Structures. Proceedings of the 23rd International Offshore and Polar Engineering Conference (ISOPE), June 2013. 455–462.
- Vina, J., Argüelles, A. & Canteli, A. F. 2011. Influence of Temperature on the Fatigue Behaviour of Glass Fibre Reinforced Polypropylene. *Strain*, 47, 222–226.
- Walters, C. L. 2014. The effect of low temperatures on the fatigue of high-strength structural grade steels. *20th European Conference on Fracture (ECF20)*. Trondheim, Norway.
- Wang, G. R., Chen, L. Y., Zhao, M., Li, R. & Huang, B. S. 2014. The research on failure analysis of fluid cylinder and fatigue life prediction. *Engineering Failure Analysis*, 40, 48–57.
- Wang, X. G., Crupi, V., Guo, X. L. & Zhao, Y. G. 2010. Quantitative thermographic methodology for fatigue assessment and stress measurement. *International Journal of Fatigue*, 32, 1970–1976.

- Wu, M., Itoh, T., Shimizu, Y., Nakamura, H. & Takanashi, M. 2012. Low cycle fatigue life of Ti-6Al-4V alloy under non-proportional loading. *International Journal of Fatigue*, 44, 14–20.
- Yajima, H., Watanabe, E., Jia, Z., Yoshimoto, K., Ishikawa, T. & Funatsu, Y. 2011. Study on Fracture Toughness Evaluation by centre-notched small size specimen for heavy-thick steel plates. *Welding World*, 55, 78–83.
- Yamamoto, N., Mouri, M., Okada, T. & Mori, T. Analytical and Experimental Study on the Thickness Effect to Fatigue Strength (1st Report—Results of Fundamental Specimens). Proceedings of the Twenty-second International Offshore and Polar Engineering Conference, 2012 Rhodes, Greece.
- Yang, Y. & Vormwald, M. 2013. Three-dimensional Fatigue Crack Growth Path Simulation under Nonproportional Mixed-mode Loading. In *ICF13*.
- Yekta, R. T., Ghahremani, K. & Walbridge, S. 2013. Effect of quality control parameter variations on the fatigue performance of ultrasonic impact treated welds. *International Journal of Fatigue*, 55, 245–256.
- Yildirim, H. C. 2013. *Design aspects of high strength steel welded structures improved by high frequency mechanical impact (HFMI) treatment*. Ph.D. Thesis, Aalto University.
- Yildirim, H. C. & Marquis, G. 2014. Fatigue design of axially-loaded high frequency treated welds by effective notch stress method. *Materials and Design*, 58, 543–550.
- Yu, J., Sun, X., Jin, T., Zhao, N., Guan, H. & Hu, Z. 2010. High Temperature Creep and Low-Cycle Fatigue of a Nickel-Base Superalloy. *Materials Science and Engineering: A*, 527, 2379–2389.
- Yu, Y. H., Kim, B. G. & Lee, D. G. 2013. Cryogenic reliability of the sandwich insulation board for LNG ship. *Composite Structures*, 95, 547–556.
- Yuen, B. K., Koko, T. S., Polezhayeva, H. & Jiang, L. 2013. Mean Stress Assessment in Fatigue Analysis and Design', Ship Structure Committee, Report No. 466. Canada: Martec Limited.
- Zappalorto, M. & Lazzarin, P. 2014. Some remarks on the Neuber rule applied to a control volume surrounding sharp and blunt notch tips. *Fatigue & Fracture of Engineering Materials & Structures*, 37, 349–358.
- Zayed, A., Garbatov, Y. & Guedes Soares, C. 2013a. Reliability of ship hulls subjected to corrosion and maintenance. *Structural Safety*, 43, 1–11.
- Zayed, A., Garbatov, Y. & Guedes Soares, C. 2013b. Time variant reliability assessment of ship structures with fast integration techniques. *Probabilistic Eng. Mech*, 32, 93–102.
- Zerres, P. & Vormwald, M. 2013. Review of fatigue crack growth under non-proportional mixed-mode loading. *International Journal of Fatigue*, 58, 75–83.
- Zhan, W., Lu, N. & Zhang, C. 2014. A new approximate model for the R-ratio effect on fatigue crack growth rate. *Engineering Fracture Mechanics*, 119, 85–96.
- Zhang, G. 2012. Method of effective stress for fatigue: Part I—A general theory. *International Journal of Fatigue*, 37, 17–23.
- Zhang, G., Sonsino, C. M. & Sundermeier, R. 2012a. Method of effective stress for fatigue: part II – applications to V-notches and seam welds. *Int. J. of Fatigue*, 37, 24–40.
- Zhang, Q., Zuo, Z. & Liu, J. 2012b. High-Temperature Low-Cycle Fatigue Behavior of a Cast Al-12Si-CuNiMg Alloy. *Fatigue & Fracture of Engineering Materials & Structures*, 36, 623–630.
- Zhang, R. & He, L. 2012. Measurement of mixed-mode stress intensity factors using digital image correlation method. *Optics and Lasers in Engineering*, 50, 1001–1007.
- Zhang, S., Bridges, R. & Tong, J. Fatigue Design Assessment of Ship Structures Induced by Ice Loading - An introduction to the ShipRight FDA ICE Procedure. Proceedings of the Twenty-first International Offshore and Polar Engineering Conference, 2011 Maui, Hawaii, USA. 19–24.
- Zhang, W. & Liu, Y. 2012. Investigation of incremental fatigue crack growth mechanisms using in situ SEM testing. *International Journal of Fatigue*, 42, 14–23.
- Zhu, B. & Frangopol, D. M. 2013. Incorporation of structural health monitoring data on load effects in the reliability and redundancy assessment of ship cross-sections using Bayesian updating. *Structural Health Monitoring*, 12, 377–392.
- Zhu, S. P., Huang, H. Z., Smith, R., Ontiveros, V., He, L. P. & Modarres, M. 2013. Bayesian framework for probabilistic low cycle fatigue life prediction and uncertainty modeling of aircraft turbine disk alloys. *Probabilistic Engineering Mechanics*, 34, 114–122.
- Zhu, X.-K. & Joyce, J. A. 2012. Review of fracture toughness (G, K, J, CTOD, CTOA) testing and standardization. *Engineering Fracture Mechanics*, 85, 1–46.
- Zilakos, I. K., Karatzas, V. A., Chatzidouros, E. V., Papazoglou, V. J. & Tsouvalis, N. G. 2013. A FE based numerical tool for crack assessment in ship structures employing the CSR loading scheme'. *Analysis and Design of Marine Structures*, 281.